Modeling and CFD simulation of Abrasive Flow Machining Process

A THESIS SUBMITTED IN FULFILLMENT OF THE
REQUIREMENT FOR THE AWARD OF THE DEGREE
OF

Master of Technology (Research)

In

Mechanical Engineering

Submitted by
RUPALIKA DASH
(Roll no. 613ME3007)

Under the supervision of
Prof. K. P. MAITY

DEPARTMENT OF MECHANICAL ENGINEERING
National Institute of Technology Rourkela
India

DECLARATION

I, **Rupalika Dash,** a student of Department of **Mechanical Engineering**, National Institute of Technology Rourkela, bearing Roll No. **613ME3007** hereby declare that my M. Tech (Research) project report entitled "**Modeling and CFD simulation of Abrasive Flow Machining Process**", under the guidance of **Prof. K. P. Maity** at **National Institute of Technology Rourkela** is being submitted in partial fulfilment of the requirements for the Degree of **Master of Technology (Research)** in **Mechanical Engineering.** This is a record of bonafide work carried out by me and the results embodied in the project report have not been copied from any source. The results embodied in this project report have not been submitted to any other University or Institute for the award of any other certificate or degree.

Date:
Place: Rourkela

Rupalika Dash
Roll No. 613ME3007
Department of Mechanical Engg.
NIT Rourkela

CERTIFICATE

This is to certify that the thesis entitled "**Modeling and CFD simulation of Abrasive Flow Machining Process**" submitted by **Rupalika Dash** for the award of the degree of **Master of Technology (Research)**, **Mechanical Engineering** of NIT Rourkela, is a record of bonafide research work carried out by her under my guidance and supervision. The results of the investigation enclosed in this report have been verified and found to be more than satisfactory. The results embodied in this project report have not been submitted to any other University or Institute for the award of any other degree or certificate.

Date:
Place: Rourkela

Dr. Kalipada Maity
Professor
Department of Mechanical Engineering
National Institute of Technology
Rourkela

ACKNOWLEDGEMENT

This report is a result of my efforts as a research scholar towards my M. Tech (R) in Department of Mechanical Engineering, National Institute of Technology Rourkela. During this time, I have been supported by so many people to whom I wish to express my gratitude.

It is a great pleasure to express my deep sense of gratitude and sincere thanks to my research supervisor **Prof. K. P. Maity**, Department of Mechanical Engineering, NIT Rourkela, for his excellent guidance, constant encouragement, critical review and valuable suggestions throughout this research work. It would have not been possible for me to bring out this project report without his help and constant encouragement. His profound experience, incomparable expertise along with supportive nature has been a substantial asset for me throughout my learning experience. I am extremely thankful to **Prof. Sunil Kumar Sarangi**, (Director, NIT Rourkela) for giving me an opportunity to work under the supervision of Prof**. K. P. Maity.**

I am very much thankful to **Prof. S. S. Mohapatra**, HOD, Department of Mechanical Engineering for his continuous encouragement. Also, I am indebted to him for providing the entire official as well as laboratory facilities.

I am indebted to the members of my Masters Scrutiny Committee; **Prof. S. K. Sahoo** (chairman), **Prof. B. B. Biswal**, **Prof. M. Kumar** and **Dr. M. K. Moharana** for their useful suggestions during the discussion. I would also like to thank other faculty members of the institute for their co-operation and help. They offered me the possibility to work in a liberal environment and gave me the freedom to carry out my research in an independent way. Also, I thank to all the teaching & non-teaching staffs of Mechanical Engineering Departments for their kind cooperation.

In addition, I take this opportunity to express my gratitude to all of my friends and research scholars for being with me during the research work. My special thanks

to Mr. Kasinath Das Mohapatra, Ms. Munmun Bhaumik, Mrs. Padmaja Tripathy, Mr. Kumar Samal and Mr. Peri Raghava Ravi Teja for their help and support.

My thesis would remain incomplete without mentioning the contributions of my parents. My parents deserve special mention for their constant support, motivation and prayers during the research work. My hearty regards to all my family members for encouraging me in all aspects for carrying out the research work.

Last, but not the least, I am thankful to the omnipresent almighty for making me patient and strong enough to face the hard times during my research work.

Rupalika Dash
Department of Mechanical Engg.
NIT Rourkela

ABSTRACT

The abrasive flow machining (AFM) is a new finishing operation that involves abrasive particles as the tool to remove work material. AFM is broadly known as “no-tool” precision finishing operation and the carrier media containing abrasive particles is called as “self-deformable stone”. In AFM, a semi-solid polymer-based media containing abrasive powders in a particular proportion is flown through the work-piece at a certain pressure. The AFM consists of three major components, i.e. machine, media and tooling or fixture. The machine consists of a frame structure, control system, hydraulic cylinder and the media cylinder. The extrusion pressure for a standard AFM process varies from 10 bars to 100-200 bars. The function of tooling and fixture is to position the work-piece and provide direction to the media flow through the work-piece. The media consists of a carrier, abrasive powder and some additives. The flow of the media can be modeled using finite volume method as it deals with flow of a fluid. In the present work, FLUID FLOW FLUENT available in ANSYS 15 software package was used for the modeling and simulation. A 2D model for a cylindrical work-piece and a 3D model for four rotary swaging dies along with the fixtures have been prepared. Validation has been done for the two models with the existing experimental data. The most affecting flow output parameters like dynamic pressure, velocity and strain rate for different volume fraction and media speed have been analysed. The 3D model was simulated for both the non-granular and granular flow. The effects of different abrasive particles for variable diameter and volume fraction on the flow output parameters like granular pressure and skin friction coefficient have been studied. The flow analysis of the outputs gives a prediction of material removal efficiency.

Keywords: *Finite Volume Method, Fluid Flow Fluent, Granular and non-granular*

TABLE OFCONTENTS

List of Tables

List of Figures

NOMENCLATURE

2D	Two-dimensional
3D	Three dimensional
ρ_m	Mixture density
v_m	Mass-averaged velocity
α	Volume fraction
n	Number of phases
g	Gravitational acceleration
F	Body force
μ_m	Dynamic viscosity
E	Energy
p	Pressure
m	Mass
k_{eff}	Effective conductivity
k_{pq}	Exchange coefficient
f	Drag function
τ_p	Particle relaxation time
d_p	Diameter of fluid droplet
C_D	Drag coefficient
R_e	Reynolds number
k_{sl}	Fluid-solid exchange coefficient
g_0	Radial distribution function
θ	Granular temperature
e_{ss}	Particle restitution coefficient
F_n	Radial force
D_g	Diameter of the abrasive particle

τ_0 Shear stress

D_i Indentation diameter

t Depth of indentation

A’ Area of shaded portion

R_a^0 Initial surface roughness

R_a^i Roughness after ith stroke

L_a Actual contact length

L_w Length of work-piece

V_i Volume of material removed

N_s Number of abrasive particles in one stroke

R_w Radius of the work-piece

N_a Number of active particles per unit area

L_s Stroke length

R_m Radius of media cylinder

Subscripts

k Phase k

dr Drift

p Secondary phase

q Primary phase

s Solid phase

l Liquid phase

ss Solid shear

Superscripts

T Turbulent

CHAPTER 1

INTRODUCTION

Chapter-1

INTRODUCTION

1.1 General

The researches and innovations in the area of manufacturing technology are improving day by day to achieve a highly finished surface using reduced machining and labour cost. Now-a-days materials like ceramics, metal matrix composites, polymers and super alloys have replaced the traditional materials, which were commonly used in the aerospace, chemical and automobile industries. It has increased the need for sophisticated machining operation with high precision and accuracy. The work-pieces having complex shape and geometries, which are difficult to be machined with conventional machining process, demand for a new and advanced machining operation. Conventional machining operation involves a direct interaction of tool and work-piece, driven by an electric motor or a hydraulic pump. The advanced machining requires energy from sources such as plasma, electrochemical reactions, high-velocity water jet, abrasive jet and abrasive media. These sources give a better surface finish to parts in a convenient way with high accuracy and precision. The abrasive flow machining (AFM) is a new finishing operation that involves abrasive particles as the tool to remove work material. The conventional machining operations are used for the producing the flat and cylindrical work-pieces only and unable to machine complex shapes. AFM is capable of finishing complex shaped work-pieces as well as various materials ranging from aluminium, brass to ceramic carbides and nickel alloys. AFM is generally used for polishing, deburring and removing recast layer from the EDMed surface [1]. It also induces residual stresses on the work-piece. AFM is broadly known as “no-tool” precision finishing operation and the carrier media containing abrasive particles is called as “self-deformable stone”.

AFM is an internal finishing operation that incorporates the flow of abrasive media across the surface to be finished. The media containing abrasive is extruded either in a single direction or in two axial directions, thereby leading to a finished surface. AFM process is categorized as

1. One-way abrasive flow machining process
2. Two-way abrasive flow machining process

In one-way abrasive flow machining process, the abrasive media is extruded in one direction and collected in other direction. It is a prior stage of AFM that reciprocates the piston for a single stroke.

Unlikely, in two-way abrasive flow machining process, the abrasive media is flown through the work piece in a back and forth motion. The media is allowed to flow into the passage for a particular number of cycles and changed at specific intervals.

1.2 Working principle of AFM

The significant aspect of AFM is based on the abrasive media being used. A semi-solid polymer-based media containing abrasive powders in a particular proportion is flown through the work-piece at a certain pressure. The self-deformable property of the media enables it to move through restricted passages and acts as a flexible abrasive stone to give a finished surface [2]. A fixture arrangement is provided to create a restricted passage between the abrasive media cylinder and the work-piece so that the abrasion affects the desired locations. The required volume of abrasive media is filled in the lower media cylinder and it is extruded through the work-piece to the upper media cylinder. A single cycle in AFM contains a downward and an upward stroke of the piston. The AFM consists of three major components, i.e. machine, media and tooling or fixture. The machine determines the extent of abrasion, medium defines the type of abrasion. It is the work of tool or fixture to decide the location for abrasion [3].

1.3 Components of AFM system

In brief, AFM system is framed of components like a hydraulic pump, hydraulic cylinder, abrasive medium cylinder, pressure gauge, pistons, tooling and fixture arrangements for the work-piece. If the working and extent of machining in AFM is focussed, the system broadly consists of three major components i.e. machine, media and tooling. A simple diagram of AFM is given in Fig.1.

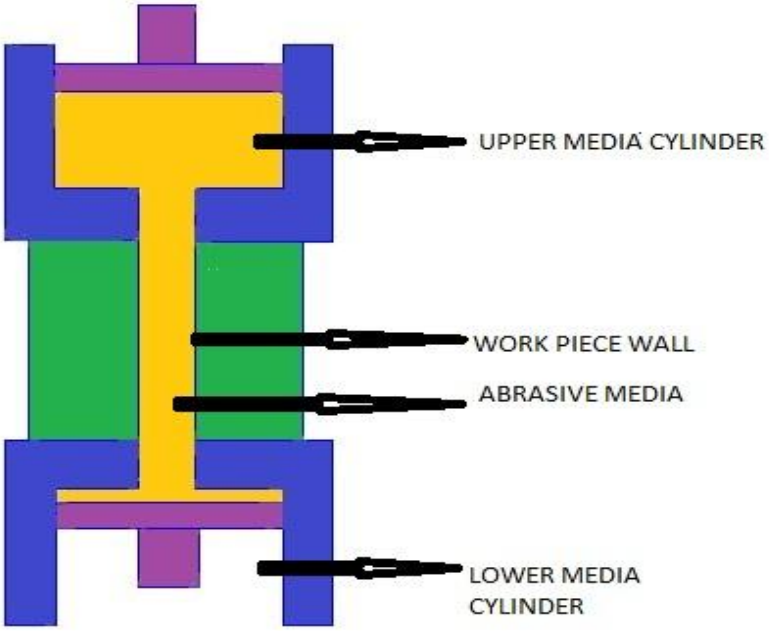

Fig. 1 Abrasive Flow Machining Process [92]

1.3.1 Machine

The capacity of AFM process determines the size of the machine. The machine consists of a frame structure, control system, hydraulic cylinder and the media cylinder. All the hydraulic pumps used in AFM are positive displacement pumps. The entire hydraulic system forces the media to flow from one media cylinder to another media cylinder through the work-piece at a particular media flow speed and pressure. The extrusion pressure for a standard AFM process varies from 10 bars to 100-200 bars. AFM systems are provided with controls on the hydraulic systems, volume flow rate of the media, the advancement of the piston, clamping and positioning fixtures. To measure and analyse the flow process, components like cycle counters, pressure and temperature controlling mechanisms and heat exchangers are incorporated for industrial use.

1.3.2 Tooling and fixture

The function of tooling and fixture is to position the work-piece and provides direction to the media flow through the work-piece. The fixture also restricts the abrasion in the area required on the work-piece. The fixture can be simple or complicated depending upon the shape and size of the work-piece**.** For small and

complex micro channels, the fixture arrangement is more complicated than that of a flat work-piece.

1.3.3 Media

Media is the most important component of AFM that controls the finishing operation extensively. The performance of AFM finishing is directly dependent on the concentration, viscosity, type of fluid and type of abrasive used in the process. The media consists of a carrier, abrasive powders and some additives. The carrier used in this process is extremely viscous and has a higher degree of cohesion to drag the abrasive particles through the work-piece passages. Abrasives used generally are aluminium oxide and silicon carbide. Boron carbide and diamond are used as abrasives for special purpose finishing. The ratio of the abrasive powder to carrier varies from 2 to 10. Special additives are mixed with the media to get the desired rheological properties and flowing conditions. The abrasive powder, polymer based carrier and the additives are employed to make a mixture in a fixed proportion. A schematic diagram of AFM process is given in Fig. 2.

1.4 AFM characteristics

- AFM works in a restricted passage to deburr and polish the inaccessible and complex work-pieces.
- Unlike other finishing processes, AFM maintains its consistency and precision for a broad range of applications.
- High-level surface finish and materials up to micron level are obtained using AFM process.

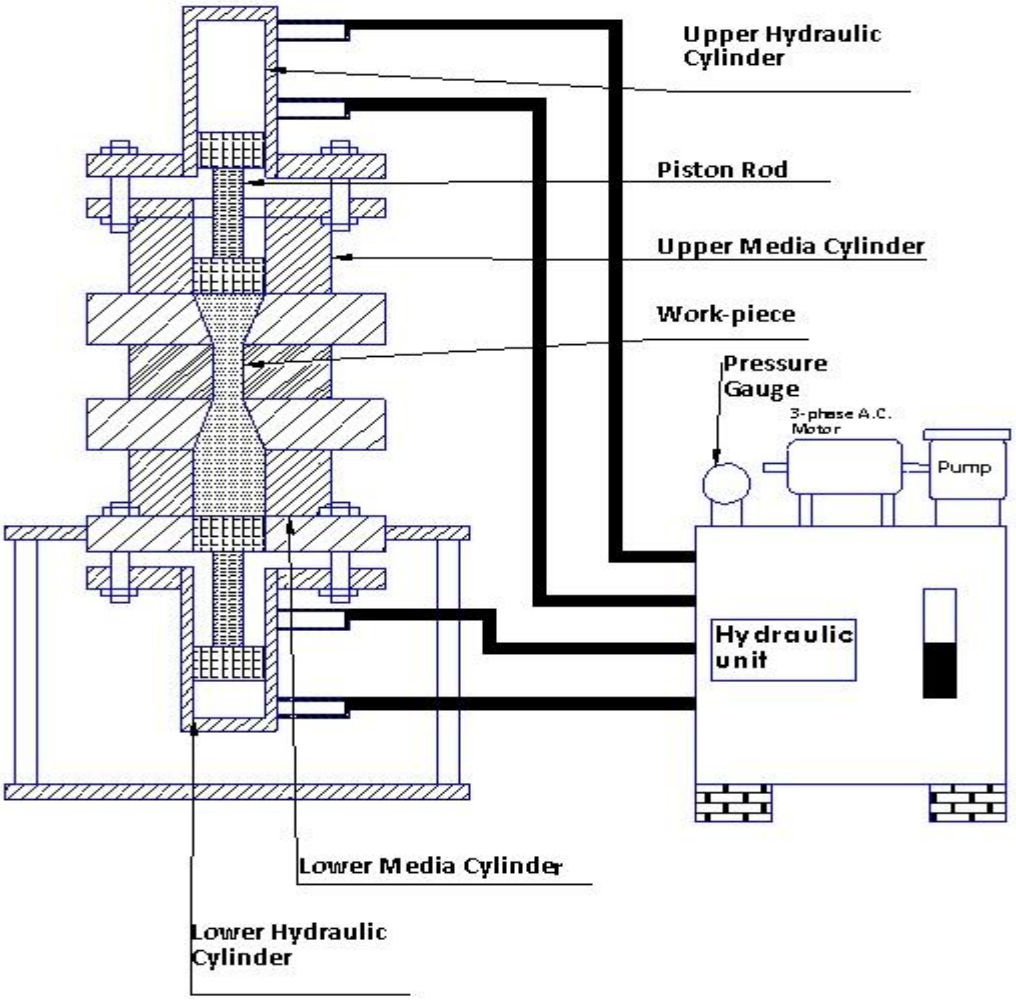

Fig. 2 Schematic diagram of AFM process [14]

1.5 Types of AFM

Many researchers are investigating to improve the performance of AFM and to reduce the time as well as labour required for the process. Recent modifications to AFM process are categorized into

a) Centrifugal force assisted AFM
b) Rotary AFM
c) Magneto-rheological AFM
d) Ultrasonic assisted AFM
e) Spiral AFM
f) Electro-chemically assisted AFM

Centrifugal force assisted AFM

Centrifugal force assisted AFM incorporates a centrifugal force generating rod inside the work-piece passage and the rod is provided with a rotary motion that causes a random interaction of abrasives in the work-piece wall with a centrifugal force. The performance of the process is dependent upon the rotational speed of the rod that increases the residual stresses and micro-hardness of the work-piece.

Rotary AFM

Rotary AFM is a modified AFM that assists the rotary movement of complete tooling arrangement with the work-piece and the media reciprocates within, with the help of hydraulic mechanism. Improvement in surface finish and an increase in MRR are also observed in rotary AFM.

Magneto-rheological AFM

Magneto-rheological AFM is a combination of magnetic finishing and AFM process. In this process, two magnets are provided around the finishing passage. A special type of media containing micro-sized soft iron particles is used to enhance the polishing. It is observed that the process increases MRR and surface finish visibly.

Ultrasonic assisted AFM

Ultrasonic assisted AFM describes a process that gives a vibration to the work-piece in a direction normal to the flow of media using a piezo actuator. The movement of the media and the abrasive action in the presence of vibration results in increased MRR up to a certain frequency.

Spiral AFM

In spiral AFM, a spiral-fluted screw is placed in the centre of work-piece passage. The rotational motion given by the screw moves the media from the lower to the upper cylinder and tries to finish the work-piece in the meantime.

Electrochemically assisted AFM

In this process, a polymeric electrolyte or water gel is used as a base carrier. The conductivity of electrolyte used for chemical machining is lower than ionic polymer

electrolyte. The polymer electrolyte medium is forced through the electrode gap and a semi solid paste flows through the passage, resulting in the finishing operation.

1.6 Critical process parameters

AFM is controlled and regulated by numerous process parameters [4-6]. Process parameters are classified into three categories. These are as follows: (i) Machine parameters, (ii) media based parameters and (iii) work-piece based parameters. Machine parameters include extrusion pressure, number of cycles, media flow speed and media flow volume. Type of abrasive, the size of the abrasive particle, abrasive concentration and viscosity of the media are included in the abrasive media parameters. Work-piece length and area are considered as the process parameters.

1.6.1 Machine parameters

Extrusion pressure

Extrusion pressure regulates the force applied to the abrasive media that affects MRR and surface roughness. The extrusion pressure affects the process upto a critical pressure value. MRR and surface finish remain unaffected after the critical extrusion pressure.

Media flow rate

According to literature survey, media flow rate has the least effect on MRR and surface finish.

Media flow speed

Experiments reveal that the increase in media flow speed affects the performance of AFM to some extent. An increase in media flow speed increases MRR and surface finish.

Number of cycles

A cycle in AFM is defined as the travel of media from one cylinder to another cylinder and flows back to the first cylinder. The number of cycles is varied to observe the change in MRR and surface finish.

1.6.2 Media parameters

Media parameters:

Abrasives used in AFM process are silicon carbide and aluminium oxide. Boron carbide and diamond are also employed in super finishing operations.

Abrasive concentration:

Abrasive concentration is an important parameter that is considered in AFM process. Higher concentration of abrasives increases the material removal rate.

Abrasive grain size

Abrasive grit size 8 is used for roughing operation. For finishing operations, finer grits of size 500 is used that provides excellent surface finish, removes less material and can easily access through the small and difficult-to-reach passages.

Media viscosity

Media viscosity is a parameter that has significant effects on the surface finish and material removal. Media viscosity is affected by the concentration of abrasive, type of abrasives and temperature of the media. The viscosity of the media decreases with increase in temperature. The temperature of the media is kept constant during the machining.

1.6.3 Work-piece parameters

Cross-sectional area

Cross sectional area of the work-piece also affects the machining performance. Decrease in the passage area increases the interaction of the media with the work-piece, leading to a rise in the material removal rate.

Length of the work-piece

Length of the work-piece is not that much significant. An increase in length decreases the finishing quality.

1.7 Mechanism of material removal

Material removal phenomenon in AFM process can be described in two modes, ploughing and abrasion [8, 9]. High pressure produced in the process makes the abrasive particle come in contact with the wall of work material due to the rubbing action. The flow of material occurs in the direction of abrasive as well as in the lateral direction. A continuous flow of abrasive results in leap formation and the work hardening of leaps cause intense stress concentration and plastic flow. The interaction of the abrasive grains with the work-piece wall is shown in Fig. 3.

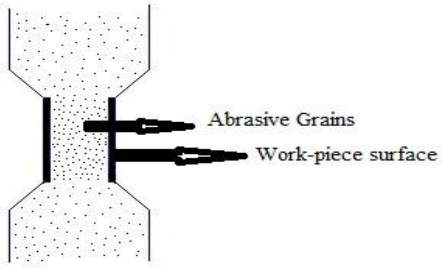

Fig. 3 Abrasive action on the wall of work-piece

Micro-cutting or abrasion is another important phenomenon in the material removal of AFM. Unlike ploughing, abrasives remove material in small amount limiting side flow of the abrasive grain during micro-cutting.

1.8 Applications of AFM

Initially AFM was developed for aerospace, automotive, medicine, chemical, die and mould industries. AFM is used for improving the surface finish of airfoils and edge rounding of blades, shafts and discs. AFM is also used to introduce residual stress and increases the fatigue strength of turbine and automotive components. The use of AFM is diversified nowadays and it is used for high-quality polishing of biomedical components and defence industry. Some manufacturing industries also prefer AFM process to other conventional finishing methods to get a better surface finish.

1.9 Advantages of AFM

1.9.1 Aerospace industry

The application of AFM in aerospace industry provides excellent surface quality, longer component life, high fatigue strength to the components used because of which increase in airflow and optimized combustion of fluid flow is observed.

1.9.2 Automotive industry

Uniform and better surface quality is noticed in the finished components of automotive industry due to the application of AFM. Enhanced engine performance, increase in velocity and volume, better fuel economy, reduced emissions, less wear of the component and a longer life span are resulted due to the finishing operation.

1.9.3 Dies and mould industry

Enhanced surface uniformity and cleanliness is observed in dies and mould industries by AFM process. The performance of dies is increased and life span of the moulds and dies are increased. Production cost is reduced and output is enhanced.

1.9.4 Medical industry

The application of AFM process in medical industry eliminates the surface imperfections and contaminations. The durability, functionality and reliability of the components are increased.

1.10 Objectives of the present work

The main objectives of the present work are as follows:

(a) Development of a 2D model for a cylindrical work-piece and a 3D model for a flow passage other than cylindrical shape
(b) Validation of the 2D and 3D model with the existing experimental data
(c) Study the most affecting flow output parameters like dynamic pressure, velocity and strain rate for different volume fraction and media speed for the 2D model and prediction of the material removal efficiency from the flow outputs
(d) Study both non-granular and granular flow of the 3D model.

(e) Study the effects of different abrasive particles for variable diameter and volume fraction on the flow output parameters and predict the material removal efficiency from the flow outputs.

1.11 Organisation of thesis

Chapter 1: ***Introduction***

The first chapter includes an introduction and incisive details about the AFM process, its types, operation, applications and advantages. The chapter also provides an objective of the present work.

Chapter 2: ***Literature survey***

This chapter reviews the literatures those provide a basic background and the ideas for the present work. The literatures discussed in this chapter are relevant for the present study and emphasize the key research work done. The study is categorised into five sections based on the major work done in the articles. The chapter describes the research gap and need of research in the field.

Chapter 3**:** ***Types of AFM: A brief study***

Different AFM processes discovered till today are described in this chapter. Schematic diagram of the process and details of the operation along with the machining effects are discussed briefly.

Chapter 4**:** ***CFD modeling and analysis***

The details regarding mathematical modeling and steps of simulation using CFD are described in this chapter. The governing equations associated with the present modeling work and the multiphase modeling along with the boundary conditions is defined.

Chapter 5: ***Flow analysis of AFM for a 2D model***

The chapter analyses different flow parameters and its variation at different positions of the flow domain of a 2D model for a cylindrical work-piece. It also predicts material removal efficiency using different theories. The variation of the flow

parameters at various media flow speed and volume fraction of the secondary phase are discussed in the chapter.

Chapter 6: ***Numerical Simulation of AFM for a 3D model***

The present chapter focuses on a 3D geometry created for four rotary swaging dies. The 3D model has been simulated for both the non-granular and granular flow. The parameters like dynamic pressure, strain rate, velocity, granular pressure and skin friction coefficient are studied.

Chapter 7: ***Partial validation of the models***

In this chapter, the mathematical modeling for the change in surface roughness has been given. The validation of the 2D and 3D model with the benchmark experimental data is given.

Chapter 8: ***Conclusions***

The last chapter gives a summary of the major findings and conclusions from all the results and discussions. The future scope in the field is also presented.

CHAPTER 2

LITERATURE SURVEY

Chapter-2

LITERATURE SURVEY

2.1 Introduction

The current chapter summarises the researches related to abrasive flow machining and its modeling using computational fluid dynamics (CFD). The purpose of the literature survey is to provide background information and highlight the important investigations related to the present work. The various aspects and researches are classified into four sections based on the major research done in the literature. The sections are based on

1. Mechanism of abrasive flow machining process
2. The study of material removal rate and surface finish
3. Important papers on CFD simulation for AJM, AWJM and slurry flow those inspired the current work
4. Modeling work done on AFM

2.2 Abrasive flow machining (AFM) process mechanism:

Jain et al. [1] developed a neural network model in which the effects of experimental parameters were analysed for material removal and surface finish. The input and output parameters were chosen and off-line model training was carried out by using back-propagation method. The simulation results were seen to have a good agreement with the theoretical and experimental results. Jain et al. [2] developed a model using finite element analysis for the media flow analysis and evaluated the stresses generated during the process. The results from the theoretical analysis were compared to that of the available experimental data and a good agreement was found by the two. Jain and Adsul [3] experimented various parameters regulating the process and the effects of MRR and surface finish were analysed. The work-piece materials considered for the analysis were brass and aluminium. The dominant process parameters were found to be abrasive concentration, number of cycles, abrasive mesh size and media flow speed. It was observed that the machining action was same as a grinding or lapping operation as the abrasive media gently and uniformly abraded the

surfaces or edges [4]. Jain and Jain [5] described the generated profile and material removal as the interaction of abrasive particles with the work-piece. Experiments were conducted as per response surface methodology and simulation was done. The results were predicted from the simulation. The profile of the finished surface was found to be a function of extrusion pressure, number of cycles, abrasive mesh size and concentration of abrasive particles. Jain and Jain [6] proposed a model to determine the tangential forces and specific energy acting in AFM process. The model took into account the applied pressure, the active grains, grain size, the hardness of work-piece and the number of cycles. Heat transfer during the finishing process was analyzed and compared with the temperature studied experimentally. The model also depicted the amount of heat flowing through the medium and the work-piece. Jain et al. [7] attempted to study the tolerance and surface finish with economically acceptable surface profile using finite element analysis and compared the data with the experimentally generated surface profile. Gorana [8] made theoretical analysis to study the forces acting on the single grain in abrasive flow machining. The research was carried out to find the axial force, radial force and active grain density during the process. The grain work-piece interaction or the minimum depth of indentation and minimum load required were the two parameters considered here. Gorana et al. [9] also studied that the cutting forces and active grain density were the important parameters, which governed the surface roughness. A disc dynamometer was used to measure the axial and radial forces during the AFM and the effects of three parameters like extrusion pressure, abrasive concentration and the grain size were studied upon the response parameters like material removal, cutting pressure and surface roughness. The surface texture was studied using scanning electron microscope. Rhoades [10-12] studied the basic principle of AFM and reported that the depth of cut primarily depended upon the abrasive grain size, relative hardness, sharpness, and the extrusion pressure. Perry [13] reported that abrasion was high where the medium velocity was high. An increase in pressure and medium viscosity increased the material removal rate while surface finish value decreased. The type of machining operation used to prepare the specimens prior to AFM was found to be significantly affecting the improvement in the surface finish. Ravi Shankar et al. [14] studied the abrasive flow finishing and effects of its parameters on aluminium composites (MMC- aluminium alloy and its reinforcement with SiC). The effects of extrusion pressure, number of cycles and viscosity of the medium were studied on

material removal rate and surface finish. The relationship of extrusion pressure and ΔRa were found to be optimum for 6 MPa and the graph between weight percentage of processing oil and ΔRa was found to be optimum for 10% wt of the plasticizer. The surface finish and material removal rate are different for alloy to MMCs for varying parameters. Shankar et al. [15] studied the AFF (Abrasive flow finishing process) which evolved as an important finishing operation in the industries to avoid the power loss due to friction and control the sharp increase in cost. They developed an advanced AFF process by providing a rotary motion to work-piece (R-AFF i.e. rotary abrasive flow finishing). In the preliminary stage, they compared the response parameters like material removal and surface roughness for both AFF and R-AFF. In the later stage, experiments were done by using MMCs as the work-piece to study R-AFF using RSM methodology. It was observed that the rotating motion of the work-piece led to a significant improvement in surface finish. Ravishankar et al. [16] characterized the rheological behaviour of the styrene-butadiene media and its performance using R-AFF process. They described that the media should have the good flowability, deformability along with good abrading quality. They prepared different media using soft butadiene rubber along with plasticizers and abrasives. Various flow, deformation behaviour of the media and the static, dynamic rheological properties of the media were studied. The polymer media was seen to have shear thinning nature. With increase in temperature, it lost its properties. To study the static rheological properties, flow test, creep compliance test and stress relaxation test were done and in order to study the dynamic properties, amplitude sweep and frequency sweep were performed. Later, the effect of each rheological parameter such as shear stress, percentage of viscous component, stress relaxation modulus, storage modulus on the change in average surface roughness (DRa) and material removal rate during R-AFF were found out. The work-piece used was aluminium MMC. Ravishankar et al. [17] in another experiment studied the surface topography and the optimum conditions for higher surface roughness. The work piece along with the entire tooling was revolved externally and the media was flown into it. It was observed that with the increase in rotational speed from 2 to 10 RPM, the helix angle decreased from 22 degrees to 9 degrees with increasing the helical path. Using the R-AFF, reinforcement was applied on MMCs and the three methods to study the MRR of reinforcement were also explained. The scanning electron microscope graphs revealed the crosshatch pattern, helical patch directions and micro scratch width and depth. Ultimately, the

study developed that the R-AFF produced 44% better surface finish and 88.1% better material removal compared to AFF process. Rajesha et al. [18] attempted to develop a new carrier media as an alternative to the existing media. The new carrier media was developed using Fourier transform infrared spectroscopy and thermo gravimetric analysis. Performance evaluation of the media was carried out by considering the extrusion pressure, abrasive concentration, viscosity of media, flow rate as the process parameters and material removal, surface finish as the response parameters. The new media, a derivative of ester group was capable of withstanding the temperature up-to 71 degrees. The new media was flexible enough and a great improvement was observed in surface finish and in material removal of AFM process. The study revealed that the surface finish was significantly influenced by the media flow rate. Bahrea et al. [19] studied the parameters to explore the influence of lead-time and medium pressure on the surface quality. The work piece used in this case was AISI steel. The silicate media containing abrasive particles like carbide and diamond were used for the finishing operation. The motive of the experiment was to not only watch the surface finish but also reduce the stress concentration. Soft materials like aluminium and brass were also studied. The extrusion pressure and the number of cycles were the most important machining parameters. Siddiqui and Hameedullah [20] attempted to show experimentally the effects of number of vents and passages of outflow on the surface roughness. Cylindrical work-pieces having varying cross-sections and lengths along with the varying number of vent passages of outflow were considered. R_a value was taken as a performance measure, indicating the output responses. Experiments were performed with constant parameters like mesh size of abrasives, abrasive concentration, number of cycles and media flow on the work-piece like brass. The results demonstrated that the work-piece with a single vent or passage had a higher material removal and improved surface roughness in comparison to the work-pieces with multiple vents or passages. Komanduri et al. [21] emphasized on material removal on brittle materials. Indentation models are proposed to study the abrasion polishing. To develop an analytical model for the prediction of surface finish using the abrasion mechanism, an overall understanding of the process involving abrasives as the finishing tool is needed. In this paper, an attempt was made to rationalize various models by linking conventional machining, grinding, ultra precision machining, and indentation sliding as a cognate transition for material removal operations. Kimberly et al. [22] gave another neural network model to predict

the dimensional change and surface finish in AFM process. The neural network was then paired with a heuristic search algorithm to select the machining parameters. The complete model was validated with experiments and the results were promising. The model can be used in industrial approach also. Venkatesh et al. [23] experimented the finishing operation in case of a micro channel. They fabricated flexible tooling for the micro channel, which was created on a rectangular work-piece. Micro channels were made by using silicon wafers and the variable parameters like extrusion pressure, the weight percentage of processing oil and the processing time were taken into consideration. Venkatesh et al. [24] investigated the effects of parameters such as processing time, extrusion pressure, number of cycles and the abrasive mesh size on a EN-8 steel bevel gear. A new fixture arrangement was developed to restrict the abrasion only to the gear tooth. The initial surface roughness was 1.4-1.8 micrometre. Taguchi orthogonal array was used to study the parametric optimization. The roughness after machining was checked at five different locations and the improvement in roughness was found to be 50%. The extrusion pressure was found to have the highest contribution to MRR and the processing time and abrasive mesh size were the other parameters having lower effects on the MRR. Cheema et al. [25] reviewed the AFM process briefly. The process can be of three types such as one way, two way and orbital AFM process. Variants of abrasive flow machining were magnetically assisted AFM, magneto-rheological AFM, and electro chemical aided AFM, centrifugal flow assisted AFM, drill bit guided AFM, rotary AFM, ultrasonic assisted AFM and spiral flow assisted AFM. A clear study on different parameters controlling the process was also done. The parameters like work-piece, abrasives used, abrasive carrier and concentration were also analysed. The effects of different media like rubber, natural polymer based media and silicon based media were observed on AFM. Chouhan and Mittal [26] used a L9 orthogonal array for experimentation, optimized the results obtained using ANOVA and verified that the output responses were affected by the input parameters strongly. The work-piece used by them was AISI D2 steel. Chouhan and Mittal [27] did a review of the AFM process. A brief idea about one-way and two-way AFM was discussed. Works of different authors regarding the parameters controlling the machining were analysed. An experimental setup was also done to see the variation of MRR at a different cross sectional area of the work-piece. Li et al. [28] employed the nonlinear tube as the research object in this case. The non-linear tube is used as the research object in

military application and civil uses in which the performance is confirmed by the surface quality. For the non-linear tube, a nozzle was considered for the research purpose and the effects of controlling parameters through the nozzle surface topography and scanning electron microscope (SEM) was explored. The optimum parameters for the abrasive flow machining were determined. Abbas et al. [29] used L18 orthogonal array in Taguchi experimental concept to determine the S/N ratio and optimize AFM parameters. The experimental procedure verified the AFM parameters such as length of stroke, extrusion pressure, number of cycles, percentage abrasive concentration and abrasive grain size. The statistical model predicted about 91.39% and 96.4% surface roughness and material removal respectively. Length of stroke was found to have more effect on the surface roughness and the percentage of abrasive concentration affected the material removal. Abbas Ibrahim [30] predicted the material removal rate in multiple regression analysis by using RSM in Minitab. From the results of the experiment R^2 value was found to be 92.3% and extrusion pressure was found to be the most significant parameter. Kenda et al. [31] experimented the profile polishing of plastic gears using AFM process. The surface roughness decreased visibly after 120s. The effect of time required for the polishing operation on the final surface roughness was studied. Polishing parameters depended upon the flow media and the geometry of the work-piece. Roughness prediction model and the thickness of the material removal model were prepared. The plastic gear finishing operation is an important technological innovation for injection moulding manufactures. Kenda [32] investigated the effects of process parameters and the fluid flow on the surface roughness and micro-structure. Along with the abrasive flow, they developed a model for the surface roughness using a rotating mandrel. The energy consumption was also studied to verify the efficiency of the process. It was concluded that the rotating mandrel was able to finish the WEDM-ed surface, induce residual stress and polish the surface. Walia et al. [33] tried to improve the performance of AFM process using a Centrifugal force generating (CFG) rod. CFG rod enhanced the efficiency by increasing the number of active abrasive particles that take part in the finishing operation. The process involving the CFG rod is also affected by the extrusion pressure, speed of the CFG rod and the number of cycles. Increase in percentage improvement of surface roughness was found using the process. The work-piece used here was a cylindrical one. There was a significant improvement in the surface roughness in the centrifugal force assisted abrasive flow machining

process in comparison to the AFM process. Mali and Kishan [34] experimented and developed a new media for the AFM process. The properties of the media were the key elements in the polishing operation. The media available commercially is expensive and not generally affordable. The new media was prepared by using a polymer as the base, liquid synthesizer and some additives. The effects of the parameters like abrasive concentration, abrasive mesh size, temperature and percentage of liquid synthesizer were studied to confirm the rheological properties of the newly developed media. The inner surface finishing of HSS was experimented using the new developed gel. The surface roughness was found to decrease visibly from 3.5μm to 0.6μm for 50 cycles. Kavithaa et al. [35] worked on the abrasive flow finishing machining (AFFM) for the deburring as well as finishing of an extrusion die, shuttle valve and modular head of the hip joint. The optimized results were calculated and the surface characterization was done using the optimal results. The paper proved the capability of the AFFM process for radiusing, nano-finishing and deburring of ferrous and non-ferrous materials. Brar et al. [36] tried to improve the finishing operation by using a drill bit in the centre of the work piece so that the abrasive particles move in a helical path inside the finishing area increasing the abrasive action. The results revealed that the use of helical drill bit increased both the material removal and surface finish. The number of cycles and presence of drill bit were the significant parameters while extrusion pressure and media flow rate were insignificant. Kumar et al. [37] worked on helical AFM process that involved a drill bit at the centre of a cylindrical work-piece having a three-piece nylon fixture in the same axis as the drill bit. An improvement in the surface finish was found by the helical movement of the abrasive media. The contribution of extrusion pressure towards the MRR was 20.43%, type of material contributed 29.57% and the number of cycles added 26.09%.

2.3 Surface finish and material removal

Williams and Rajurker experimented on the effects of viscosity and piston pressure on material removal (MR) and surface finish. The conclusion was derived by a scanning electron microscope. There was a significant improvement in surface finish within the initial few cycles [38-40]. Przyklenk [41] gave an idea that the media temperature should not exceed 100°C. Loveless et al. [42] performed some

experiments and concluded that the media viscosity is an important parameter to determine the material removal efficiency. Wang and Weng [43] developed a polymer-based gel for abrasive flow machining process that removed recast layer formed by WEDM operation. Vinyl-silicone polymer has a good deformation property and can pass through complex holes easily. Temperature can be maintained constant when it is used in high concentration with a minimum value [44]. High viscosity media has higher deformation rate and can finish the WEDM recast layers. High abrasive concentrations have fine finishing results. The experiments showed that the roughness improvement rate was more for higher abrasive concentration. On the other side, small abrasive particles produced finer surface in comparison to bigger abrasive particles, but the smaller sized particles need more number of finishing cycles than the bigger particles. Gov et al. [45] studied the effect of work-piece hardness on AFM process. The work-piece was cut by wire EDM and roughness measurement was done before and after AFM process. The improvement of surfaces with respect to hardness was observed. It was observed that the white layer formed by WEDM process was successfully removed by AFM process and the surface cracks were also removed with increase in fatigue strength. Harder materials have more surface improvement than softer materials. Agrawal et al. [46] used polyborosiloxane as media and predicted the viscoelastic properties of media such as viscosity, creep compliance and bulk modulus. Kendaa et al. [47] experimented the influence of process parameters on the surface roughness and the residual stresses induced. The work-piece used in this case was AISI D2 steel, which was pre-machined by EDM. The AFM process removes all the surface damages and induces high compressive residual stresses to the machined surface in a very thin sub layer up to 10 microns. AFM improves the surface integrity in comparison to other finishing operations. The rheological properties of the AFM media play an important role in the material removal rate. Uhlmann et al. [48] studied the AFM process for ceramic materials. A specified pressure and temperature is applied when the fluid is flown in the contours of the work-piece. AFM process was studied in correlation with the flow parameters, surface formation and edge rounding. Model simulation techniques were developed to give an insight to the process. The overall objective was to check the surface quality and edge rounding. Uhlmann [49] reported about the changing behaviour of the shear modulus of the media due to change in design of work-piece holding device and variable flow rate. AFM is a complex process because of the shear thinning and visco-

elastic property of the media. This paper is based on the model using the Maxwell model of elastomers and generalized Maxwell model. The conventional simulation process was used to develop the material model. The model was validated by suitable experiments. Tzeng et al. [50] fabricated a micro slit using wire EDM, Taguchi experimental method was applied to investigate experimentally the parameters of AFM including extrusion pressure, concentration of abrasives, abrasive particle size and machining time. The surface roughness was measured using SEM and the optimum parameters were calculated using ANNOVA and S/N ratio response graph. ANNOVA was proposed to study the surface finishing and shape precision. Tzeng et al. [51] also worked on finishing of micro channel to study the self-modulating behaviour of the abrasive media. They prepared a micro channel of stainless steel with the help of WEDM and studied the effects of different parameters. The results show that the roughness for a coarse particle is less in comparison to a fine particle. The machining quality increases with the increase in machining time and extrusion pressure. The self modulating property of the media affects the machining in a large amount. Tool marks and burrs produced by WEDM process are removed by AFM. AFM improves the finishing of micro channels at low cost and in an efficient way. Fang et al. [52] gave an idea about the particle movements in AFM process, i.e. sliding, rubbing or rolling. The material removal can also occur in three different ways, i.e. sliding deformation or grooving, plastic deformation by rolling of the particle, micro-cutting, ridge formation or by fatigue wear. The machining efficiency is dependent upon the wear mass loss, speed of the material and results in particle movement. The paper concentrated the attention upon elliptical particle, the movement pattern, normal load, ellipticity, particle size and hardness. The analytical model and movement pattern were studied using C++ programming language. Large ellipticity increased grooving particle numbers. Lower particle hardness, larger particle radius and higher normal load tend to increase the grooving of the particle. An increase in the sharpness of the particle increased the grooving. The optimum ellipticity value for the grooving is 0.8. The combination of hard work piece and softer abrasive led to particle rolling. Walia et al. [53] experimented on the recently developed hybrid finishing operation, i.e. centrifugal force assisted abrasive flow machining (CFAAFM) process in which the centrifugal force was applied to the abrasive laden media with the help of a centrifugal force generating rod, which was introduced into the work-piece. The surfaces generated in this case by the random

attack of the abrasive grains and finishing was unidirectional. The experiments were done by increasing the rotational speed of the rod while keeping the other parameters constant. The micro hardness, X-ray analysis, residual stresses and surface morphology were analysed after the finishing operation. An increase in surface micro hardness and compressive residual stress were observed with the increase in rotational speed of the rod. Walia et al. [54] analysed the CFAAFM (centrifugal force assisted abrasive flow machining) process. In CFAAFM process, the surface was attacked by the abrasive grains randomly. The surface generated was also random, but unidirectional. The surface micro hardness, residual stress, surface morphology and X-ray analysis were done. The surface micro hardness and residual stress were found to increase with the increase in rotating speed of the CFG rod. Hiremath et al. [55] experimented on the finishing operation of the intricate profiles and inaccessible areas using a special type of set-up. The machining operation was done for a special type of aerospace material named nitralloy collar sleeve. Progressive reduction in surface roughness was observed after much number of passes. Recast layer produced by EDM was also removed by the process. Very high surface finish was achieved by the increase in the number of passes in finishing. The set-up was ideal for the finishing of complex areas successfully with an increase in compressive residual stress. Kim and Kim [56] used AFM for deburring of spring collets for chrome-molybdenum using micro-grooves. The test was conducted for both SiC and Al_2O_3 media, the aluminium oxide media was found to be superior to silicon carbide media. The AFM process was found to be independent of the deburring pressure at different circularity and concentricity. The high viscosity of the media increased the deburring action and improved the surface roughness. Singh et al. [57] developed a model of AFF (Abrasive Flow Finishing) process for the force and surface roughness using the previous equations and mathematical model by Jain et. al. The shearing action of the abrasive particles at different concentration of plasticizer was studied. The radial force and axial forces were determined by the mathematical formulations and rheological property of the media. The surface roughness was studied theoretically at different extrusion pressure, number of strokes and percentage of plasticizer. The theoretical results were validated with the available experimental results. Gupta and Wandra [58] experimented on centrifugal assisted abrasive flow machining in L9 orthogonal array and studied the effects of abrasive concentration, abrasive mesh size, number of cycles and centrifugal force. Centrifugal force enhanced the efficiency, performance,

surface quality and reduced the machining time. The abrasive mesh size was observed to have the largest effects followed by the speed of the rod, the number of cycles and abrasive concentration. Wang et al. [59] carried out experiments on AFM for helical passages. Usually AFM process is applicable for a smooth one-way motion. In the helical passage, the media gets multiple flow direction and interact with the wall properly to reduce the surface roughness. The roughness improvement was found to increase 76% in comparison to 60% that of the conventional AFM. Use of a helical core improved the surface finish as well as performance of AFM. Brar et al. [60] tried to couple the ECM process with the AFM process. The work piece was taken as the anode and the abrasive media as cathode. A DC current was applied for the anodic dissolution of the work-piece and it enhanced the material removal by the dual action of ECM and AFM. The experiment was done using L29 orthogonal array and the process parameters were optimized using the Taguchi method. The surface finish was found to increase and modified further by using some electrolyte salts in AFM media. Wani et al. [61] focussed on the modeling and simulation for the prediction of surface roughness on the work piece surface finished by MAFF process. Magnetic abrasive flow finishing (MAFF) is a new modification in AFM process and sufficient experimental results regarding the material removal is not available. The initial stages of the research were given. A finite element model was developed to find the magnetic potential distribution in the magnetic abrasive brush formed during finishing action and then it was used to evaluate machining pressure, surface finish and material removal. Shinmura et al. [62-64] carried out experimental as well as analytical studies on MAF using magnetic abrasives in which the surface finish was generated with the help of magnetic field. Shinmura [65, 66] examined the microscopic changes in the surface texture resulting from an internal magnetic abrasive finishing process. Jha and Jain [67, 68] gave a design and simulation of magneto-rheological abrasive flow finishing (MRAFF). In this experiment a smart magneto rheological fluid (MR) was used which consisted of carbonyl iron powder and silicon carbide abrasive dispersed in base medium of grease and mineral oil. This MR polishing fluid was used to control the final surface finish. No measurable change in surface finish was found at zero magnetic fields where as for same number of cycles, the roughness was found to decrease with application of magnetic field. With increase in magnetic field, the carbonyl iron powder held the abrasive particles more firmly leading to better surface finish. At higher magnetic flux density, abrasive marks in the direction of motion

were also observed due to deep penetration of some abrasive particles during MRAFF in the work piece surface. Scientists at Belarus explored the new possibilities of using slurry comprised of aqueous MR fluid and cerium oxide abrasives to polish glass up to nanometre level [69].

2.4 CFD simulation

The modeling of abrasive flow machining (AFM) is done using the computational fluid dynamics as the machining operation involving fluid flow. The flow parameters and the motion of the fluid can be easily analysed by using CFD. CFD is also used for the abrasive jet machining process, which involves the abrasive particles flowing in the form of a jet or with the help of a water jet. The modeling in CFD is generally done using commercially available FLUENT and CFD ACE+ softwares. Das et al. [70] studied the CFD simulation for nano-finishing operations like magneto-rheological abrasive flow machining. Magneto-rheological abrasive flow machining is the conjugation of magneto-rheological finishing operation with abrasive flow machining. As it is a nano finishing operation, material is removed in the form of small chips. The CFD simulation and the flow governing equations were done in this paper. Paramvir et al. [71] did the experiments and analysed the results using a two dimensional CFD model. The axial and radial forces were calculated for the flow of polishing medium in the work piece passage. Wang and Wang [72] developed a model for abrasive water jet machining. A control volume method was used to discretize the equations and study the velocity-pressure coupling. The abrasive media was assumed to be a pseudo-fluid phase and a two fluid model was created using a phase coupled SIMPLE algorithm. The two-dimensional flow outside the nozzle was analysed and the results were validated and compared with the experimental results. Deam et al. [73] prepared a model for the water jet cutting to avoid the fluctuation rising in local cutting face. The simulation process considered the properties of the material being cut, the cutting or erosion by abrasive particles, jet inlet boundary conditions, particle distribution in the jet, the fluid dynamic model produced and the kerf profile produced. A CFD software package was used to analyse the flow motion of the abrasive jet. Narayanan et al. [74] made a three-phase flow model. The particle size distribution and the effects of particle breakage were taken into account. The model was validated with the experimental data of abrasive mass

flow rate, operating pressure and cutting head geometry. The cross sectional averaged particle velocity outside the nozzle was validated with the experimental ones and found to have a good agreement. Annoni et al. [75] established a model for water jet cutting assisting airflow along with the jet. In the system, a controlled flow of air was given through an orifice into the jet to stop the instabilities in the jet. The flow and motion of the water jet were studied with the help of ANSYS FLUENT CFD package. The CFD simulation provided the information on how the airflow inside the orifice tube protected the capillarity from the disturbances. The model was validated by pressure and jet velocity and improvement in the real cutting experiments was observed by entering air through the orifice. Liu [76] studied the kerf produced by the abrasive water jet using CFD model. Different boundary conditions were given to the abrasives and the water jet. The model gave a better insight into the dynamics of the flow during the process. Initially there was a declination in velocity rapidly and the decay in velocity for different particles was also studied. The motion of the jet predicted the kerfs to be produced. Deepak et al. [77] analysed the suspension in abrasive water jet to study the erosion inside a nozzle. The skin friction effects and jet kinetic energy were observed in the presence of abrasives. The skin friction was found to vary along with change in nozzle diameter. The skin friction coefficients caused due to wall shear and jet kinetic energy values changed for different abrasive particles. The research work was conducted for three different abrasive particles. The result explained that the abrasive particles with low density produced a lower skin friction coefficient and higher jet kinetic energy. From the three types of abrasives, garnet was found to have a higher kinetic energy of the jet in comparison to aluminium oxide and silicon carbide. Deepak et al. [78] studied the effects of inlet pressure on the wall shear and jet kinetic energy. The increase in inlet pressure increased the wall shear significantly. The wall shear reached the peak value in the critical cross section of the flow passage. The inlet was found to have more effects on the wall shear in comparison to jet kinetic energy because the jet kinetic energy increases linearly unlike wall shear. Deepak et al. [79] established a model and studied the effects of the ratio of the diameter of the nozzle to the particle size. The alterations in the exit velocity and nozzle diameter were found to have visible change in the wall shear. A design of experiment using ANOVA was used for the simulation and the simulated results were analysed. The exit velocity was found to decrease with an increase in diameter of the nozzle. Effects of particle size and volume fraction were

found to have no significant effects. Deepak et al. [80] worked on the effects of inlet pressure and the volume fraction on the skin friction coefficient. Increase in inlet pressure increased both the skin friction coefficient and jet kinetic energy and increase in volume fraction decreased the both. The increase in skin friction coefficient affected the diameter of the nozzle, which in turn changes the jet kinetic energy. Lagumbay [81] developed a new homogenous equilibrium mixture approach with proper numerical methods that agreed with the experimental data in a wide range. This is an idealized fluid model flow for both multiphase and multicomponent flow in comparison to the conventional methods, which are able to solve only multiphase or multicomponent flow. Exact solution of the flow can be achieved by this method. The initial idea of multi phase flow was taken from the paper by Manninen [82]. Zivkovic et al. [83] studied various granular phenomena like heat transfer, erosion, aggregation, attrition and segregation using granular phase variables like granular pressure and granular temperature. Diffusion wave spectroscopy phenomena were used to determine both granular pressure and granular temperature. The fluidized bed phenomena were used to derive the kinetic theory of granular flow. The determined variation of granular pressure with solid volume fraction was compared with the previously determined experimental and theoretical data.

2.5 Modeling in AFM

Abrasive flow machining is a new finishing method used for fine finishing of complex and very small flow passages. It includes fluid flow, so the flow characteristics analysis is done to predict the behaviour of the polishing media inside the flow passage. CFD formulations are used to establish the relations between the input parameters and output flow parameters. The flow can be assumed differently basing on input parameters because there are several parameters, which affect the solid-liquid flow inside the work-piece. The particle-laden flow can be assumed as a homogenous multiphase flow if the velocities of both the phases are same and there is no slip velocity. The solid phase can also be assumed as a granular phase and according to that, the granular pressure and other parameters can be analysed. The literature review explains that the modeling of abrasive flow machining is done by using different multiphase models like volume of flow, Eulerian and mixture model. Fang et al. [84] considered the important governing factors in abrasive flow

machining like temperature, viscosity, abrasive hardness, particle sharpness, pressure, piston moving speed, etc. According to their experiment, the effect of temperature is very critical. He did the experiments for different grades of steel and it was observed that with the increase of temperature, the viscosity of media decreased. Increase in number of cycles extensively decreased the material removal and surface roughness. With high viscous media, the material removal efficiency increases initially, but decreases with substantial increase in the number of cycles. The Mooney-viscosity temperature relation of media was used to study the effect of temperature on media viscosity. In order to study the mechanism, a CFD approach into the experiment was done to predict the abrasive particle-moving tendency. A two-dimensional model was constructed to study the effects of viscosity at different extrusion pressures. Tang et al. [85] aimed to improve the surface roughness of precision mould structural surface in finishing using a no-tool precision polishing method based on softness abrasive flow. A zigzag micro channel was taken as the research object and standard k-epsilon turbulence and volume of flow (VOF) model were considered in the analysis. The simulation considered the solid phase as a continuous phase as the particles were very small and in very less amount. The simulation results implied that with an increase in velocity of the media, the efficiency of abrasive flow machining increased, but the effect of finish machining declined. The structure of the channel was also an important factor, which affected the turbulent kinetic energy and axial velocity. Li et al. [86] investigated that the abrasive flow machining was an important finishing process for the precise micro holes. The paper explored the polishing and finishing operation of the common rail tube. They designed the holes of the common rail tube with fixture arrangement and calculated the strength. Finite element analysis of the whole part was done and the flow passage for the abrasive flow machining was prepared. The velocity and pressure profiles were shown at different inlet conditions. The simulations were done differently for different branches. Li et al. [87] gave a CFD analysis on U-tubes, which were generally used in military applications. Its internal surface finish is the governing factor of its performance in the machine on which this is incorporated. Using the results of numerical analysis of the thermodynamic energy balance equation of a two-phase solid-liquid flow, numerical simulations for heat transfer and surface processing for the U-tube was carried out. Using different inlet conditions, the turbulent kinetic energy for different temperature was analysed. The relationship between temperature and turbulent kinetic energy was

analysed at different cross sections. The parameter relationships obtained in this study is used for the determination of optimum parameters of abrasive flow machining. Liu et al. [88] designed the nozzle micro hole and its precision finishing. The nozzle is an important part in oil supply system of the engine. The paper is based on the dynamic design and stress calculation by using a model in a commercial software CATIA followed by finite element analysis of the structure. Lastly, the internal finishing of the micro hole was done by using Fluent. Zheng et al. [89] reported about the micro-cutting in the abrasive flow machining process using the modern technology and proper modeling methods. The solid-liquid flow was analysed to study the turbulence, pressure and velocity for a three dimensional simulation. The simulated results were used for a brief theoretical explanation for abrasive flow machining. Guo et al. [90] proposed a numerical modeling for common-rail pipe. The common rail pipe is used for the injection system and has a number of complex cavities, which require precision finishing operation. The model of the rail-pipe was made using gambit and the fluent analysis was done using mixture model at various inlet and outlet pressures. The pressure variation at different branches of common rail pipe was studied. The pressure and velocity variation in different volume fraction were also studied. A process program was developed at the end. Liu et al. [91] explored the equipment design of the common-rail and analysed the dynamic simulation using ANSYS. The analysis confirmed the stability of the design. The abrasive flow machining experiment was done afterwards to study the influence of viscosity, extrusion pressure, machining time and diameter of abrasive particle on the machining operation. Wan et al. [92] examined a simple, zero-order mechanistic approach towards the analysis of the two-way abrasive flow machining to reduce the time and labour to find the experimental results. The numerical simulation gave a description of a set of coupled models, which considered the fluid flow to be the non-Newtonian flow, and the wall slip was taken into account to study the wall shear-rate. The relative motion between the wall and the media was studied. The model also predicted the stock removal. The simulated results were benchmarked against the experiment with a straight tube with an ellipsoidal cross section. Jhi-Shi Ming et al. [93] aimed at a problem of difficult contact machining for the mini structural surface of the mould-manufacturing using SAFM (soft abrasive flow machining). In this paper a two-phase dynamic model of SAFM was taken into consideration for the analysis, which used Eulerian discrete phase modeling for the precision finishing of the surface. Simulation

results indicated that the ablating surface was influenced by the granular pressure and inlet velocity of the abrasive flow media. Preston equation was established to create a relationship between the granular pressure, the velocity and the material removal rate. Li et al. [94] studied the SAF process further for a U-shape restrained passage using the appropriate frictional coefficients. A k-ε turbulent model and Eulerian multiphase model was used to describe the flow-field and the flow kinetics using the discrete phase model. The pressure distribution at different velocities and the turbulent parameters were studied at different inlet conditions. The solid phase pressures trail at increasing velocity giving a stochastic and random distribution, which is an important parameter for finishing. By analysing the flow parameters, the best area for the finishing was found. Experiments were conducted and found to be good agreement with the analytical data. Wang et al. [95] used a CFD simulation method for getting smooth roughness in passage holes in AFM. The shear forces in the polishing process and the nature of the media plays a vital role in controlling the roughness of the wall. In this case, a power law was established first by using the effects of shear rate in media viscosity and the coefficients of power law were found out of the algebraic equations from the relation between viscosities and shear rate. Applying the equations, the strain rate, the wall shear and the velocities were obtained. The simulation was considered with and without the mould. Various parameters gave the optimal results for the material removed. Venkatesh et al. [96] used ultrasonic assisted abrasive flow machining as a new variant of AFM in which the work piece was subjected to a vibration in orthogonal direction to the media flow. A special type of fixture was designed for the process and piezoelectric actuator provided the vibration. Commercially available simulation tool was used for the analysis of media responses in different machining parameters in terms of pressure, velocity distribution and temperature. The abrasive particles hit the wall at an angle, which affected the basic mechanisms involved, and the effectiveness of the process was increased. The high frequency assisted AFM mainly affected the wall shear more in comparison to the pressure and velocity profiles. It also revealed that the temperature had no effect on the stability of the media. Venkatesh et al. [97] used the ultrasonic assisted AFM for finishing of bevel gears. In the analysis, two simulations were done for conventional AFM and ultrasonic vibration. The pressure, velocity and temperature were studied for both the simulations. A 3D model was prepared for the bevel gear to study the flow on its outer wall using CFD. An experimental trial was done by using the

pressure, velocity and temperature as the input parameters and the material removal, surface finish as the output parameters. It was concluded at the end that the outputs were significantly higher in comparison to conventional machining. Qiaoling et al. [98] considered a variable V-shaped channel for soft abrasive flow machining. Based on Eulerian-Lagrangian multiphase flow model, an analytical method was proposed to describe the optimum parameters for softness abrasive flow machining. The simulation resulted that the variation in the volume fraction had more effects on flow pressure in comparison to velocity. An experiment was carried out to verify the simulation results. Arora et al. [99] studied on enhancing the efficiency of abrasive flow machining through the restricted passage. The material removal efficiency is increased by using various electrical, mechanical and magnetic techniques. The spiral flow assisted abrasive flow machining is a type of AFM process in which a spiral rod rotates inside the work-piece during machining for homogenously finished work-piece. The pressure and velocity distribution using FEM method for spiral assisted AFM for a polymer based media has been analysed. Finite element analysis was done by using software SOLIDWORKS (COSMO-FLO WORKS).

Chen and Cheng [100] developed an analytical model to study the flow of abrasive media in complex passages using CFD-ACE+ software followed by series of experiments to verify the simulated results. The numerical simulation demonstrated that the helical passageways created interactive changes in the velocities in two-axes and resulted in multiple direction motion of the abrasive media. Replacement of a helical passage by a square passage reduced the strain rate deviation from 72 to 40%. A small deviation in the strain rate gives better uniformity in case of a polygonal hole. Experimental results indicated that the helical passageways perform better than polygonal passageways during AFM in terms efficiency and a polishing uniformity was produced in helical passageways than polygonal passageways. Dong et al. [101] studied analytically and developed a model for the viscoelastic fluid having abrasives through a slit flow channel. In the model flow, controlling factors like difference of high visco-elastic fluid abrasives, wall slip, normal stress and cutting coefficient were considered. The variations of wall pressure and wall slip velocities were characterised but the processing characteristics were analysed by using Preston equation. The effects of normal stress, cutting coefficients and viscosity of the fluid on the wall slip were studied. The pressure gradient was found to be constantly up to the critical point

and after that it also increased exponentially. The higher viscosity of the abrasive media is an important reason for the high velocity near the wall. Wang et al. [102] developed a model for the abrasive flow. The flow was assumed to be a non-Newtonian flow and power law was applied to describe the motion of the abrasive fluid. Shear rates and viscosities of different abrasive gels were established by using the software CFD-ACE+. The simulated results were compared with the experimental results. From the simulated results, it was clear that the higher viscosity of the media increased the shear force and deformed the hole to be finished. The strain rate increased, when the media directed through a narrow passage. The results were found to be in a good agreement with the simulated results. Das et al. [103,104] studied the nano-finishing operation using RMRAFF (rotational magneto-rheological abrasive flow finishing). In RMRAFF, the electromagnets are provided a rotational motion and forces the magneto-rheological fluid undergo a rotary motion within the work-piece.

2.6 Need of research

The details of abrasive flow machining process and the exhaustive literature survey indicate that the abrasive flow machining is a fine finishing operation. It is mostly affected by the abrasive media content and the type of abrasive used. The literature survey briefly describes the experimental details carried out on different work piece materials with different input parameters. The papers available for the modeling and simulation of AFM concentrated on some particular process parameters and ignored other parameters. AFM works on the concept of fluid flow. Most of the modeling is based on FLUENT simulation. Noticeable work had been done in the realm of AFM using FLUENT by Fang et al. [84], Jhi shi Ming et al.[93], Wan et al. [92], Wang et al. [102] and Li et al. [94]. The researches are solely based on the flow analysis in the geometry and the study is limited to some parameters, which open up the avenues for downstream applications. The analysis of flow parameters for different abrasive particles and the prediction of the material removal efficiency still lacks behind. This necessitates the study of various flow parameters intensively for different machining conditions and carrier media. The study of flow parameters for different abrasive particles is an important aspect of finishing operation that involves abrasives.

2.7 Conclusion

The chapter entails concise literature survey on the researches done on the present topic and the knowledge gap and the need for more research.

CHAPTER 3

TYPES OF AFM: A BRIEF STUDY

Chapter-3

TYPES OF AFM: A BRIEF STUDY

3.1 Introduction

AFM is a finishing operation used for complex shapes and geometry. The operation and basic mechanism of AFM has been described in the previous chapter. Hybridization of AFM process was started to increase the versatility of the process and to improve the material removal rate as well as surface finish. AFM is associated with magnetic force, vibration, centrifugal force and rotational motion to increase the interaction of the media with the work-piece wall. The hybridization of AFM makes more number of abrasive particles to be exposed to the work-piece wall thereby improving the surface finish. The significant amalgamation of the AFM process and their schematic diagrams of the experimental setups are described in this chapter.

3.2 Magneto-rheological abrasive flow finishing (MRAFF)

Advance finishing processes are those, which include abrasives and magnetic force, magnetic abrasive finishing (MAF), magnetic float polishing (MFP) and magneto-rheological finishing (MRF). In these processes, a magnetic field is used to control the abrading forces and limited to simple geometries. Abrasive flow machining is applicable for both simple as well as complex geometries. The finishing operation in AFM is dependent on the rheological behaviour of abrasive media used. It is not controlled fully by external means. In order to improve the adaptability of AFM process and to have a better control on the rheological behaviour of the polishing media, a new finishing process termed as "Magneto-rheological abrasive flow finishing" was developed by Jha and Jain [67-68]. The magneto-rheological abrasive flow finishing (MRAFF) is the association of magneto-rheological finishing process and (MRF) and abrasive flow finishing process (AFF). Smart magneto-rheological (MR) fluids are used and controlled by external magnetic field.

MRP (magneto-rheological polishing) fluid is a special rheological fluid whose properties can be controlled by external magnetic field. MR-fluid consists of a non magnetic carrier medium like mineral oil, silicon oil or water and the magnetisable particles like carbonyl iron (CIP) along with nonmagnetic abrasive particles are

dispersed in it. In the presence of external magnetic field, the magneto-rheological behaviour of the media is observed. The viscosity of the MRP fluid and the yield stress of the medium can be controlled by controlling the current flowing through the electromagnets placed externally. The CIPs gain dipole moments are proportional to the magnetic strength and they form a chain like structure aligned in the same direction of the applied magnetic field. The abrasive particles are embedded within the CIP chain. The bonding strength between the abrasives and CIPs depend on the volume, size and concentration of abrasives and CIPs. The MRP fluid is extruded back and forth through the work-piece surface in the presence of a magnetic field. The abrading action of the abrasive particles is controlled by varying the magnetizing current and desired finishing is obtained. In the presence of magnetic field, the media behaves as a Bingham plastic with a field dependent shear stress. After removing the magnetic effect, it again acts as a Newtonian fluid.

The MRAFF set up consists of MRPF cylinders with pistons, work-piece fixtures, hydraulic drive, electromagnet, controls and frame as shown in Fig. 4. The primary function of the MRPF cylinder is to contain sufficient quantities of MRPF fluid and extrude it through the piston movement at the desired extrusion pressure. The gap between the electromagnets is kept at 30 mm to obtain higher magnetic field and the work-pieces are fixed at different sizes. The fixture for guiding the MRP fluid into the work-piece is nonmagnetic i.e. stainless steel. The electromagnet is designed for a maximum flux density of 0.6 Tesla. Core diameter is taken higher than the work-piece to avoid magnetic field gradient at the corners. A number of factors such as wire gauge, number of layers, number of turns, coil diameter and geometric factor are tested before arranging the set up. The values taken by Jha and Jain [67] were maximum current = 6A, number of turns = 200, coil diameter = 170 mm, core length =90 mm and cold rolled annealed steel were used as the core material.

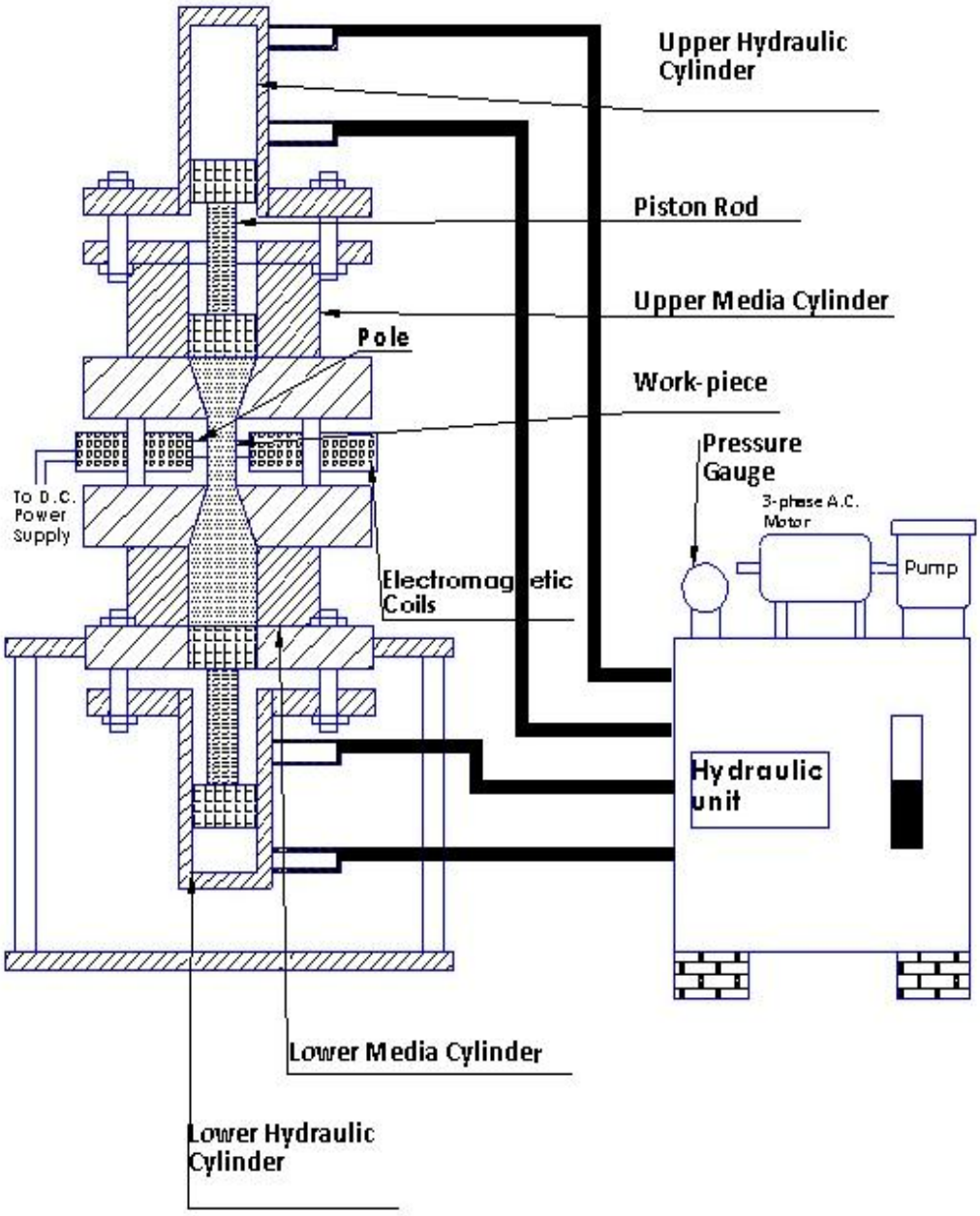

Fig. 4 Schematic diagram of MRAFF experimental set-up by Jha and Jain [67]

There is a significant improvement in surface finish at higher magnetic field. The magnetic field is increased by increasing the magnetizing current. More abrasive action is observed at increasing magnetic field because the CIP chains are able to hold the abrasives tightly at a high magnetic field. Further increase in magnetic field results a bad surface finish because of more depth of indentation of the abrasives.

3.3 Centrifugal-force-assisted abrasive flow machining (CFAAFM)

Centrifugal-force-assisted abrasive flow machining was developed by Walia et al. [54] at IIT Roorkee to provide a centrifugal motion to the media inside the work-piece passage with the help of centrifugal force generating (CFG) rod as shown in Fig. 5.

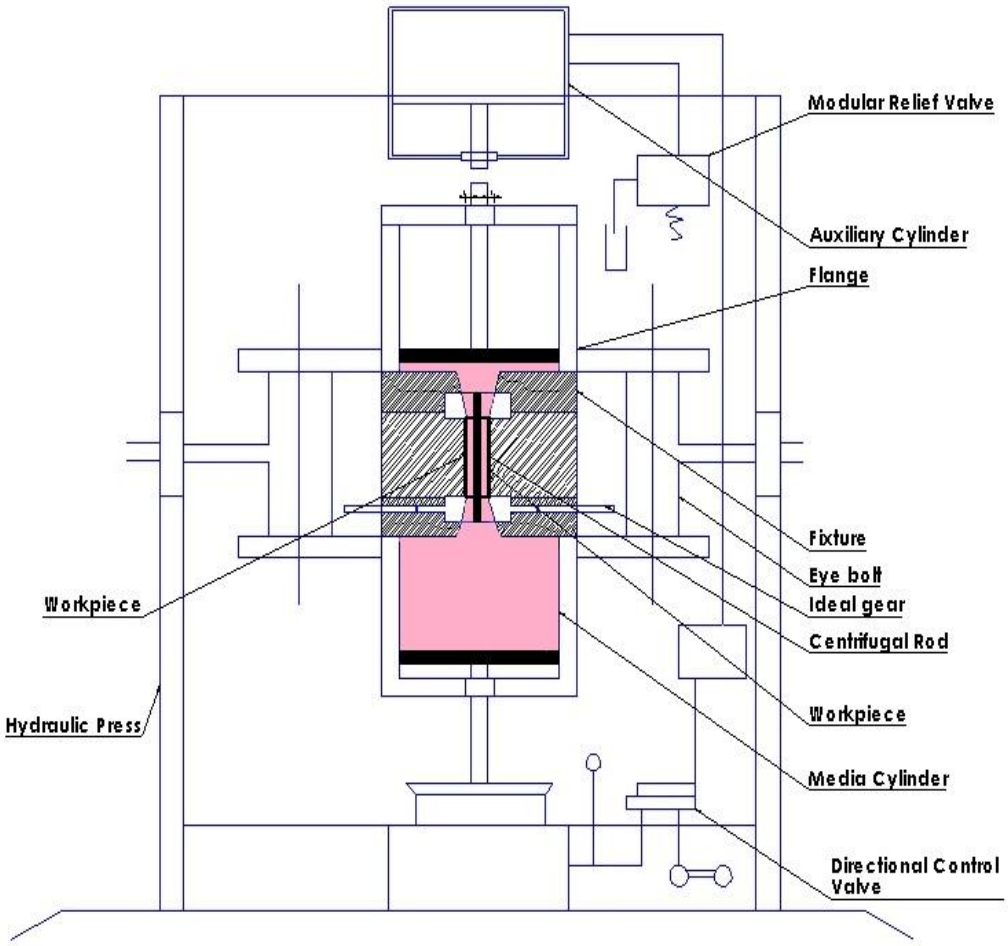

Fig. 5 Schematic diagram of CAAFM experimental set-up by Walia et al. [53]

The fixture used in this process is made of three parts to place the work-piece and CFG rod in position. The media flows through the central hole inside the work-piece. Special drive and attachments are attached to the work-piece as well as the CFG rod to provide required rotational movement of the rod. The rotational movement of the CFG rod develops a centrifugal motion in the media inside the work-piece passage and throws it towards the wall of work-piece thereby developing interaction of more number of abrasive particles on the wall. More particles come in contact with the wall and some particles also indent the work-piece wall at some incident angle. In

CFAAFM, the media is subjected to extrusion pressure as well as centrifugal pressure. Although a significant change in surface micro layer is not found in CFAAFM process, a better surface finish can be achieved at an optimum value of centrifugal force and extrusion pressure. Fig. 5 shows the schematic diagram of CAAFM set-up by Walia et al. [54].

3.4 Rotational abrasive flow finishing (RAFF)

A better surface finishing can be achieved in any abrasive finishing process by imparting a random motion of the abrasive particles. To enhance the finishing action, MRAFF and RMRAFF are used to impose a magnetic field along with a centrifugal force to the medium. Some researchers used a drill bit or spiral rod in the middle of the work-piece to improve the abrasive action, but it was less effective as the force was produced at the centre and it was not enough to increase the random action of the abrasives. In RAFF as described by Ravishankar et al. [17], rotational motion is provided to the work-piece to exert a tangential force on the abrasive grain in contact with the work-piece. A linear motion along the axis of the hydraulic piston as well as a rotational motion of the work-piece wall is imposed upon the abrasive media. The media undergoes a helical motion inside the work-piece and shears off the peaks on the surface in a helical path. The performance of RAFF process depends on the extrusion pressure, number of cycles, medium viscosity and rotational speed of the work-piece. It was verified experimentally that the shearing of surface peaks in case of RAFF is more than that of AFF. The tangential force resulted due to the helical motion assist the radial and axial force in finishing operation.

3.5 Rotational magneto-rheological abrasive flow machining (RMRAFF)

To overcome the limitations by MRAFF and AFF, RMRAFF process was developed. The limitation of MRAFF includes its lower abrasion for hard materials and finishing at a particular region due to the arrangement of the abrasives in the chains of CIP. The whole work-piece surface is not abraded equally. There is a need of interaction of abrasives to a larger area of work-piece surface and reduce the machining time.

In RMRAFF process, a rotational motion is provided to the MRP fluid by a rotating magnetic field so that the abrasive particles interact with a larger area. The reciprocating motion of the MRP fluid by the piston rod along with the rotational motion results in an increase in the material removal rate and decrease in the surface roughness.

The axial motion of the MRP fluid is caused by to and fro motion of the piston rod as it is used for the simple AFM process. The rotational motion is given to the MRP fluid by rotating the permanent magnets. The permanent magnets are associated with the work-piece surface through a magnetic fixture. The magnetic fixture has four slots in 90-degree direction to each other and accommodates four electromagnets. The set up was fabricated by Das and Jain [103]. They maintained a gap of 26 mm between the electromagnets and a distance of 1 mm from the pole tip and work-piece. A variable frequency drive is connected to control the frequency of the motor, which in turn controls the rotation of the permanent magnet. In RMRAFF process, along with the axial force (results due to the axial movement of the media) and radial force (results due to the extrusion pressure) as in AFF, a centrifugal force also acts on the abrasive particle due to the rotational motion of the MRP fluid. The indentation force on the abrasive particle for RMRAFF is the summation of axial force, radial force and centrifugal force. The experimental verifications confirmed that RMRAFF is more efficient than MRAFF in reducing surface roughness. Both RMRAFF and MRAFF are found to be less efficient in finishing a magnetic work-piece as compared to a non-magnetic one. With the increase in rotational speed of the magnet, the surface finish increases, but there is an optimum value of the rotational speed for which surface finish is the best. Fig. 6 shows the schematic diagram of RMRAFF set-up by Das et al. [103, 104].

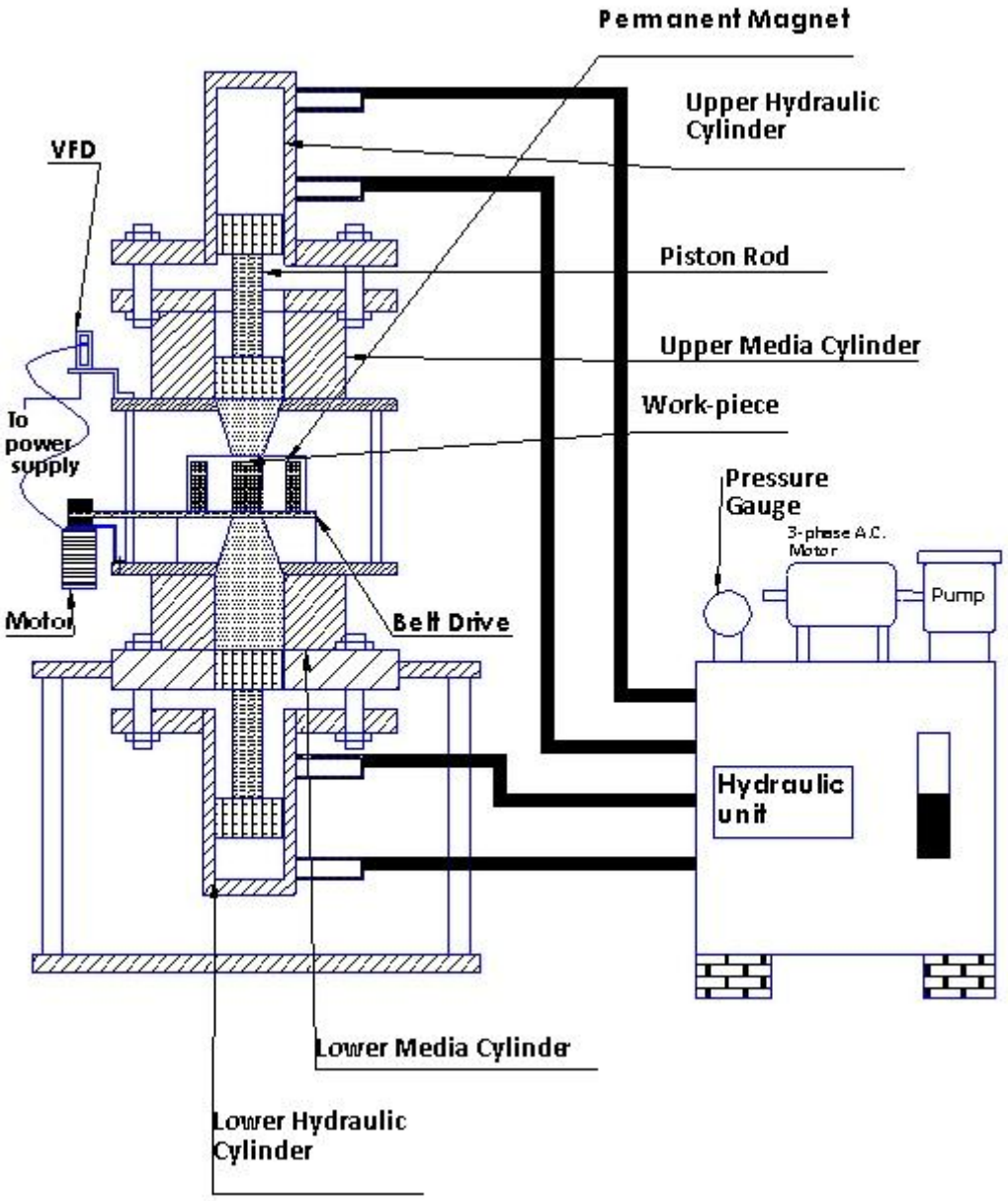

Fig. 6 Schematic diagram of RMRAFF experimental set-up by Das et al. [103]

3.6 Ultrasonic-assisted abrasive flow machining (UAAFM)

Fusion of advanced technical applications to the basic AFM process is made to improve the performance of the finishing. The motive behind the hybridization is to increase the interaction of a number of active abrasive particles on the walls of the work-piece. As the name suggests, a frequency mechanical vibration with a predetermined amplitude and frequency is applied to the work-piece. This process is known as Vibration assisted or Ultrasonic vibration assisted-AFM. Micro-motion is applied to the work-piece controlled by a function generator through a computer. Two

fixture arrangements are provided to the process. One is to accommodate the cylindrical work-piece and the vibrating actuator. Second one is to transmit the vibration from the ultrasonic actuator to the work-piece. The frequency used by Venkatesh et al. [96] was in the range of 0-20 kHz and the amplitude of 10-50 µm. The vibration provided to the work-piece causes a force in a particular pattern, e.g. sinusoidal on the media and abrasives present in the media, get a larger contact surface. Consequently, a larger material removal rate and better surface finish is resulted. An improved surface finish and material removal is observed in UAAFM as compared to AFM. The schematic diagram of UAAFM set-up by Venkatesh et al. [96] is shown in Fig. 7.

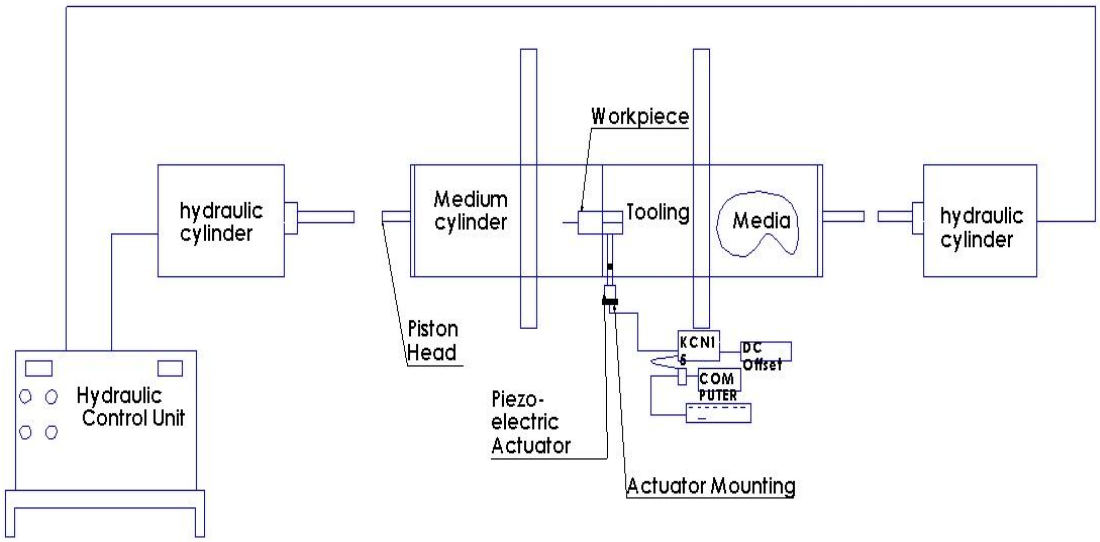

Fig. 7 Schematic diagram UAAFM experimental set-up by Venkatesh et al. [97]

3.7 Conclusion

In the chapter, a brief study has been done on various AFM process and its mechanism and schematic diagram of the experimental set-up is presented using Solid Works. The setups were associated with AFM process to improve the interaction of the more number of active particles on the work-piece wall to increase the abrasion. An increase in the action of abrasive particles increases the surface finish.

CHAPTER 4

CFD MODELING AND ANALYSIS

Chapter-4

CFD MODELING AND ANALYSIS

4.1 Introduction

Computational fluid dynamics (CFD) is advancement in the area of fluid flow analysis that deals with algorithms and numerical methods to simplify and study the critical fluid flow. The last three decades have witnessed a great deal of use of CFD in the industries and problems of practical interest. CFD demonstrates an approximate solution to the fluid through space and time. The approach of CFD is to get the solution using digital computers for thermo-fluid problems. The basis of the approximate numerical solution is the fundamental laws of mass, momentum and energy. Physical principles are expressed either in terms of integral equations or in terms of partial differential equations. Broadly, the steps of CFD are categorized into two major operations such as are the discretization of the governing equation and to obtain the solution by using high-speed supercomputers upto a level of accuracy. Initially CFD was applied for aerospace application by NASA and meteorological applications for weather forecast. Now-a-days CFD is being used for industrial R&D and basic level research. The expansive areas for the use of CFD are chemical industries, aerospace, bio-medical applications, turbo-machineries, energy systems, engines, hydraulics and hydrology. Some commercial codes of CFD are available like ANSYS FLUENT, ANSYS CFX, COMSOL, FORTRAN and STARCD.

4.2 Advantages of CFD

CFD is useful for study of complicated and difficult flow patterns and obtain an approximate solution of desired accuracy. Major advantages of CFD can be classified into five.

(a) Decreases the time required for design and analysis
(b) Flow domains those cannot be verified experimentally can be simulated with the help of CFD
(c) CFD is cost effective in comparison with other experimental tests
(d) Exact and detailed information regarding the simulation is obtained by CFD
(e) CFD is reliable as it is a dependable tool in design and analysis

4.3 Applications of CFD

In a large aspect, CFD is concerned with the areas covering fluid flow and thermal analysis. Recent researches have expanded the range of using CFD. The applications of CFD are assorted as follows:

(a) Aerospace: Design of aerofoils and aerodynamic design of aero parts
(b) Meteorology: Weather forecast
(c) Engines: Combustion in internal combustion engines
(d) Chemical engineering: chemical process and slurry flow
(e) Marine: Design of ships and analysis of wind flow
(f) Turbo-machineries: Hydrodynamic design of different types of turbines, pumps, compressors and blades
(g) Hydraulics: Flow of water through pipes, rivers
(h) Thermal analysis: Heat exchangers, conduction, convection and radiation
(i) Biomedical: Flow of blood through arteries, fluid flow in renal and ocular systems
(j) Energy systems: Nuclear power plant and thermal industries

4.4 Process of numerical simulation using CFD

A physical problem for numerical simulation using CFD includes modeling of geometry, selection of appropriate mathematical model, numerical solution methods, and implementation of algorithms into the computer and analysis of data. The steps can be briefly written as

(a) Model of the geometry of the flow domain
(b) Appropriate mathematical model for the numerical problem
(c) Selection of correct discretization method
(d) Generate the grids and discretize the numerical problem
(e) Choose a solution technique to solve the discretized problem
(f) Proper convergence criteria for the problem
(g) Numerical results for analysis

4.4.1 Geometrical modeling

Geometrical modeling is the initial step in CFD simulation that prepares the flow field for the simulation. Always the geometry is made a simpler one, it is tried to limit the geometry to the area involving flow of fluid, and the finer details in the model are avoided. Intricate details make it difficult to generate grids and simulate.

4.4.2 Mathematical model

The mathematical model is an important aspect of the CFD simulation and the objective of the solution along with the physical conditions are considered in choosing a proper mathematical model. Incompressible Navier Stoke's equation and Euler's equation are applied according to the flow Mach number. The mathematical model selection is also dependent on the accuracy required.

4.4.3 Discretization method

The discretization approaches are used to convert a mathematical model to a discrete system of an algebraic equation. Generally, there are three types of approaches used for the discretization. Finite element method (FEM) is used for the stress analysis, but fluid flows use finite difference method (FDM) and commercial codes of CFD use finite volume method (FVM).

4.4.4 Grid generation

The grids are the discrete representation of the geometrical domain. The geometrical model is discretized into mesh or grids according to the discretization method. It divides the domain into some finite sub-domains. There are two types of grids known as structured and unstructured grids. The FEM modeling prefers structured grids and both the structured and unstructured grids can be used for FVM and FDM with quality checking of the mesh. Structured grids have certain families of grid lines and member of a particular family of grid lines do not cross the lines of other families. Structured grids are used for simpler solutions and distribution of grids is difficult to control. The unstructured grid system is the most flexible one and it can adapt to any complex geometrical boundary. It is easy to run the computer codes for unstructured grids.

4.4.5 Numerical solution

The discretization of the problem leads to a system of discrete equations such as a set of ordinary differential equations in time to unsteady problems and a set of algebraic equations for steady state model. Time integration for initial value problems are applied to unsteady state problems and the differential equations are converted to some algebraic equations. The iterative method is used to get the solution. The solution method is independent of the grid sizes. The accuracy of the solution is determined from the convergence criterion.

4.4.6 Post-processing

The values of field variables are found at from numerical simulation at different computational nodes with respect to space and time. Stress and flux analysis are done for the design analysis. CFD codes provide own post processor for the calculation of the field variables in the form of contours and x-y plots. Further approximation is done by using interpolation of the nodal variables.

4.4.7 Validation

The numerical solution is always validated with the available experimental results. In most of the cases, the simulation is chosen for a problem that has no experimental values and in those cases simulation process is validated for scale model having experimental values. The convergence criteria of the iterative solution are set and the accuracy of the solution is tested. Convergence and residuals for momentum, continuity, turbulence and energy are dependent on the model selected.

4.5 Steps for simulation

The CFD simulation is classified into three important stages such as pre-processing stage, solution stage and post-processing stage. The pre-processing stage includes creation of problem geometry, construction of mesh, selection of model and providing the boundary conditions. Discretization of the equations and solving the problem using an iterative method are included in the solution stage. Post processing stage includes the analysis of the results, i.e. calculation of pressure drop, velocity, forces and heat transfer and plotting of contours and graphs.

4.6 Multiphase models

Multiphase phase flow can be defined as a traceable class of materials that has a particular inertial and dynamic response as well as interaction with the continuous flow field in which it is submerged. The multiphase can be liquid-liquid, liquid-solid, liquid-gas, gas-solid, gas-gas and all the three phases.

4.6.1 Numerical modeling of liquid-solid flow

Three types of flow regimes can be considered for liquid-solid flow. These are slurry flow, hydro-transport and sedimentation.

4.6.2 Approaches to modeling of liquid-solid flow

The multiphase liquid-solid flow can be modeled using two types of multiphase model, i.e. Eulerian model or mixture model. Eulerian model is the most complex among all the multiphase models. It solves n number of momentum and continuity equations. The phase coupling in this case is different for fluid-fluid and fluid-solid flow. In the fluid-solid flow, the granular properties are defined by the help of kinetic theory of gases. The exchange of momentum is also based upon the coupling of phases. Mixture model is also used for two or more phases (fluid or particulate). Mixture momentum equation is solved and relative velocities are assigned to the dispersed phases. It is used to lower particulate loading flow. The mixture models can also assume the granular phase to be a continuous phase for smaller volume fraction in order to solve the equations.

The Eulerian model is computationally unstable and solves many equations. If the exact interphase drag is not known and the computational accuracy is not mandatory, mixture model is applicable as it is computationally stable and less complex.

4.6.3 Coupling between phases

Coupling between phases can be described as the interaction between the phases in multiphase modeling. It is an important aspect for solving equations of continuity and momentum exchange between the phases.

4.6.3.1 One-way coupling

The secondary phase is very less in amount and diluted one. The secondary phase does not affect the continuous phase and moves along with primary phase.

4.6.3.2 Two-way coupling

In two-way coupling, sufficient numbers of particles are present in the carrier phase and the momentum exchange occurs between the two phases. The drag and turbulence of the dispersed phase affect the dynamics of the continuous phase.

4.6.3.3 Four-way coupling

Four-way coupling is applicable for dense fluidized bed as the interaction of the particulates with the continuous phase along with the particles is considered in this case. Viscous forces and the particle pressure are resulted from the particle interaction.

4.6.4 Overview of mixture model

Mixture model is a simplified substitution of the complex Eulerian model and phases may move at different velocities assuming local equilibrium. As an Eulerian multiphase model, mixture model also solves n number of continuity, momentum and energy equations. It also solves equations for volume fraction of secondary phases. The mixture model has also some limitations and those are as follows

(a) The mixture model is applicable only for pressure-based solver
(b) The specified mass flow rate for streamline periodic flow cannot be modeled using mixture model
(c) It is difficult to track particles in discrete phase model (DPM) along with the mixture model
(d) Melting and solidification are not modeled using mixture model
(e) Inviscid flow is not modeled in mixture model
(f) Interpenetrating phases are allowed in mixture model
(g) Slip velocity option can be opted in mixture model to provide different velocities to the phases

The governing equations such as continuity, momentum, volume fraction and solid pressure of the mixture model are as follows

4.6.4.1 Continuity equation

The continuity equation for the mixture is given by

$$\frac{\partial}{\partial t}(\rho_m) + \nabla.(\rho_m \vec{\upsilon}_m) = 0 \tag{1}$$

where $\vec{\upsilon}_m$ is the mass-averaged velocity and ρ_m is the mixture density.

$$\vec{\upsilon}_m = \frac{\sum_{k=1}^{n} \alpha_k \rho_k \vec{\upsilon}_k}{\rho_m} \tag{2}$$

$$\rho_m = \sum_{k=1}^{n} \alpha_k \rho_k \tag{3}$$

4.6.4.2 Momentum equation

The momentum equation for the mixture is obtained by adding up all the individual momentum equations of all the phases.

$$\begin{aligned} &\frac{\partial}{\partial t}(\rho_m \vec{\upsilon}_m) + \nabla.(\rho_m \vec{\upsilon}_m \vec{\upsilon}_m) = \nabla p + \nabla.\left[\mu_m \left(\nabla \vec{\upsilon}_m + \nabla \vec{\upsilon}_m^{T}\right)\right] \\ &+ \rho_m \vec{g} + \vec{F} + \nabla.\left(\sum_{k=1}^{n} \alpha_k \rho_k \vec{\upsilon}_{dr,k} \vec{\upsilon}_{dr,k}\right) \end{aligned} \tag{4}$$

where, n is the number of phases, $\vec{F}$ is the body force and μ_m is the viscosity of the mixture

$$\mu_m = \sum_{k=1}^{n} \alpha_k \mu_k \tag{5}$$

$$\vec{\upsilon}_{dr,k} = \vec{\upsilon}_k - \vec{\upsilon}_m \tag{6}$$

$\vec{\upsilon}_{dr,k}$ is the drift velocity of secondary phase k.

4.6.4.3 Energy equation

Energy equation of the mixture model is given by

$$\frac{\partial}{\partial t}\sum_{k=1}^{n}\left(\alpha_k \rho_k E_k\right) + \nabla.\sum_{k=1}^{n}\left(\alpha_k \vec{\upsilon}_k\left(\rho_k E_k + p\right)\right) = \nabla.\left(k_{eff}\,\nabla T\right) + S_E \tag{7}$$

k_{eff}. is the effective conductivity

4.6.4.4 Volume fraction equation for the secondary phase

$$\frac{\partial}{\partial t}\left(\alpha_p \rho_p\right) + \nabla.\left(\alpha_p \rho_p \vec{\upsilon}_m\right) = -\nabla.\left(\alpha_p \rho_p \vec{\upsilon}_{dr,p}\right) + \sum_{q=1}^{n} \dot{m}_{qp} - \dot{m}_{pq} \tag{8}$$

4.6.4.5 Fluid-fluid exchange coefficient

For fluid-fluid flows, the secondary phase is assumed to act as small bubbles. Between the two fluids, the fluid having lower volume fraction is assumed to be droplets and the predominant phase is assumed to be primary phase or carrier phase. The exchange coefficient for fluid-fluid, gas-fluid and gas-gas is considered the same and the formula written as

$$k_{pq} = \frac{\alpha_p \rho_p f}{\tau_p} \tag{9}$$

where k_{pq} is the exchange coefficient, α_p is the volume fraction of secondary phase, f is the drag function and τ_p is the particulate relaxation time.

The particulate relaxation time is given by

$$\tau_p = \frac{\rho_p d_p^2}{18\mu_q} \tag{10}$$

d_p is the diameter of the fluid droplets for the secondary phase

The drag function f includes a drag coefficient. The default value of fluid-fluid drag is given by Schiller-Naumann

$$f = \frac{C_D R_e}{24} \tag{11}$$

C_D is the drag coefficient and R_e is the Reynolds number

4.6.4.6 Fluid-solid exchange coefficient

The general form of fluid-solid exchange coefficient is given by

$$k_{sl} = \frac{\alpha_s \rho_s f}{\tau_s} \tag{12}$$

k_{sl} is the fluid-solid exchange coefficient, f is different in this case and the formula varies according to different models used.

$$\tau_p = \frac{\rho_p d_p^2}{18\mu_s} \tag{13}$$

d_s is the diameter of particle phase s.

Syamlal-O'Brien model is used when the exact drag between fluid-solid is not known and it is used if the particle loading is low and secondary phase is not dense in the media. f, the drag function is written as:

$$f = \frac{C_D \, Re_s \, \alpha_l}{24 \upsilon_{r,s}^2} \tag{14}$$

The coefficient of drag, C_D, is given by

$$C_D = 0.63 + \frac{4.8}{\sqrt{Re_s / \sqrt{\upsilon_{r,s}}}} \tag{15}$$

In the above equations, the l is for the l^{th} fluid phase, s is for the s^{th} solid phase and d_s is the diameter of s^{th} solid phase particles.

4.6.4.7 Granular properties

The effective viscosity of the mixture is calculated from the concentration of the particles. For a granular phase, the granular viscosity is calculated to know the viscosity of the suspension. A shear viscosity arises because of translation and

collision of the particles. The volume-weighted average of the viscosity is calculated for the shear viscosity.

Shear viscosity is the summation of collisional and kinetic viscosity along with frictional viscosity.

$$\mu_s = \mu_{s,col} + \mu_{s,kin} + \mu_{s,fr} \tag{16}$$

μ_s, $\mu_{s,col}$,$\mu_{s,kin}$ and $\mu_{s,fr}$ are shear viscosity, collisional viscosity, kinetic viscosity and frictional viscosities respectively.

The collisional viscosity of the shear viscosity is given by

$$\mu_{s,col} = \frac{4}{5}\alpha_s \rho_s d_s g_{0,ss}(1+e_{ss})\left(\frac{\theta_s}{\pi}\right)^{1/2}\alpha_s \tag{17}$$

The kinetic viscosity in this case is given by default expression by Syamlal et. al [105] because it is used for lower particle loading and the cases in which the fluid-solid drag is not known. The expression by Gidaspow [106] is used for dense fluidized beds. The particle loading for the abrasive flow in AFM is less than the maximum particle concentration and the exact drag is not known in this case. So, the Syamlal et. al. [105] kinetic viscosity formula is used in this case.

$$\mu_{s,kin} = \frac{\alpha_s d_s \rho_s \sqrt{\theta_s \pi}}{6(3-e_{ss})}\left[1+\frac{2}{5}(1+e_{ss})(3e_{ss}-1)\alpha_s g_{0,ss}\right] \tag{18}$$

4.7 Conclusion

The above steps were used in FLUENT modeling and the equations were used in simulation of the mixture model.

CHAPTER 5

FLOW ANALYSIS OF AFM FOR A 2D MODEL

Chapter-5

FLOW ANALYSIS OF AFM FOR A 2D MODEL

5.1 Introduction

The mathematical representation of the flow media in AFM process involves the equations of continuity, momentum and constitutive equations. To analyze the media flow, CFD simulation is done. There are several commercial software packages those include simulation of fluid flow. In the present work, the simulation is done using commercially available ANSYS FLUENT. The work-piece considered for the present simulation, is a cylindrical one according to the dimensions given by Ravishankar et al. [15]. The hole diameter in this case was taken 10 mm which is 13.4 mm in the experiment done by Ravishankar et al. [15]. It was taken so to avoid a non-standard dimension of the hole. But later on, in the chapter of validation, the another hole diameter 13.4 mm was taken for the purpose. The solution has been done by using a multiphase mixture model and the flow is assumed to be in steady state, laminar and incompressible one. The fluid is assumed as a Newtonian fluid. The flow is modeled for only one stroke. The carrier media used in this case is a highly viscous one and extruded with the help of a piston, so the effects of the force of gravity is neglected. When a fluid is flowing through a closed channel such as pipe or between two flat plates, the flow may be taken as laminar or turbulent depending upon the velocity. Laminar flow is taken into consideration, when fluid flows in parallel layer; no disruption of layers and the velocity is lower. The media flow speed is very low in this case. Incompressible flow refers to a flow in which the material density is constant with the fluid flow. The model is validated with the benchmark experiments in chapter 7. In the present work, the flow analysis of the 2D model is done based on the theories of strain rate, dynamic pressure and velocity. The material removal efficiency is predicted based upon the theories. Fang et al. [84] studied the effects of media viscosity and extrusion pressure on the dynamic pressure and velocity earlier. An analysis on the effects of volume fraction and media flow speed of the secondary phase has been done in the present chapter.

5.2 Geometry and mesh

A 2D axisymmetric model of the Fig. 8 is developed for the CFD simulation. The meshed model of the work-piece and fixture is designed in 2D. The flow regime is considered from the abrasive cylinder along with the constricted passage of the work-piece. The abrasive particles are tiny and present in fine powder form because AFM is used for polishing operation. Some authors assumed the carrier media along with the abrasives as a continuous one because the size of the particle is very small. In some literatures, the phase was also considered as a granular discrete phase. In the present 2D model, the abrasive particles for the analysis are assumed as a continuous phase. The abrasive particles act as bubbles inside the fluid. A pressure based solver and steady formulation is taken for the purpose. The axisymmetric flow domain created after the meshing is shown in Fig. 9.

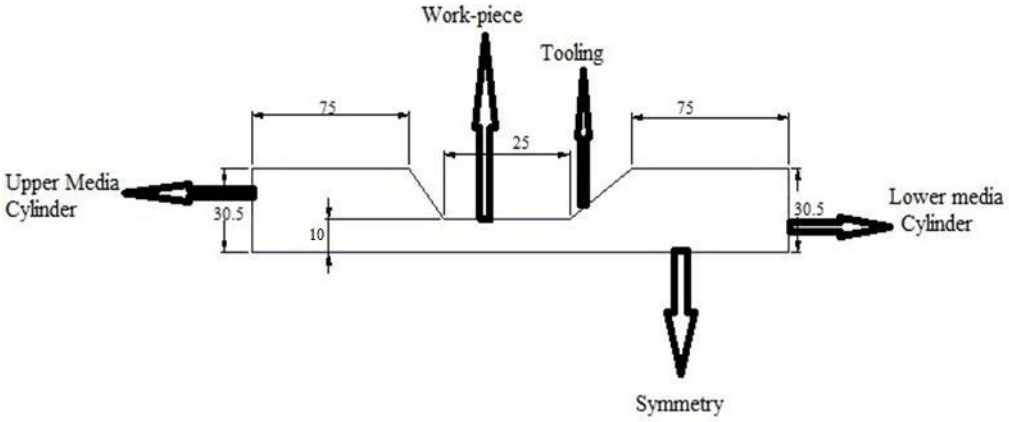

Fig. 8 Symmetrical geometry taken up for the simulation (all dimensions in millimetres)

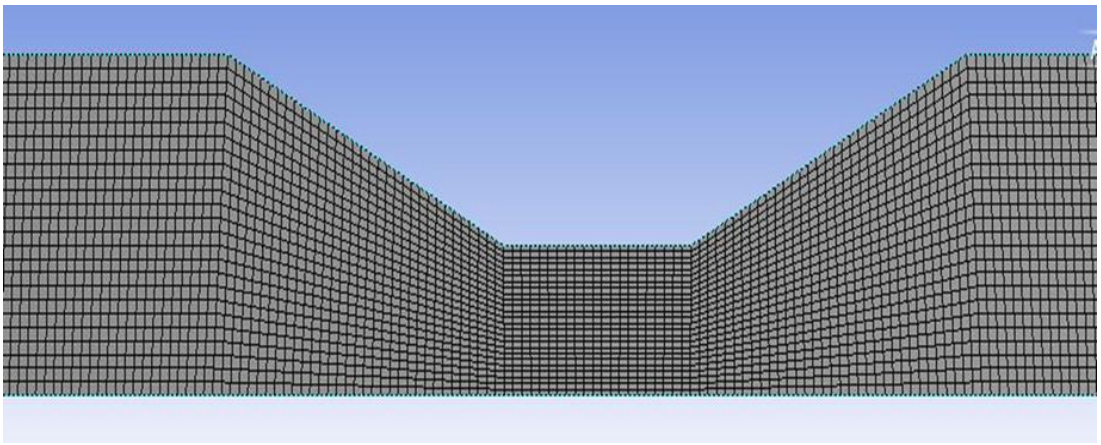

Fig. 9 Meshing of 2D computational domain

5.3 Simulation details

The simulation of the 2D model is done using a multiphase mixture model for two phases and the secondary phase is taken as a continuous phase. From the literature survey, it is clear that the carrier media of the abrasive particles can be of different types having different viscosity values. The base media can be a natural polymer, silly putty or styrene butadiene rubber along with the plasticizer. The viscosity of the media varies in a wide range. The carrier media in the present chapter is having a viscosity value 789 Pa.s. The viscosity value is selected from the FLUENT simulation of abrasive flow machining process by Li et al. [86]. The viscosity value of the media may change according to the proportion of the silly putty and the oil or the plasticizer. The carrier media behaves as a Newtonian fluid [1, 96]. The size of the abrasive is selected to be 150 µm [3]. The solid phase is present in very small volume fraction and the size of the particles is of few microns. The size of the particle is also selected after brief literature survey. The size of the particle varies between 70-165 microns in the literatures. The present chapter is based on the theories of dynamic pressure given by Fang et al. [84] and the strain rate theory. The effects of these two factors have been discussed briefly. Operating pressure for the simulation was 101325 Pa. The inlet is taken as the pressure inlet to study the effects of volume fractions of abrasive particles and velocity inlet to study the effects of media flow speeds.

5.3.1 Assumptions of the analysis

- The media used for AFM is a mixture of semisolid carrier and abrasive particles with linear viscous properties.
- The media is isotropic and homogenous.
- The properties of the media are independent of temperature and are constant with respect to time and space.
- The media flow is taken as axisymmetric for the 2D geometry.

The flow governing equations for continuity and momentum are given in chapter 4.

5.4 Grid independence test

The grid independence test is essential because the results of the numerical analysis are dependent on the grid size and number of grids. With an increase in the

number of cells (control volumes), the error tends to be less and the time required for convergence increases. Refinement of the grid is not needed after the grid independence is achieved. A grid independence test has been carried out for the 2D geometry. Five types of grids are designed to observe the variation in the numerical results. The static pressure variation is observed at a particular point in the flow domain for the five grid sizes, i.e. 1905, 2397, 3380, 4656 and 5275. The value of static pressure varies significantly for 1905 number of cells. There is no variation in the flow parameters within 2397- 5275 numbers of cells and the value is found to be constant. The grid size having 3380 number of cells is taken into account for simulation. The variation of static pressure with grid numbers is shown in Fig. 10.

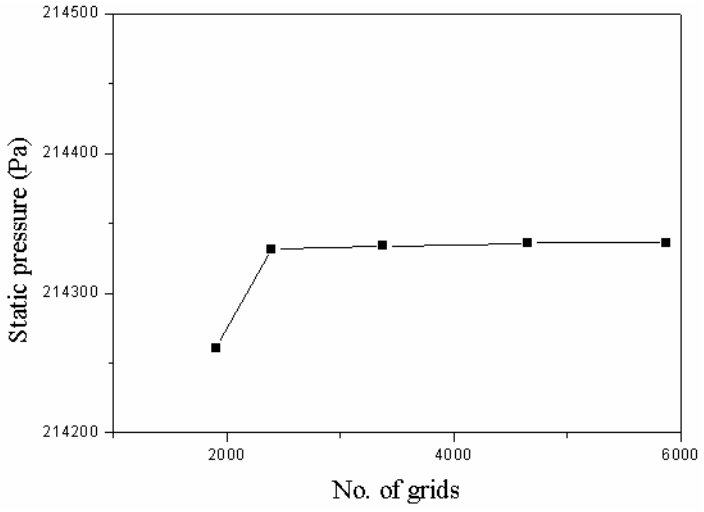

Fig. 10 Variation of Static pressure with respect to number of grids for the 2D model

5.5 Results and discussion

AFM is a precision finishing process and it is affected by process variables like extrusion pressure, velocity of media flow, viscosity of media, concentration of abrasives and size of the abrasive particles. The mathematical modeling as well as the CFD simulation for different process variables are analysed to predict the material removal efficiency. There are various theories proposed to predict the polishing action and material removal efficiency of the process based on tribology and fluid dynamics. It is difficult to determine the effects of all the parameters experimentally. The exact interphase laws during the abrasive action in AFM process are not known. The theories are based on some assumptions and concentrate on particular parameters that affect the abrasion extensively. The flow analysis using FLUENT helps to anticipate

the outcomes of the process variables. The flow outputs are studied to predict the abrasion. The details of the variables studied, are given below.

Strain rate tensor that macroscopically describes the rate of deformation of a material in the neighbourhood of a certain point at a particular time. In case of fluids, gradual change in its deformation gives rise to viscous forces in its interior, due to friction between adjacent fluid elements that tend to oppose the change. The viscous stresses are determined completely by the strain rate tensor and some intrinsic fluid properties. The viscous stress and the deformation are dependent on the velocity and fluid properties. The increase in rate of change of the fluid layers increases the active number of particles, increasing the material removal efficiency. Although the strain rate does not depend on the material of the solid and force applied directly, it is affected by the fluid viscosity and concentration. The strain rate of a two-phase fluid is changed according to the concentration of the secondary phase. In the present study, it can be written that the strain rate is the deformable value per unit time of the abrasive medium in the polished area. Larger strain rates in a particular area lead to larger abrasive force on that area [95].

On the profile of an abrasive particle, total pressure in the tunnel is the load acting in normal direction and the horizontal driving force is transferred by the carrier media. The analysis of a single grain shows that the force acting upon a particle is the resultant of four forces acting together. First one is the force acting in the normal direction that is produced by the cylindrical pressure and the second one is the horizontal force caused by the media flow. Other two forces are the resistive forces offered by the wall and the deformation force. The horizontal driving force by the media flow is the important one to study the particle movement as well as the behaviour. It can be predicted by analysis of the velocity and pressure of the abrasive media. The total pressure in the AFM flow passage can be resolved into two parts those are static pressure and dynamic pressure. The static pressure is responsible for the flow of the media through the passage and the dynamic pressure is important to study particle rolling. The static pressure and dynamic pressure are significant controlling parameters for estimation of horizontal force as described by Fang et al. [84]. Dynamic pressure distribution is not same as the static pressure inside the flow passage. Dynamic pressure variation is in a direction normal to the flow direction while static pressure varies along the direction of flow. The static pressure is

considered to be the load acting upon the particle and sliding motion of the particle is the result of this static pressure. The dynamic pressure is considered to be the driving factor for particle rolling because of a large normal pressure gradient. Increase in particle rolling decreases the material removal efficiency [84]. If the contours of dynamic pressure are closely observed, it approaches to zero as a limit from maximum in the near wall region (Fig. 11). Therefore, it can be assessed that the horizontal force acted by media is different in accordance with the specimen surface.

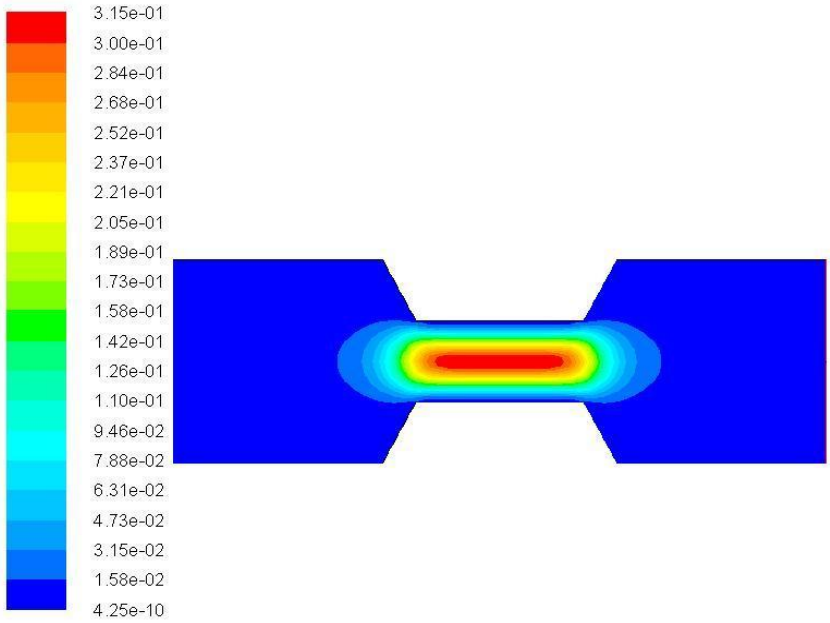

Fig. 11 Dynamic pressure contour (in Pa)

The colour bar on the left side indicates the related pressure value with different colour blocks in pascal. Red colour shows the maximum pressure and blue colour shows the minimum pressure.

Similarly, increase in horizontal velocity is same as the increase in dynamic pressure. An increase in velocity gradient strengthens particle rolling. The horizontal flow velocity along with the dynamic pressure is considered the vital factors to study the particle rolling. According to Fang et al. [84], the particle will roll instead of sliding if flow criterion is satisfied. The ratio of material yield resistance to the normal load is equal to the ratio of the frictional coefficient of rolling of the particle to the actual frictional coefficient. So, the material removal efficiency decreases with the increase in particle rolling. The material removal efficiency is predicted at different inlet parameters. In the simulation, the flow velocity is observed to study the rolling of the

particles only. The assumptions for the FLUENT simulation are taken according to the theories of material removal efficiency considered and a no-wall slip boundary condition is taken for convenience..

The concept of strain rate and dynamic pressure are two contradictory statements. The significance of the parameters according to the flow simulation is discussed in the next two segments.

5.5.1 Effects of volume fraction of secondary phase

The effects of volume fraction of abrasive particles on parameters like dynamic pressure, horizontal velocity and strain rate are plotted keeping other parameters constant. The simulation parameters are shown in Table 1.

Table 1 Simulation parameters for variable volume fraction

Parameters	**Values**
Primary phase	Polyborosiloxane, density-1219 kg/m^3, viscosity-789 kg/m-s
Secondary phase	Silicon carbide, density-3170 kg/m^3
Diameter of secondary phase	150 µm
Inlet pressure	2.5 MPa
Volume fraction of secondary phase	0.2, 0.25, 0.3, 0.35, 0.4, 0.45, 0.5

Drag coefficient is given by Schiller-naumann because the secondary phase is assumed as fluid or continuous phase for this simulation. The variations of dynamic pressure, velocity and strain rate are plotted in the radial direction in the middle position of the flow domain (constricted portion of the geometry). The graphs of velocity and dynamic pressure are plotted for both the symmetric section of the geometry to observe the pattern of the curve. The strain rate is plotted from the wall towards centre for only one symmetric section. The volume fractions of the secondary phase are indicated in the graphs and the contours are plotted for the same. The contour plots for a single volume fraction is shown for every parameter because the distribution is similar for all the volume fractions.

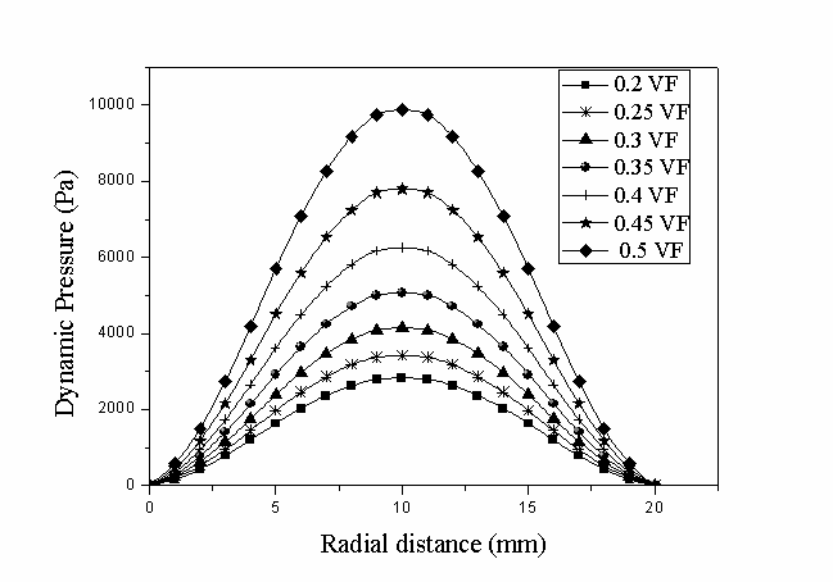

Fig. 12 Variation of dynamic pressure with respect to radial distance from wall

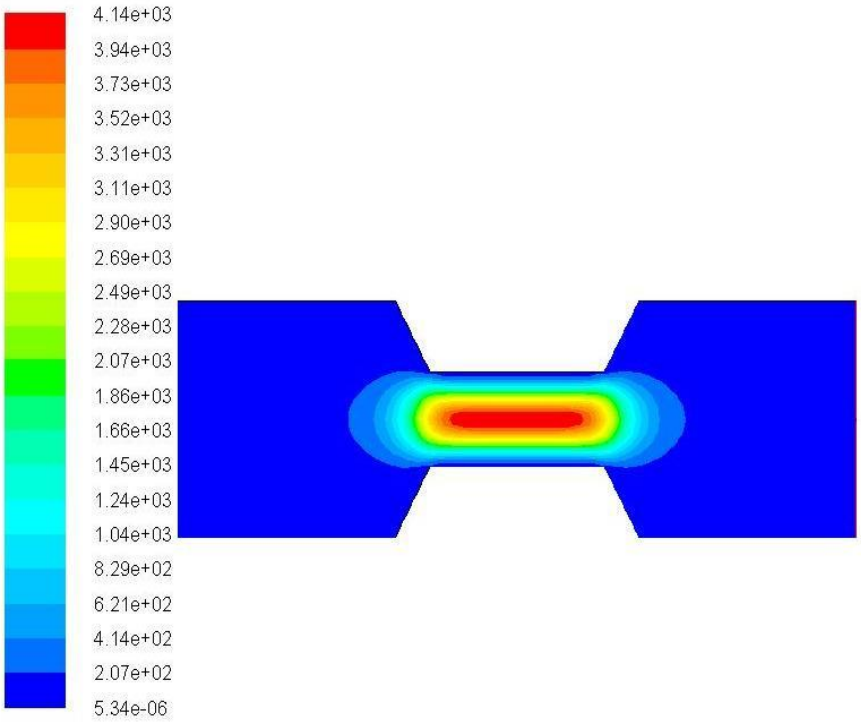

Fig. 13 Contour of dynamic pressure in Pa for volume fraction 0.3

The graph from Fig. 12 depicts that the dynamic pressure value is maximum in the centre of flow domain and decreases in the near wall region. The dynamic pressure increases with the increase in volume fraction of the secondary phase. The variation of dynamic pressure is more uniform upto 0.35 volume fraction, but the non-uniformity increases for the volume fraction more than 0.35. The colour blocks in the

contour plot (Fig. 13) for the volume fractions 0.3 give a clear image regarding the distribution of the dynamic pressure in the flow area. The maximum value of dynamic pressure for 0.3 volume fraction is 4.14×10^3 Pa in the centre of the constriction. The value gradually decreases towards the wall. It is inferred from the above graphs and contours that the rolling tendency of the particles is maximum at the centre due to the high value of dynamic pressure and the particle rolling decreases in the near wall region. The dynamic pressure is found to increase with the increase in volume fraction.

The strain rate for the different volume fractions are plotted in the radial direction in the centre of the flow domain. The contours for strain rates are shown to observe the exact values of strain rate at different positions of the work-piece.

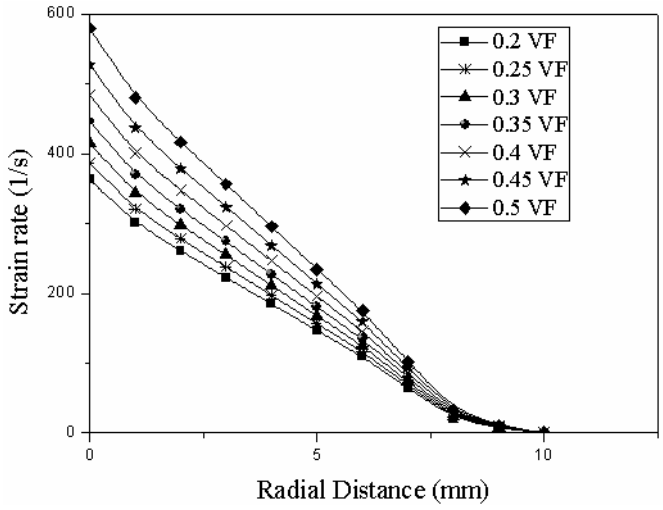

Fig. 14 Variation of strain rate with respect to radial distance from the wall

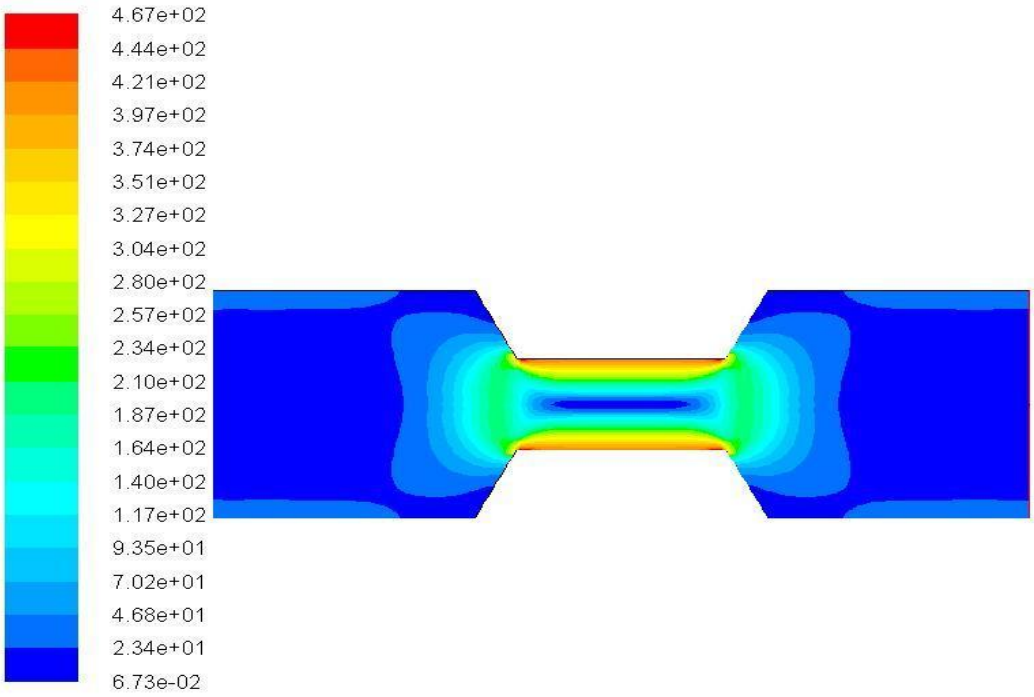

Fig. 15 Contour of strain rate in s^{-1} for volume fraction 0.3

The graph in Fig. 14 gives the strain rate distribution at different volume fraction in the radial direction of the flow domain. The strain rate increases from the centre towards the wall and the values increase with increase in volume fraction. The increase in strain rate increases the deformation per unit time and shear stress in the near wall region. Maximum strain rate is observed on the wall of the constriction. More strain rate in the narrow passage increases the abrasive force and polishing action. The maximum strain rate from the contour plot in Fig. 15 for 0.3 volume fraction is 4.67×10^{2} s^{-1}.

The velocity variation for different volume fraction has been plotted in the radial direction in the centre of the constriction. The velocity contour for 0.3 volume fraction of secondary phase is shown.

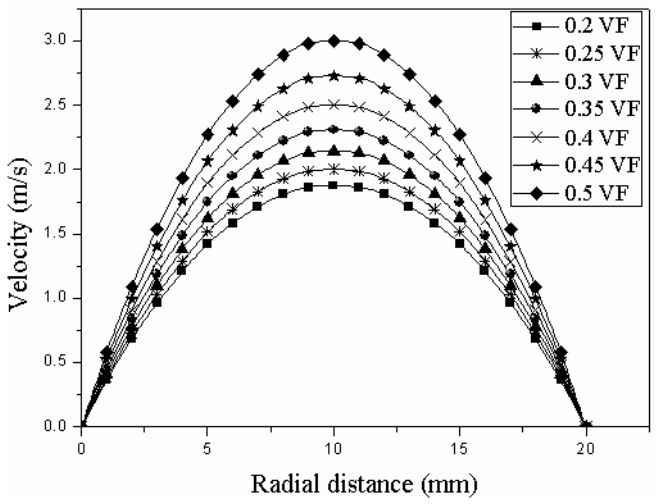

Fig. 16 Variation of velocity with respect to radial distance from the wall

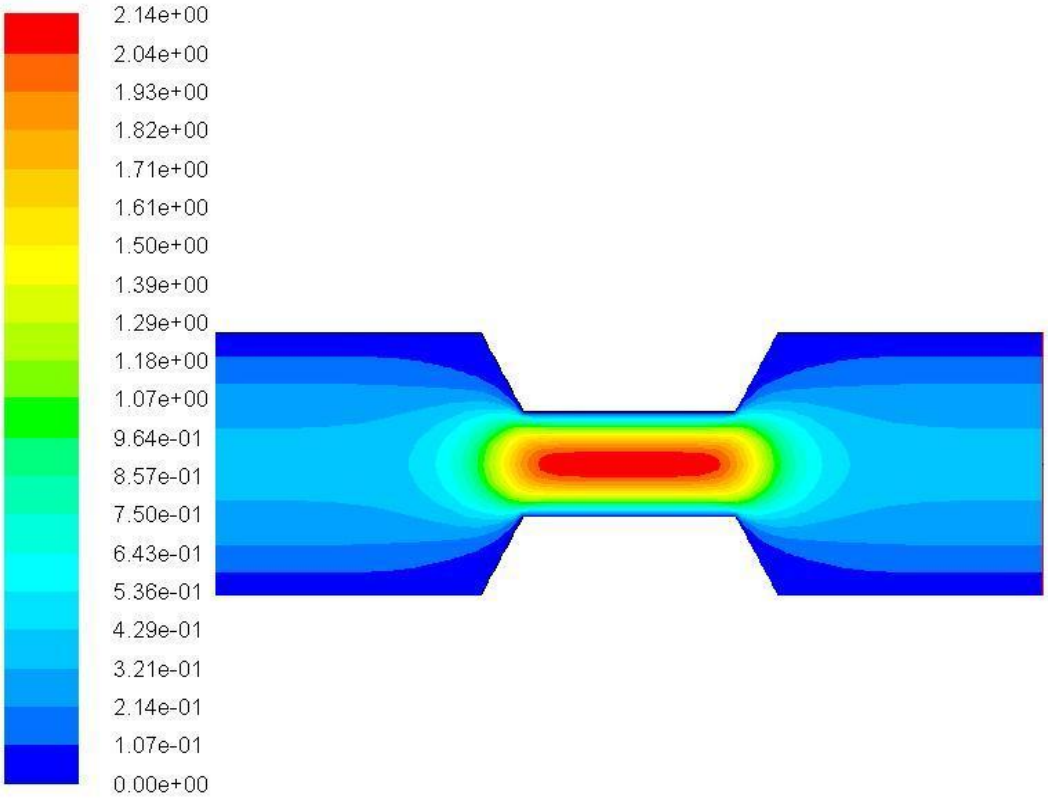

Fig. 17 Contour of velocity in $m.s^{-1}$ for volume fraction 0.3

The velocity graph in Fig. 16 illustrates that the velocity is maximum at the centre of flow domain and it decreases towards the wall. The increase in volume fraction of the secondary phase tends to increase the magnitude of velocity. An increase in velocity increases the velocity gradient leading to an increase in shear stress. The contour plot

(Fig. 17) of the velocity shows that the maximum value of the velocity is at the centre of flow area. The maximum value of velocity is 2.14 m/s for 0.3 volume fraction.

The flow analysis for variable volume fraction of the abrasive particles gives a better view on the simulation results like dynamic pressure, velocity magnitude and strain rate. The dynamic pressure is maximum at the centre, but it decreases towards the wall, decreasing the rolling tendency of particles. AFM is a finishing operation and the values in the near wall region are taken into account. The dynamic pressure and velocity for different volume fractions increase with the increase in volume fraction, but the effects of both the parameters are less or negligible in the near wall region. To predict the polishing action, the strain rate is taken into consideration in comparison to the effects of dynamic pressure and velocity. The strain rate is maximized near the wall of the narrow work piece surface. Larger strain rate results in larger abrasive force and increases in number of active particles. There is a uniform variation of the strain rate at different volume fraction unlike that of the dynamic pressure and velocity. MRR has been determined by experiments [5], [8]. The volume fraction of the secondary phase is increased to increase the material removal rate in the experiments. The experiments depict that the increase in concentration of abrasive above 60 % causes more wear and affects the final surface finish.

5.5.2 Effects of media flow speed

The effects of flow speed of media on parameters like dynamic pressure, horizontal velocity and strain rate have been plotted keeping other parameters constant. The simulation parameters are given in Table 2.

Table 2 Simulation parameters for variable media flow speed

Parameters	Values
Primary phase	Polyborosiloxane, density-1219 kg/m^3, viscosity-789 kg/m-s
Secondary phase	silicon carbide, density-3170 kg/m^3
Diameter of secondary phase	150μm
Inlet velocity	0.00068 m/s, 0.0086 m/s, 0.011 m/s, 0.014 m/s
Volume fraction of secondary phase	0.35

The variation of dynamic pressure, velocity and strain rate is plotted in the radial direction in constricted portion of the geometry.

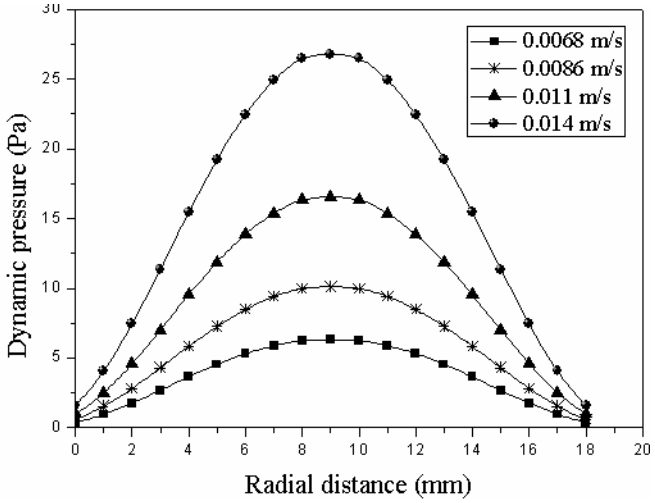

Fig. 18 Variation of dynamic pressure with respect to radial distance from the wall

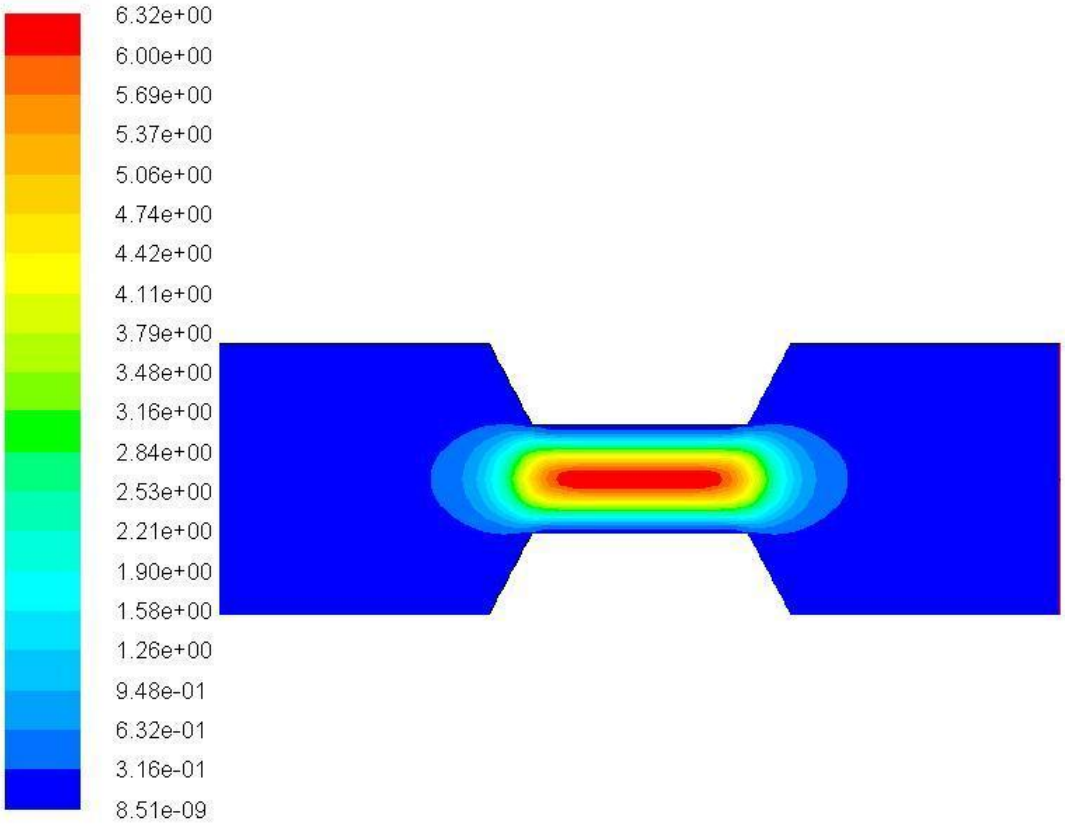

Fig. 19 Contour of dynamic pressure in Pa at media flow speed of 0.0068 m/s

Referring to Fig. 18, there is an increase in dynamic pressure with the increase in media flow speed. The contour of dynamic pressure is shown in Fig. 19. The value of dynamic pressure is maximum at the centre of the constricted passage and it gradually decreases towards the wall. The maximum value of dynamic pressure for media flow speed 0.0068 m/s is 6.32 Pa.

Variation of strain rate with respect to radial distance is shown in Fig. 20. The strain rate increases with the increase in media flow speed. Strain rate tensor in case of fluid is a shear stress and proportional to the macroscopic velocity. Increase in strain rate among the adjacent fluid layers increases the abrasion and activity of the abrasive particles. The distribution of strain rate is shown in contour plot (Fig. 21). The maximum value of strain rate for 0.0086 m/s is 19.0 s^{-1}.

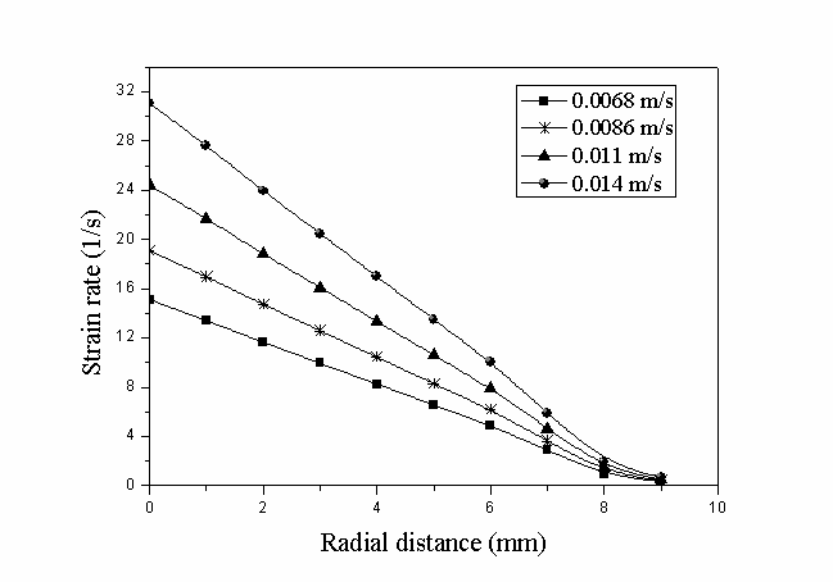

Fig. 20 Variation of strain rate with respect to radial distance from the wall

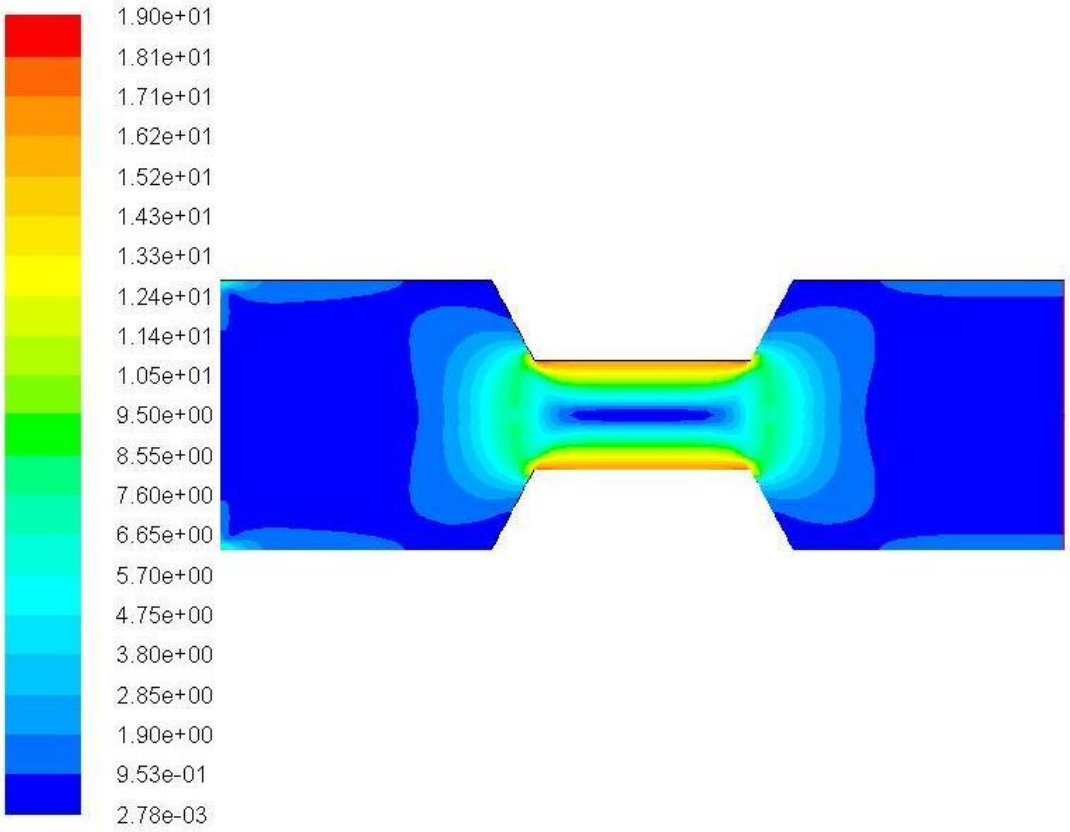

Fig. 21 Contour of strain rate in s^{-1} at media flow velocity 0.0086 m/s

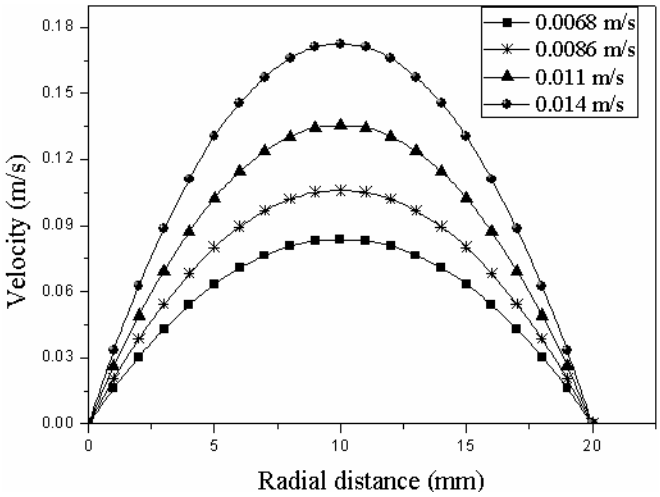

Fig. 22 Variation of velocity with respect to radial distance from the wall

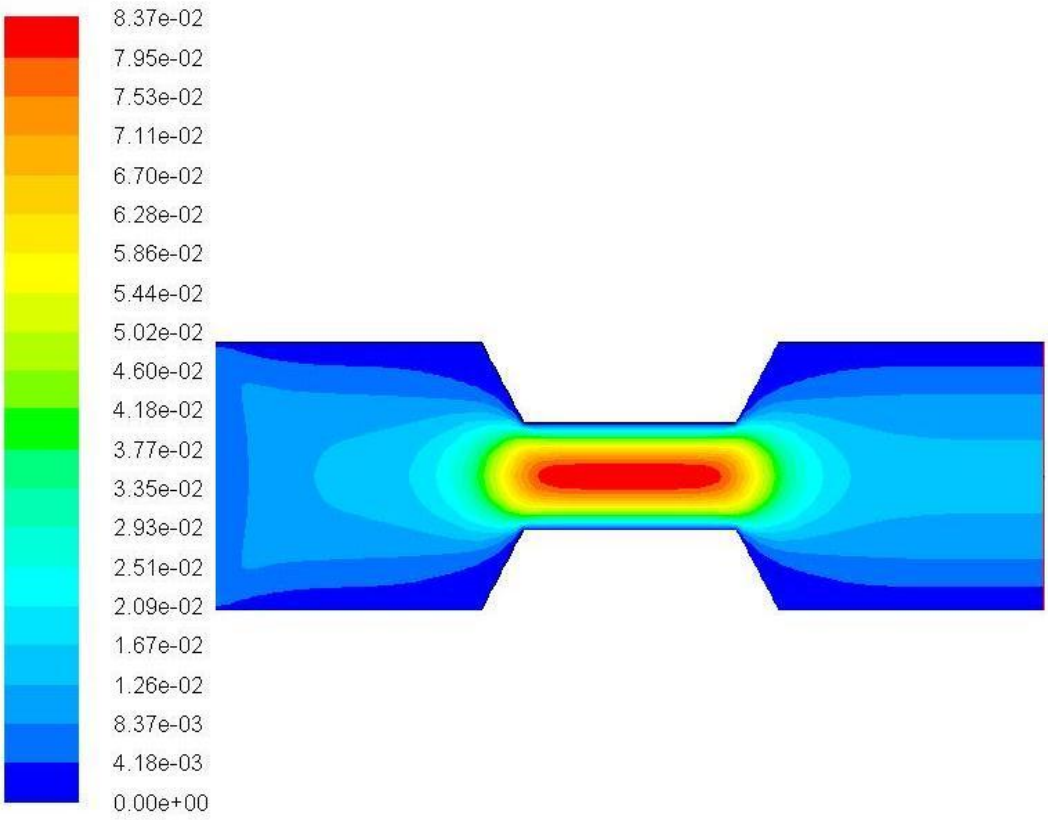

Fig. 23 Contour for velocity distribution at media flow speed 0.0068 ms^{-1}

The variation of velocity with respect to radial distance for different media flow speeds is shown in Fig. 22. The value of maximum velocity increases with the increase in media flow speed. Maximum velocity for 0.0068 ms^{-1} media flow speed is 8.37×10^{-2} ms^{-1} as shown in contour plot (Fig. 23).

The above flow analysis of AFM at different media flow speed provides a transparency of the idea on the dynamic pressure, strain rate and velocity magnitude. The strain rate in comparison to the dynamic pressure is given more preference to study the abrasion effect on the wall of the work-piece. The effects of dynamic pressure and velocity are maximum at the centre of the flow domain and become insignificant in the near wall region. The maximum value of strain rate in the near wall region leads to more abrasive force and polishing action.

The strain rate graphs for the two machining parameters of AFM i.e. volume fraction of the abrasives and media flow speed are a bit different from each other. The strain rate graph for the variable volume fraction is steeper and the value of strain rate increases at a higher rate in comparison to that of the media flow speed. As described above, the strain rate is an important flow output to determine the abrasive force and action of the abrasive particles.

5.6 Conclusion

The findings from the simulation can be summarized as follows,

- The strain rate, i.e. the deformable value per unit time in the polished area, increases in the near wall region of the narrow section on the flow domain.
- The dynamic pressure is maximum at the centre and minimum near the wall. The rolling of abrasive particles is more at the centre in comparison to the wall.
- Velocity shows a same trend as that of the dynamic pressure. The maximum velocity is observed at the centre and it is zero near the surface.
- The value of strain rate, dynamic pressure and velocity increase with the increase in volume fraction of the secondary phase and media flow speed. As it was discussed previously that the effects of dynamic pressure and velocity are negligible in the near wall regions, so the strain rate is considered to study the abrasion. The polishing action and abrasive forces are predicted from the strain rate graphs.
- The strain rate graph for the volume fraction is steeper in comparison to that of media flow speed. It is clear that the concentration of abrasive is more significant in abrasive action than media flow speed.

CHAPTER 6

NUMERICAL SIMULATION OF AFM FOR A 3D MODEL

Chapter-6

NUMERICAL SIMULATION OF AFM FOR THE 3D MODEL

6.1 Introduction

The abrasive flow machining (AFM) is a finishing process that can be used for small channels and complex work-piece passages. Initially, AFM was studied for only a cylindrical work-piece because the fixture and tooling were comparatively simpler. In recent days, AFM is being used for industrial purpose for micro-channels and other geometrical passages using proper tooling arrangement. In the present chapter, a flow passage other than the cylindrical shape is developed and simulated. It has been studied whether the concepts of the strain rate, dynamic pressure and velocity, given in the previous chapter are valid for the new model or not. Now-a-days the dies used for swaging and rotary swaging operations need smooth finishing on the surface to avoid irregularities on the work-piece. So, a 3D model is developed for four rotary swaging dies arranged with fixtures as described by Kenda et al. [47]. The validation of the model has been provided in chapter 7. The assumptions for the FLUENT analysis are same as the 2D model. The flow is assumed to be in steady state, laminar and incompressible. Initially the model is simulated for a non-granulated flow. The granular model is assumed in the subsequent simulations and modifications in the boundary conditions are provided.

6.2 Geometry and mesh

For the 3D model, the abrasive powder is assumed to be a continuous phase for initial simulations and mixture granular model is used for further analysis. For the present study, the secondary phase i.e. the abrasive particles are assumed to be a continuous phase. Details of granular phase are given in subsequent simulations. The geometry is symmetrical around two planes. The arrangement of rotary swaging dies along with the fixtures is according to the arrangement given by Kenda et al [47]. Only the geometry of Kenda et al. [47] is considered for simulation. The detail dimensions of the flow passage and the meshed model is shown in Fig. 24 (a) and (b). The symmetric section of the flow passage around two planes is considered for

FLUENT simulation to save computation time and complexity. The meshed model of the symmetric section is shown in Fig. 25.

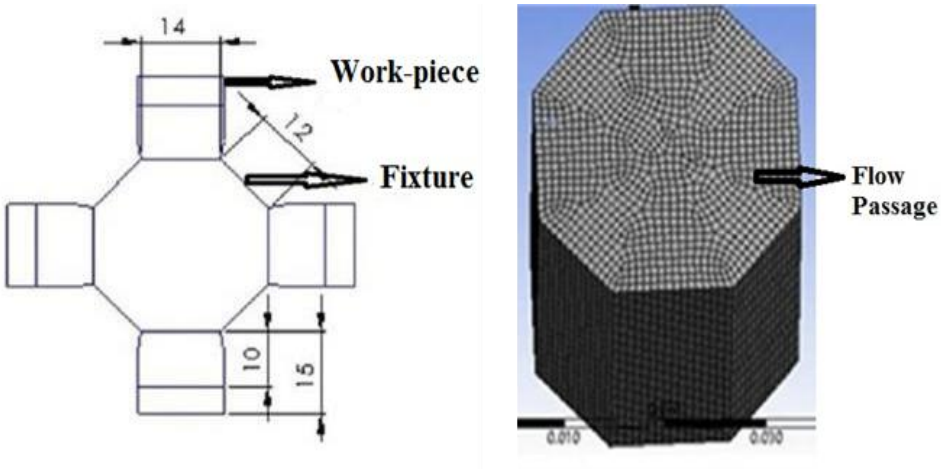

(a) (b)

Fig. 24 (a) Arrangement of work-pieces with fixtures [47] (b) 3D meshed model for FLUENT analysis of the passage

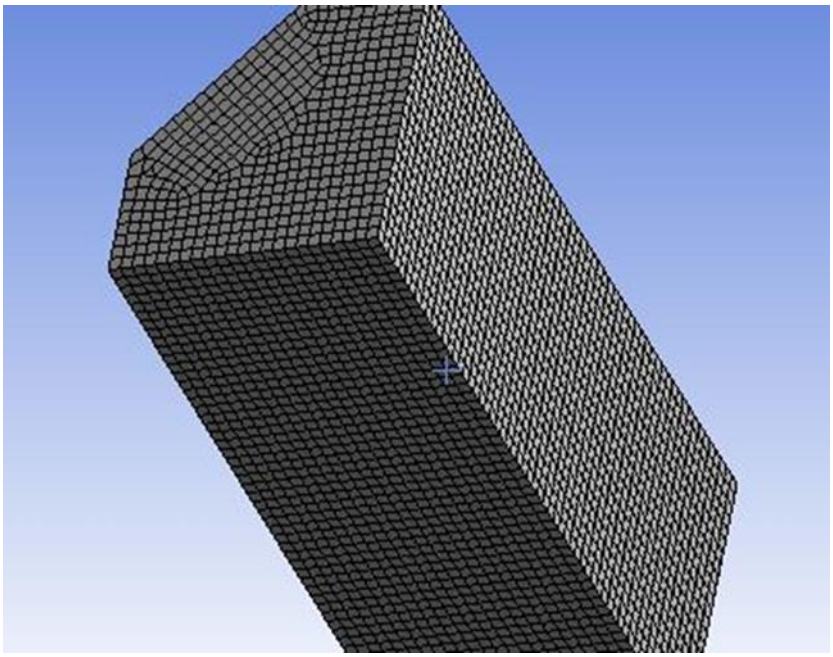

Fig. 25 Meshing of 3D computational domain

6.3 Grid independence test

The 3D model for the simulation is verified for five grid sizes to check the effects on the results. The model is simulated for five numbers of grid sizes, i.e. 10604, 16150, 25288, 41370 and 56394. At a lower number of grids, the variation of the static pressure value is more. With an increase in the number of cells, the value becomes constant. At 25288 numbers of cells, there is no change in static pressure and convergence is achieved. The graph for the grid independence test is given in Fig. 26.

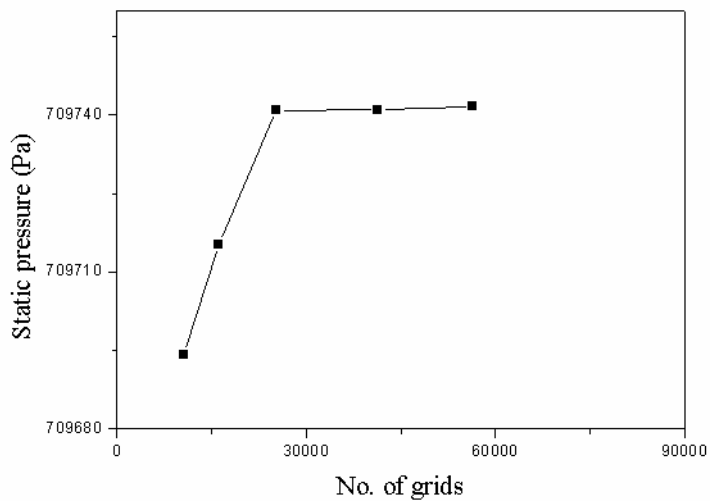

Fig. 26 Variation of static pressure with respect to number of grids

6.4 Simulation details

The simulation of the present model is done for both granular and non-granular flow. In the first set of simulations, multiphase mixture model is selected assuming the abrasive particles as a continuous phase. The effects of volume fractions on the flow outputs are studied as it is done for the 2D model. The carrier media selected for the simulations is polyborosiloxane and the abrasive is silicon carbide.

The second set of simulation involves the multiphase mixture granular model that assumes the abrasive particles to be granular. The effects of particle diameter and volume fraction of the particles are verified for three different abrasives like silicon carbide, boron carbide and corundum. The granular pressure and skin friction coefficient are plotted for variable diameter and volume fraction.

6.5 Results and discussion

Non-granular flow:

In the previous chapter, the variation of volume fraction and media flow speed has been verified for a 2D cylindrical work-piece. In the present study, the effects of volume fraction are studied assuming the secondary phase to be a continuous phase as that of the 2D model. Four different volume fractions such as 0.2, 0.3, 0.4 and 0.5 are considered for the secondary phase.

6.5.1 Effects of changing volume fraction

The effects of volume fraction of abrasives on the flow output parameters like dynamic pressure, strain rate and velocity have been studied in the previous chapter (2D model). In the current chapter, the 3D model for the flow passage is simulated for the variable volume fractions to verify the results and check whether the results are in accordance with that of the 2D model. The theories of strain rate and dynamic pressure given in the previous chapter are demonstrated for the 3D model. The simulation parameters for variable volume fraction of the secondary phase are given in table 3.

Table 3 Simulation parameters for variable viscosity of the media

Parameters	Values
Primary phase	Polyborosiloxane, density-1219 kg/m^3, viscosity- 789 kg/m-s
Secondary phase	silicon carbide, density-3170 kg/m^3
Diameter of secondary phase	150μm
Inlet pressure	2.5 MPa
Volume fraction of secondary phase	0.2, 0.3, 0.4, 0.5

The variation of dynamic pressure in the radial direction has been plotted for four volume fractions and the contours of the dynamic pressure are given.

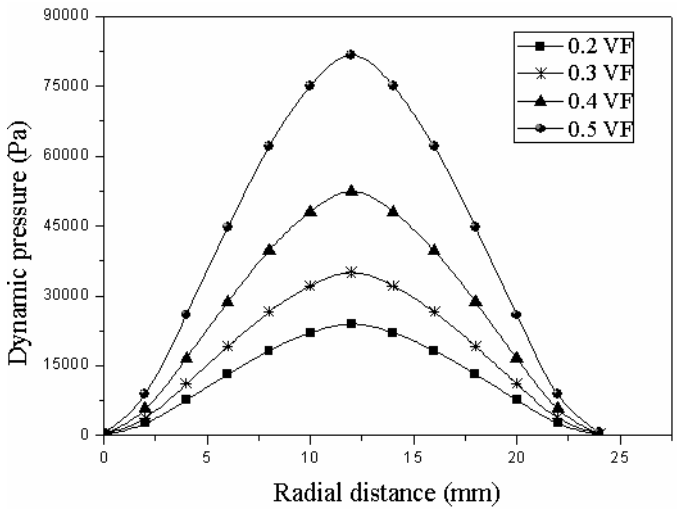

Fig. 27 Variation of dynamic pressure with respect to radial distance from the wall

The variation of dynamic pressure with respect to radial distance from the wall towards the centre is given in Fig. 27. The dynamic pressure is found to increase from the wall towards the centre. The dynamic pressure value increases with the increase in volume fraction of the secondary phase. The contour plots in Fig. 28 illustrate the distribution of dynamic pressure for 0.2 and 0.3 volume fraction of the secondary phase for a particular range. The colour blocks show the distribution of dynamic pressure and its ranges for the two volume fractions.

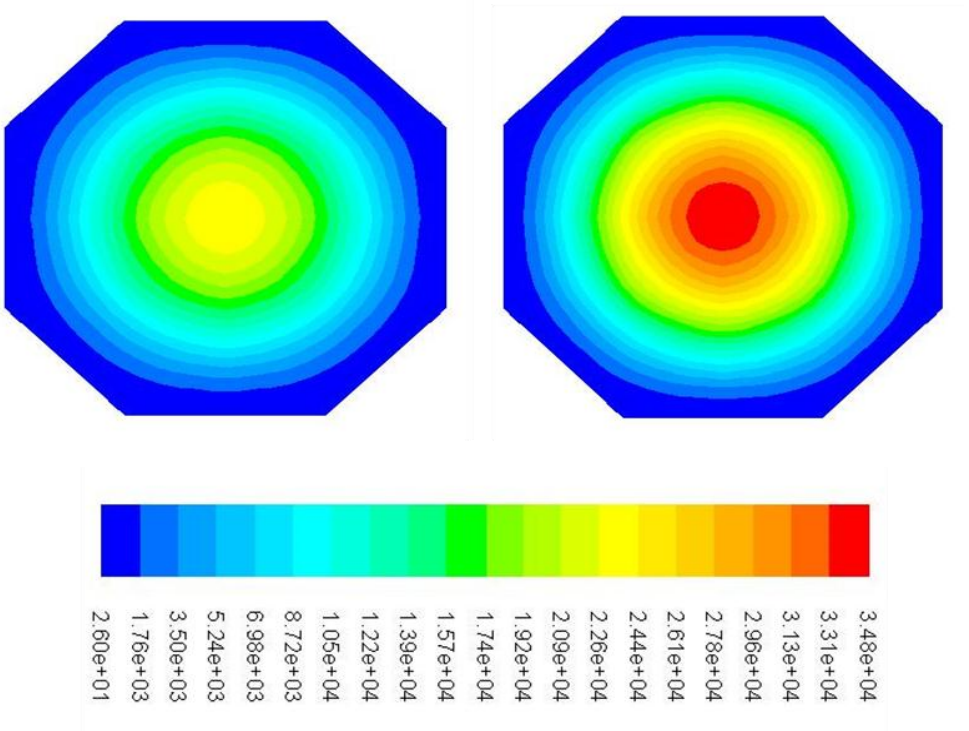

Fig. 28 Contours plot of dynamic pressure for 0.2 and 0.3 volume fractions

The variation of strain rate for four different volume fractions in radial direction and the contours of the strain rate for the 3D model are given below.

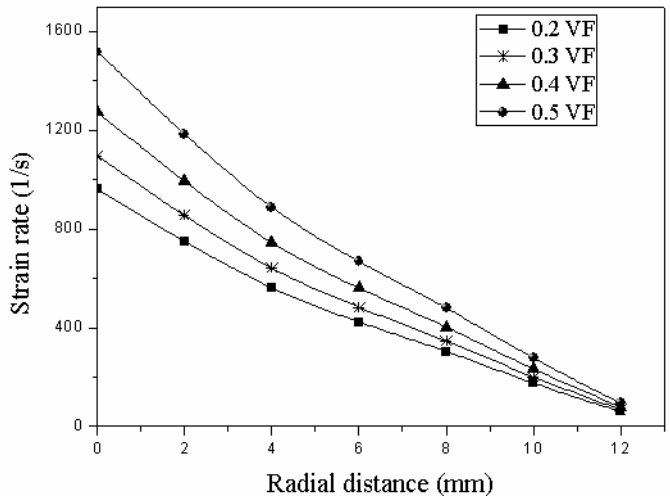

Fig. 29 Variation of strain rate with respect to radial distance from the wall

The variation of strain rate with respect to radial distance from the wall towards the centre of the flow domain is given in Fig. 29. The value of strain rate increases with the increase in volume fraction. Front view of a symmetric section is viewed to observe the variation of strain rate. The comparison of the strain rate values for 0.2 and 0.3 volume fraction of the secondary phase can be depicted from the contour plots in Fig. 30. The colour blocks provide the ranges of strain rate. It is evident from Fig. 30 that the strain rate value increases in the near wall region and decreases towards the centre. The increase in strain rate in the near wall region increases the deformation. The value of strain rate increases with the increase in volume fraction.

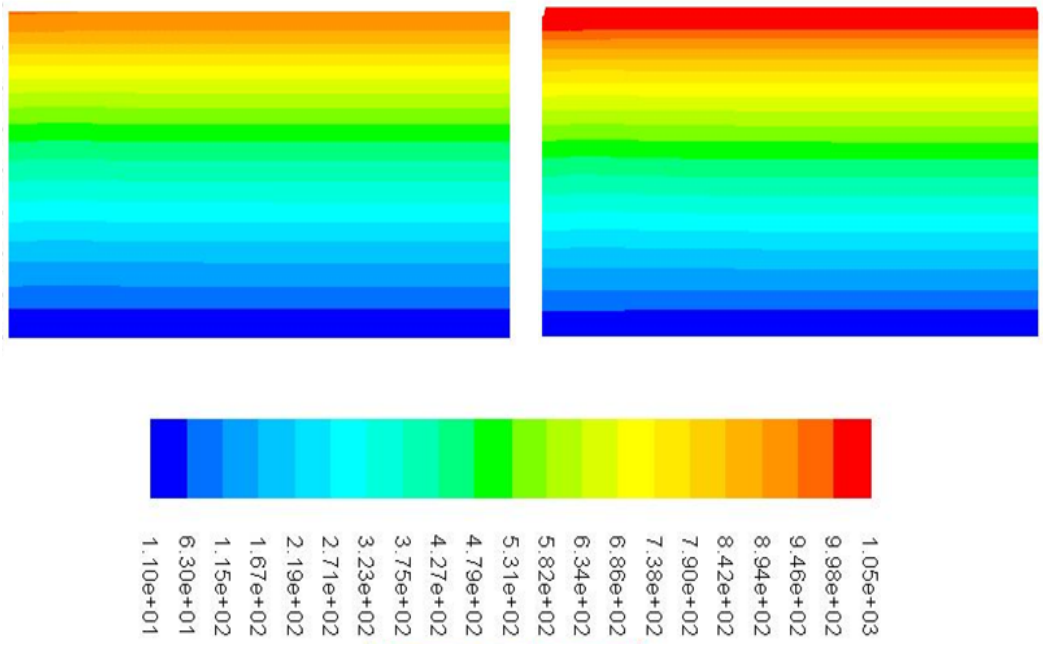

Fig. 30 Strain rate (in s^{-1}) for 0.2 and 0.3 volume fractions

The variation of strain rate with respect to distance from the centre of the wall towards the edge is given in Fig. 31. The graphs and contours are plotted for the wall only. The colour distribution of strain rate for the volume fractions 0f 0.2 and 0.3 is shown in Fig. 32. The contours are shown for the wall only.

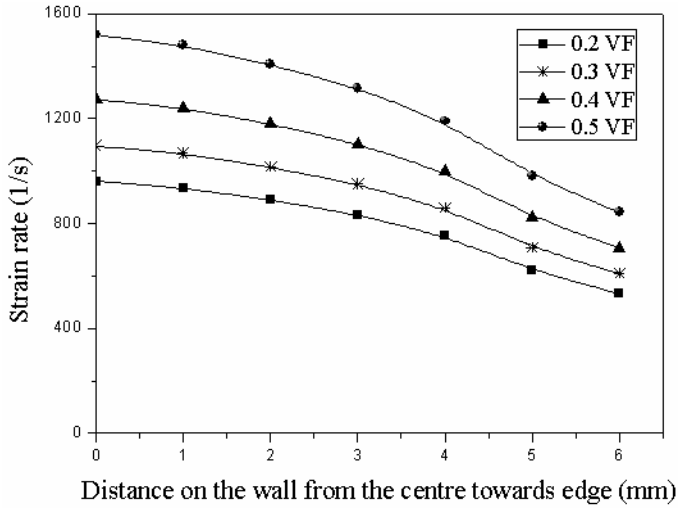

Fig. 31 Variation of strain rate with respect to radial distance on the wall

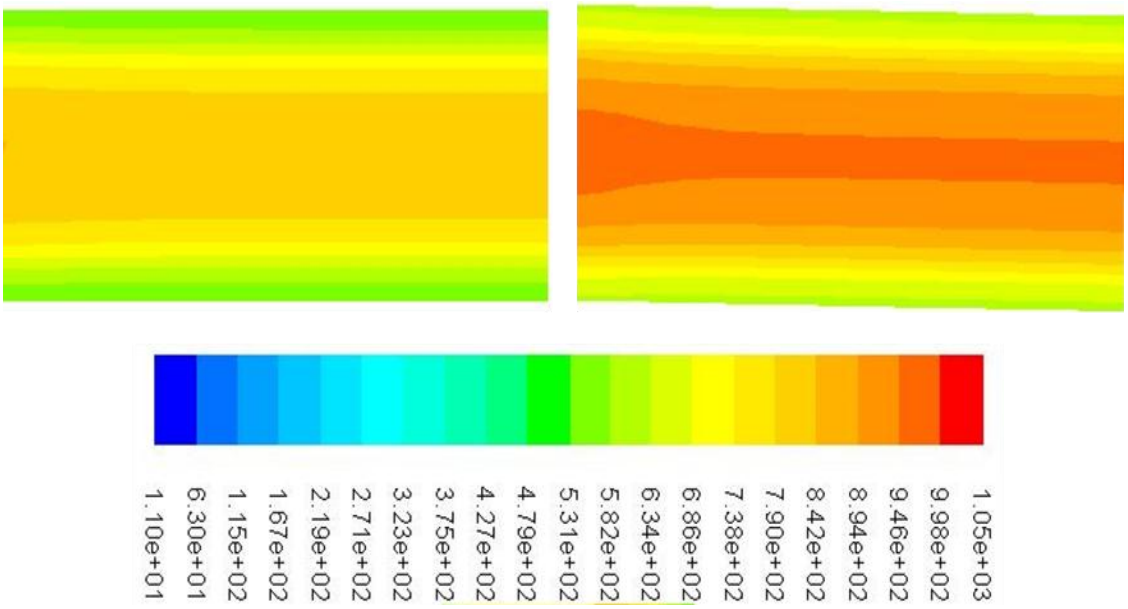

Fig. 32 Strain rate (in s^{-1}) on the wall for 0.2 and 0.3 volume fractions of secondary phase

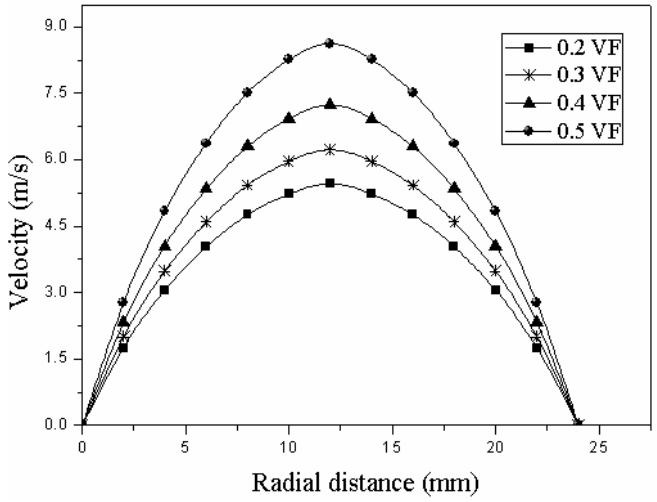

Fig. 33 Velocity (in $m.s^{-1}$) with respect to radial distance from the wall

The variation of velocity distribution in the radial direction is shown in Fig. 33 for the 3D model. The velocity is found to be maximum at the centre and decreases towards the wall. The average velocity increases with the increase in volume fraction of the secondary phase. The rolling tendency of the particle increases with the increase in velocity, thereby decreasing the efficiency of material removal as described in the previous chapter. The comparison of velocity contour for 0.2 and 0.3 volume fractions of the abrasive particles are shown by different colour blocks (Fig. 34).

The theories about the strain rate, dynamic pressure and velocities, discussed in the previous chapter, are found to be valid for the 3D model also. The strain rate is observed to be maximum in the near wall region. Increase in abrasive concentration increases the strain rate and the abrasive force. The dynamic pressure and velocity are maximum at the centre of the flow passage as that of the 2D model. The dynamic pressure has a negligible effect in the near wall region, so the strain rate is considered to predict the abrasive action. The strain rate values on the different positions of the wall are also studied. The centre of the wall is affected more by the abrasive forces in compared to the edges. The results of the simulation from both the 2D and 3D model are found to have a good agreement for an increase in volume fraction of the secondary phase.

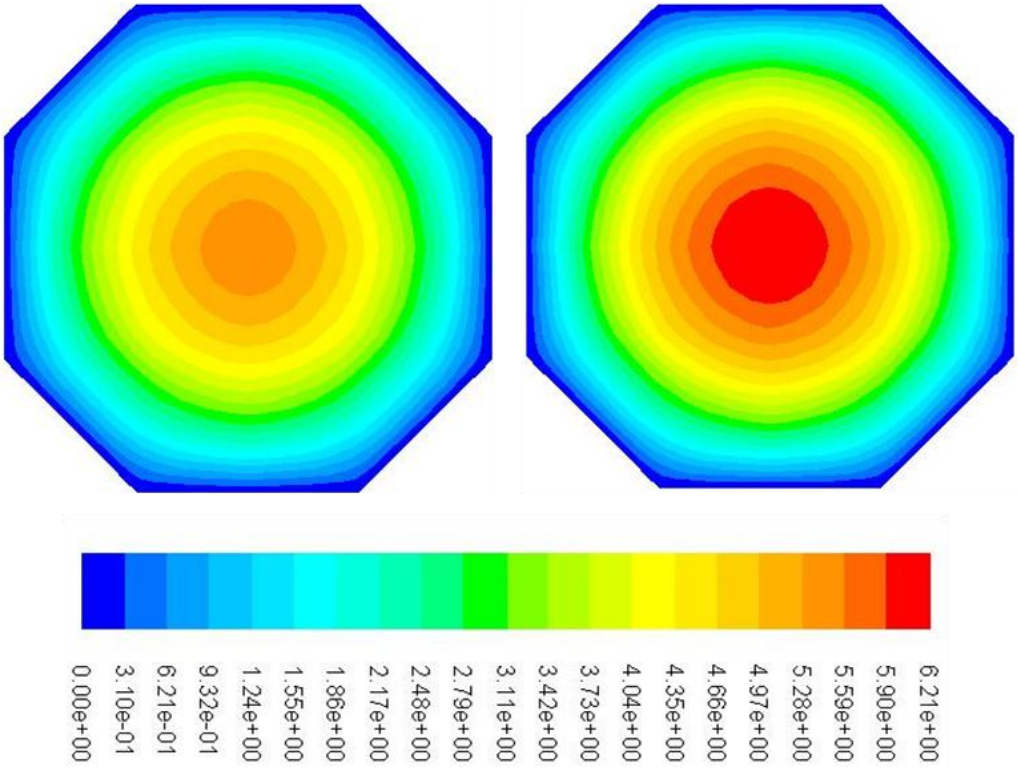

Fig. 34 Velocity magnitude (in $m.s^{-1}$) for 0.2 and 0.3 volume fractions of secondary phase

Granular flow

A multiphase granular model is selected for the simulation of the abrasive media. The granular pressure and skin friction coefficient for three different abrasives have been studied. Collisional and kinetic viscosities are added to give solid shear viscosity for the simulation of the granular flow. The expression for shear viscosity and

collisional viscosity is given by the equation 16 and 17 in chapter 4. The kinetic viscosity, in this case, is given by default expression by Syamlal et al. [105] because it is not a case of fluidized bed as described in chapter 4. The expression for kinetic viscosity by Syamlal et al. is given in equation 18. The simulation parameters for granular phase are given in table 4.

Simulation parameters

Table 4 Simulation parameters for granular phase

Parameters	Values
Primary phase	Polyborosiloxane, density-1219 kg/m^3, viscosity- 789 kg/m-s
Secondary phase	silicon carbide, density-3170 kg/m^3 corundum, density-3910 kg/m^3 boron carbide-2520 kg/m^3
Inlet pressure	5 MPa
Volume faction of the secondary phase	0.3 (for variable diameter of particles) 0.2, 0.25, 0.3, 0.35 and 0.4 (for variable volume fractions)
Particle diameter	150 micron (for variable volume fraction) 100 micron, 122 micron, 150 micron and 165 micron (for variable diameter)

6.5.2 The effect of silicon carbide, boron carbide and corundum on granular pressure

I. Granular pressure at changing volume fraction

Granular pressure is defined as the pressure exerted on the flow regime due to particle collision. It can be considered as the direct reason for abrasion of the passage wall. Granular pressure is a function of solid density and concentration of abrasive particles in the mixture. The density of the three types of abrasives used, is given by corundum

ρ=3910 kg/m^3, silicon carbide ρ=3170 kg/m^3, boron carbide=2520 kg/m^3. The variation of granular pressure for the three types of abrasive particles at changing volume fraction has been plotted in Fig. 35.

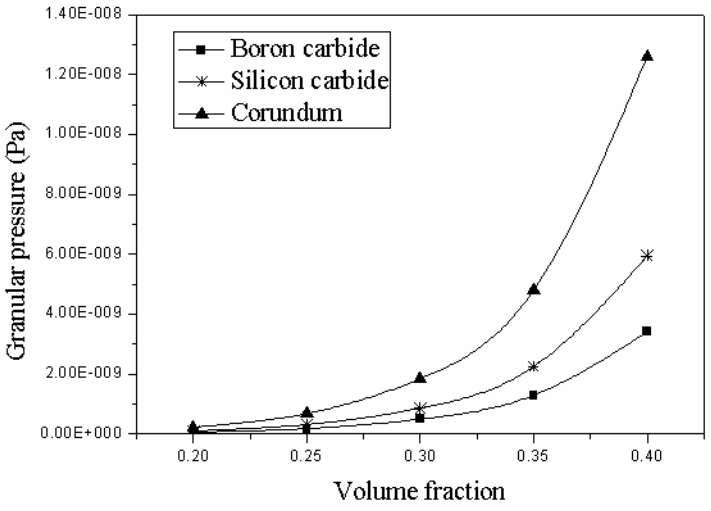

Fig. 35 Variation of granular pressure with respect to volume fraction

The increasing trend of granular pressure with the rise in volume fraction is due to the increase in particle concentration in the suspension fluid. Increase in particle concentration increases the granular pressure on the base fluid and the abrasion on the passage wall due to more particle collision on the wall.

Further, the granular pressure has been investigated for different abrasive particles. It is observed from Fig. 35 that for same inlet conditions and at increasing volume fraction, the granular pressure is maximum for corundum having the highest density. From equation number 16 and 17, it is clear that both the collisional viscosity and kinetic viscosities are the functions of the density of solid. The granular pressure is a result of these two viscosities so; the granular pressure is maximum for the abrasive particle having the highest density.

II. Granular pressure on changing mesh size of the abrasives

The granular pressure has been plotted for the three abrasives like corundum, silicon carbide and boron carbide at different mesh sizes of the abrasives. The variation of granular pressure at different mesh sizes of the abrasive particles is shown in Fig. 36.

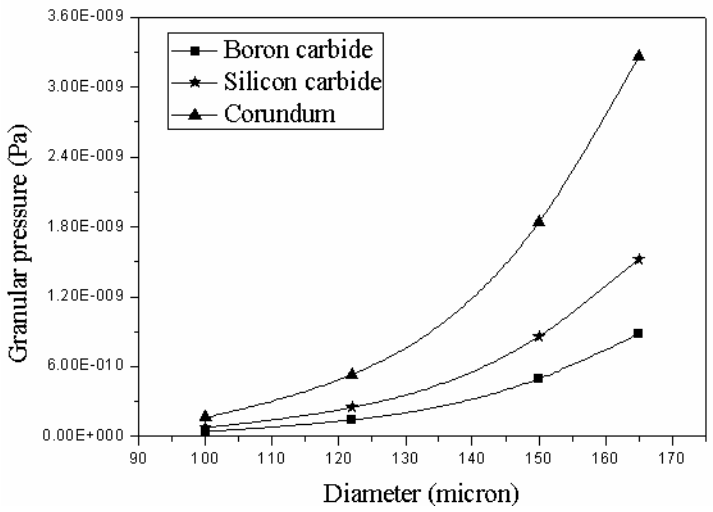

Fig. 36 Variation of granular pressure with respect to abrasive diameter

The granular pressure increases with the increase in diameter of abrasive particle. Again, it is maximum for the abrasive with the maximum density. The rise in the diameter of the abrasive particle for the same inlet pressure and volume fraction increases the granular pressure as the interaction of the abrasives with the fluid media increases.

6.5.3 The effect of silicon carbide, boron carbide and corundum on skin friction coefficient

Skin friction is a component of drag that resists the motion of a fluid across the surface of a solid boundary. The skin friction coefficient is a dimensionless drag coefficient that expresses proportionality between the frictional force per unit area and square of speed. Fig. 37 demonstrates the variation of skin friction coefficient with respect to volume fraction for three different abrasives.

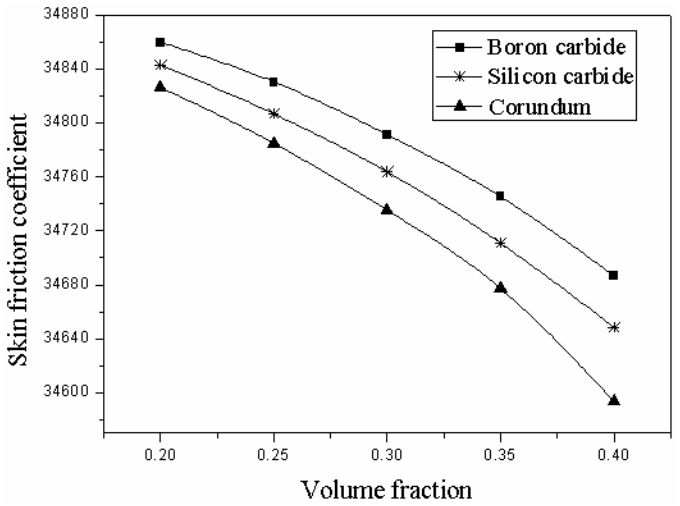

Fig. 37 Variation of skin friction coefficient with respect to volume fraction

The variation of skin friction coefficient with respect to volume fraction is shown in Fig. 37. The skin friction coefficient is observed to decrease with increase in volume fraction of the secondary phase. This is due to the increase in concentration of abrasive in the fluid media reduces the pressure energy to transport the particles in the liquid suspension that ultimately decreases the magnitude of the velocity. Hence skin friction coefficient reduces. Three abrasive particles: boron carbide, silicon carbide and corundum have been used. The skin friction is observed to be maximum for boron carbide that has the least density among the three abrasives. The increase in the density of the particles results in a decrease in the velocity of flow due to the mass inertial effect hence reducing the skin friction coefficient. The skin friction coefficient is the least for corundum and maximum for boron carbide. The skin friction coefficient was plotted for variable volume fraction. The skin friction coefficient is dependent on the velocity. The skin friction coefficient is invariant to the variation in diameter of the abrasive as there is no change in velocity magnitude.

The numerical analysis of the abrasive media demonstrated the effects of change in volume fraction and change in diameter of the abrasive on the granular pressure for three different abrasive particles. The granular pressure is the result of the presence of abrasive powder as the secondary phase in the fluid media. The increase in granular pressure increases the particle collision on the wall and this leads to more active number of particles near the wall. Pressure exerted in the suspension fluid increases the abrasive action and material removal efficiency. The increase in diameter and volume fraction of the secondary phase demonstrates an increase in granular pressure.

It is clear from the simulation results that an increase in diameter and volume fraction increases the abrasive action and the material removal efficiency. The similar thing was observed experimental investigation by Jain and Adsul [3]. The density of particles also increases the granular pressure of the media. Among the three abrasive particles, the highest granular pressure was obtained in case of corundum. The material removal efficiency of corundum is maximum among the three different abrasives used.

Decrease in skin friction coefficient with an increase in volume fraction makes it clear that pressure energy is lost due to the particle movement in the fluid media. Decrease in skin friction is the result of the decline in velocity that implies the increase in material removal efficiency. The skin friction coefficient is the least for corundum as it experiences the least velocity and the highest abrasive action. The change in skin friction is very less in comparison to the granular pressure. The media flow consists of abrasive particles, so the granular pressure significantly affects the material removal compared to the skin friction coefficient. The flow analysis of the above simulation is in good agreement with the experimental observations for the variation in concentration of abrasives and grit size of the abrasive particle.

6.6 Conclusion

The current chapter discusses both the granular and non-granular flow of the abrasive media to study different parameters that affect the material removal efficiency. The simulation has also studied the effects of three types abrasive particles on the flow outputs and material removal efficiency. The simulation results are independent of the number of grids. The major findings from the non-granular and granular phase can be written as follows

- The strain rate, i.e. the deformable value per unit time in the polished area, increases in the near wall region of the flow domain and increase in strain rate is observed with an increase in volume fraction of the secondary phase. The maximum value of the strain rate is found in the middle of the wall and the value decreases towards the edge. The effects of dynamic pressure and velocity are found to be less significant in the prediction of abrasive action.

- The granular pressure increases with an increase in volume fraction of the abrasives and the diameter of abrasives. The use of abrasive with maximum density, i.e. corundum leads to the maximum granular pressure. The skin friction coefficient decreases with the increase in volume fraction. The use of abrasive with the least density comes out to have the highest skin friction coefficient. The analysis infers that the increase in granular pressure and the decrease in skin friction coefficient tend to increase the material removal efficiency. Hence, corundum induces the maximum abrasive action on the wall of the passage in comparison to the other two abrasive particles.

CHAPTER 7

PARTIAL VALIDATION OF THE MODELS

Chapter-7

PARTIAL VALIDATION OF THE MODELS

7.1 Introduction

Validation of the models, developed using softwares, play an important role in numerical modeling. The models need to be validated with the existing experimental data. A 2D model has been developed for the cylindrical work-piece in chapter 5 and the simulation is done. Similarly, a 3D model has been developed in chapter 6. The non-granular and granular flow was simulated for the same. In the present chapter, the validation of the two models with the benchmark experimental data is given.

7.2 Validation of the 2D model

The flow analysis for the 2D (Fig. 38) model is done using a multiphase mixture model for two phases. As mentioned in chapter-5, the workpiece hole diameter was taken 13.4 mm for validation purpose. Soft styrene butadiene rubber with a weight percentage of plasticizer is used as the base and SiC as the abrasives [14]. In the validation study, the media with 10% plasticizer is taken into account. The dynamic viscosity of the media with 10% plasticizer oil is 4.57×10^5 Pa.s. The viscosity of media is very high for AFM. In the present modeling, the fluid is assumed to be a Newtonian fluid [2, 96]. The experimental results for 6MPa extrusion pressure with abrasive mesh size 220 and abrasive concentration 66.7% is used for validation of the present results.

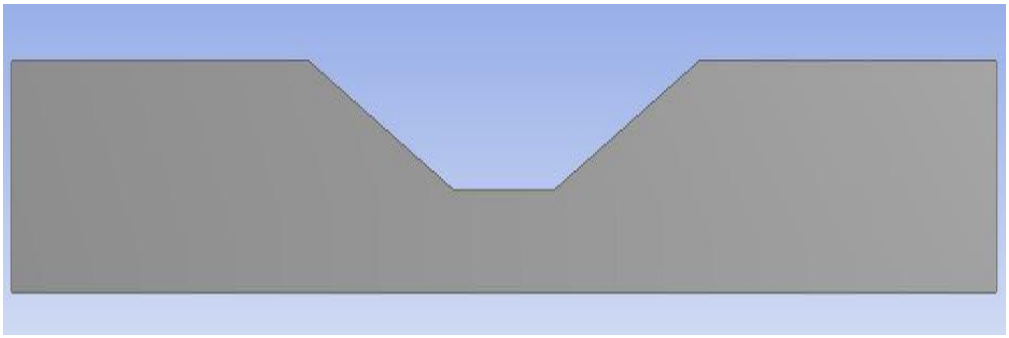

Fig. 38 Symmetrical geometry taken up for the simulation (2D)

7.2.1 Mathematical modeling of surface roughness

Abrasive flow machining as described by Jain et al. [2] is a scratching action of the abrasive particles present in the media. The normal force applied to the spherical grain will cause the penetration on the surface. The grain removes the material as it moves in the horizontal direction. The amount of stock removal is equal to the total volume of grooves produced on the work-piece wall by each grain in the media. The volume of stock removal and surface roughness can be calculated if the number of abrasive grains, the depth of the groove and their shapes are known. Fig. 39 represents a simplistic diagram of an abrasive grain and the roughness profile.

Following assumptions were made by Jain et al. [2] in their theoretical modeling:-

1. The shape of the abrasives is spherical in nature and each particle consists of a single active cutting edge.
2. The load on each abrasive particle is constant and is assumed to be equal to the average load for the convenience in mathematical calculation.
3. All the abrasive grains attain the same depth of indentation upon applied force.
4. Uniform surface roughness was assumed for the profile.

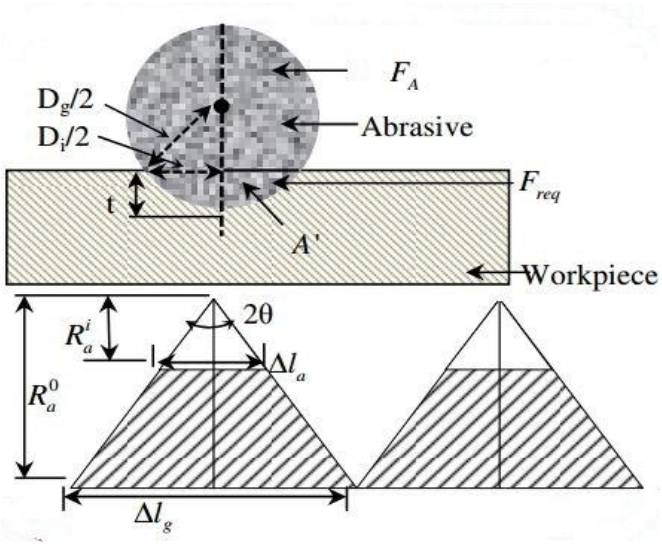

Fig. 39 Schematic diagram of an abrasive particle indenting on the work-piece and simplified geometry of roughness [57]

Singh et al. [57] also validated the results of mathematical modeling done based on previous assumptions. They calculated the shear stress using a capillary rheometer

and performed a frequency sweep. Radial force and axial force were calculated from the shear stress value. The mathematical modeling by Jain et al. [2] was used to calculate the surface roughness value and the value from the mathematical modeling was validated with the experimental data by Ravishankar et al. [14]

In the present paper, the shear stress has been calculated from the FLUENT simulation by using the same geometry and input parameters as described by Ravishankar et al. [14]. The radial force is calculated. The mathematical modeling given by Jain et al. [2] is used to calculate the theoretical roughness and it is compared with the experimental results by Ravishankar et al. [14].

Radial force (F_n) acting on a single abrasive grain is as follows,

$$F_n = \tau_0 . \pi \frac{D_g^2}{4} \tag{19}$$

where D_g is the diameter of the abrasive particle and τ_0 is the shear stress. The shear stress value in this case is nothing but the wall shear stress that is calculated from FLUENT.

Brinell hardness number is given by the formula

$$BHN = \frac{F_n}{\frac{\pi}{2} D_g \left(D_g - \sqrt{D_g^2 - D_i^2} \right)} \tag{20}$$

BHN of aluminium alloy work-piece was calculated by Singh et al. [57] and found to be 118 BHN. F_n is calculated from the equation 19. Putting the value of the diameter of abrasive particle 70 μm (220 mesh size), D_i (indentation diameter) is calculated. The mathematical formulation according to Jain et al. [2] is given as follows:

The depth of indentation (*t*) is given by

$$t = \frac{D_g}{2} - \frac{1}{2} \sqrt{\left(D_g^2 - D_i^2 \right)} \tag{21}$$

The cross-sectional area of the groove generated A’ (shaded portion of the grain) can be derived from the geometry

$$A' = \frac{D_g^2}{4}\sin^{-1}\left(\frac{2\sqrt{t(D_g - t)}}{D_g}\right) - \sqrt{t(D_g - t)}\left(\frac{D_g}{2} - t\right) \quad (22)$$

Let R_a^0 be the initial surface roughness and R_a^i is the roughness after i^{th} stroke. The actual contact length (L_a) between the work-piece and abrasive grain within the total length of the work-piece is given by:

$$L_a = \left(\frac{\Delta l_a}{\Delta l_g}\right)L_w = \left[\frac{(R_a^0 - R_a^i)\tan\theta}{R_a^0 \tan\theta}\right] \times L_w = \left[1 - \frac{R_a^i}{R_a^0}\right] \times L_w \quad (23)$$

where L_w is the length of the work-piece

Volume of material removed after *i*th stroke by a single abrasive particle is given by:

$$V_i = A' L_a \quad (24)$$

Total number of abrasive grains (N_s) during one stroke of AFF is given by

$$N_s = 2\pi R_w N_a L_s \frac{R_m^2}{R_w^2} \quad (25)$$

where R_w is the radius of the work-piece, N_a is the number of active particles per unit area, L_s is the stroke length and R_m is the radius of media cylinder.

Volumetric removal (V_i) for *i*th stroke is given by

$$V_i = A' L_a N_s \quad (26)$$

Putting the values of A', L_a, N_s as given in equation 22, 23 and 25, V_i can be written as

$$V_i = \left(\frac{D_g^2}{4}\sin^{-1}\left(\frac{2\sqrt{(t(D_g - t))}}{D_g}\right) - \sqrt{t(D_g - t)}\left(\frac{D_g}{2} - t\right)\right) \times \left[1 - \frac{R_a^i}{R_a^0}\right] L_w \times 2\pi R_w N_a L_s \frac{R_m^2}{R_w^2} \quad (27)$$

Volumetric material removal for 2n number of cycles is written as:

$$V_n = \left(\frac{D_g^2}{4} \sin^{-1}\left(\frac{2\sqrt{t(D_g - t)}}{D_g} \right) - \sqrt{t(D_g - t)} \left(\frac{D_g}{2} - t \right) \right) \times \sum_{i=1}^{2n} \left[1 - \frac{R_a^i}{R_a^0} \right] L_w \times 2\pi R_w N_a L_s \frac{R_m^2}{R_w^2} \tag{28}$$

Volumetric material removal for i^{th} stroke can also be written = height of material removed × width of work-piece × actual contact length of the work-piece. So,

$$V_i = \left[1 - \frac{R_a^i}{R_a^0} \right] L_w \times 2\pi R_w \left[R_a^{i-1} - R_a^i \right] \tag{29}$$

After simplifying the equation, the surface roughness after i^{th} stroke can be written as

$$R_a^i = R_a^{i-1} - \left\{ N_a L_s \left(\frac{R_m^2}{R_w^2} \right) \left(\frac{D_g^2}{4} \sin^{-1}\left(\frac{2\sqrt{t(D_g - t)}}{D_g} \right) - \sqrt{t(D_g - t)} \left(\frac{D_g}{2} - t \right) \right) \right\} \tag{30}$$

The change in roughness is written as described by Singh et al. [57]

$$\Delta R_a = \left\{ N_a L_s \left(\frac{R_m^2}{R_w^2} \right) \left(\frac{D_g^2}{4} \sin^{-1}\left(\frac{2\sqrt{t(D_g - t)}}{D_g} \right) - \sqrt{t(D_g - t)} \left(\frac{D_g}{2} - t \right) \right) \right\} \tag{31}$$

Putting the values of constants in equation 31 as given by Ravishankar et al. [14] i.e. R_m =30.5 mm, R_w =13.4 mm, L_s =75mm, N_s =40 grains/mm^2, change in surface roughness for one stroke is calculated and the value is multiplied by the number of strokes to obtain the change in surface roughness at the increasing number of strokes.

From the FLUENT simulations, the wall shear value is calculated to be 10113.6 Pa. The value is used to calculate the radial force in equation 19. The diameter of the abrasive particle is 70µm and the t value is calculated from equation 21 and found to be 1.5295×10^{-10} m. Solving the final equation, change in surface roughness is found out for a single stroke, subsequently for more number of strokes. The graph is plotted for the change in surface roughness at different strokes and compared with the experimental data found by Ravishankar et al. [14] as shown in Fig. 40. Singh et al. [57] also plotted the comparison graph between the experimental and simulated

values. Both the lines for simulation are found to be in the same pattern for 6 MPa extrusion pressure, 70 µm diameter of abrasive particle with concentration 66.7 %.

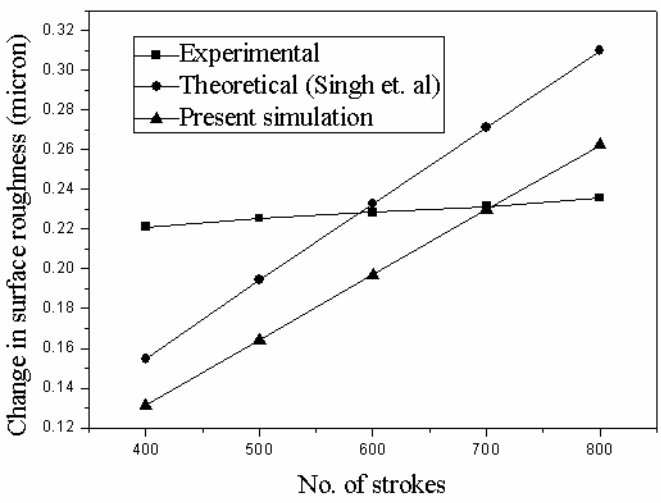

Fig. 40 Effect of number of AFF strokes on change in roughness (ΔR_a) in micron

The graph (Fig. 40) shows that the experimental change in roughness is negligible with the increase in number of strokes, but the theoretical change in roughness increases linearly with the increase in number of strokes. In theoretical modeling, it is assumed that the abrasive particles are spherical and all the particles take part in abrasion. The wear of the abrasive particles with the increase in number of strokes is not considered in the mathematical modeling. These are the important reasons for which there is deviation between the experimental and theoretical results.

7.3 Validation of the 3D model

In case of the 3D model (Fig. 41), the value of viscosity of the media is taken to be 2650 Pa.s, the abrasive diameter to be 165 micron (mesh size 80) and the volume fraction of abrasives to be 57 % as described by Kenda et al. [47]. The simulation is done for two extrusion pressures i.e. 3.5 MPa and 6MPa. Kenda et al. [47] machined the work-pieces using EDM and AFM subsequently. The image of the surface texture was distinguished between EDM + AFM with polishing media under pressure 3.5 MPa and EDM + AFM with polishing media under pressure 6 MPa. The simulation only considers the AFM part and the comparison between the polishing at 3.5 MPa and 6 MPa extrusion pressure.

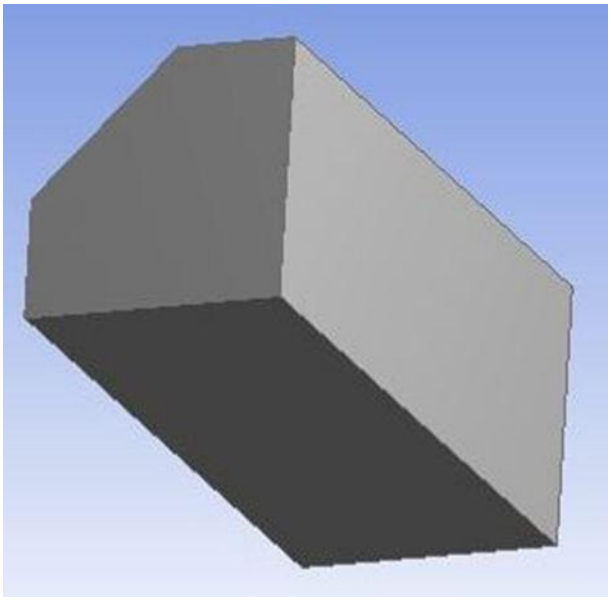

Fig. 41 Symmetrical geometry taken up for the simulation (3D)

The 3D model is simulated for two extrusion pressures i.e. 3.5 MPa and 6 MPa. The indentation force or the radial force is calculated using the wall shear stress values, found out from the FLUENT analysis. The wall shear stress for 3.5 MPa and 6 MPa are 18770.313 Pa and 32136.893 Pa. Putting the values in equation 19, the indentation force has been calculated. The hardness value as given by Kenda et al. [47] is 59 HRc. The value was converted to BHN value i.e. 613 BHN. The values are substituted in equation 20 and 21 subsequently to find the depth of indentation (t). The depth of indentation is found to be 1.288×10^{-10} m and 2.2052×10^{-10} m for 3 MPa and 6 MPa respectively. The depth of indentation is observed to be more for 6 MPa in comparison to 3.5 MPa. The roughness measurement using the mathematical formulae as given by Jain et al. [2] is not possible because the number of abrasive grains is not given in the paper. If the surface texture as given by Kenda et al. [47] is observed, more polished surface is demonstrated at 6 MPa in comparison to 3.5 MPa. Mathematically, the depth of indentation is directly proportional to the material removed from the surface peaks. For a single grain, the value of depth of indentation for 6 MPa is higher than 3.5 MPa. So, it can be inferred from the mathematical calculation that the polishing is better in case of 6 MPa than 3.5 MPa extrusion pressure.

The exact validation of the surface roughness could not be done for the 3D model as the number of abrasive particles is not provided in the paper. The depth of indentation is calculated which is directly proportional to the material removed.

7.4 Conclusion

The 2D and 3D models have been partially validated with the existing experimental data.

CHAPTER 8

CONCLUSIONS

Chapter-8

CONCLUSIONS

8.1 Summary of research findings

- Theoretical models of work-pieces for AFM process has been developed and CFD simulation done using FLUENT software.
- The 2D model has been simulated for variable volume fraction and media flow speed. The value of strain rate, dynamic pressure and velocity increase with the increase in volume fraction of the secondary phase and media flow speed. The effects of dynamic pressure and velocity were negligible in the near wall regions, so the strain rate is considered to study the abrasion. The polishing action and abrasive forces have been predicted from the strain rate graphs. The strain rate graph for the volume fraction is steeper in comparison to that of media flow speed. It is clear that the concentration of abrasive is more significant in abrasive action than media flow speed.
- The 3D model was simulated for non-granular and granular flow separately.
    - *Non-granular flow*: The distribution of dynamic pressure, velocity and strain rate has been observed at different positions in the flow domain. The strain rate, i.e. the deformable value per unit time in the polished area, increases in the near wall region of the flow domain and increase in strain rate is observed with an increase in volume fraction of the secondary phase. The maximum value of the strain rate is found in the middle of the wall and the value decreases towards the edge. The effects of dynamic pressure and velocity are found to be less significant in the prediction of abrasive action.
    - *Granular Flow*: The granular pressure increases with an increase in volume fraction of the abrasives and the diameter of abrasives. The use of abrasive with maximum density, i.e. corundum leads to the maximum granular pressure. The skin friction coefficient decreases with the increase in volume fraction. The use of abrasive with the least density has come out to have the highest skin friction coefficient. The analysis infers that the increase in granular pressure and the decrease in

skin friction coefficient tend to increase the material removal efficiency.

- The change in roughness value at the increasing number of stokes have been observed for the 2D model. The theoretical change in roughness increases in a linear fashion with the increase in the number of strokes because in modeling, it is assumed that the particle is spherical and all the particles take part in the finishing operation. The experimental change in roughness experienced negligible effects for increase in number of strokes. In case of the 3D model, the depth of indentation increases with the increase in extrusion pressure.

8.2 Future scope

The present study provides a wide future scope to the investigators working in the area of modeling of AFM. The recommendations for future research are given as follows:

- The FLUENT simulation can be done for the temperature analysis using energy equations.
- Mathematical modeling for a shape other than cylindrical can be developed.
- Processes like MRAFF and CFAAFM can be simulated using FLUENT.
- ANSYS CFX can be used to calculate the material removal more accurately.
- Different mechanical means to improve the interaction of the abrasive grains with wall can be investigated.

REFERENCES

[1] Jain, R.K., Jain, V.K. and Kalra, P.K., (1999), "Modeling of abrasive flow machining process: a neural network approach", *Wear,* Vol. 231, pp. 242-248.

[2] Jain, R.K., Jain, V.K. and Dixit, P.M., (1999), "Modeling of material removal and surface roughness in abrasive flow machining process", *International Journal of Machine Tools & Manufacture,* Vol. 39, pp. 1903-1923.

[3] Jain, V.K. and Adsul, S.G., (2000), "Experimental investigations into abrasive flow machining (AFM)",*International Journal of Machine Tools & Manufacture,* Vol. 40, pp. 1003-1021.

[4] Williams, R.E. and Rajurkar, K.P., (1992), "Stochastic modeling and analysis of abrasive flow machining", *Journal of Engineering for Industry-Transactions of the ASME,* Vol. 144, pp. 74-81.

[5] Jain R.K. and Jain V.K., (1999), "Simulation of surface generated in abrasive flow machining process", *Robotics and Computer Integrated Manufacturing,* Vol. 15, pp. 403-412.

[6] Jain, R.K. and Jain, V.K., (2001), "Specific energy and temperature determination in abrasive flow machining process", *International Journal of Machine Tools & Manufacture,* Vol. 41, pp. 1689-1704.

[7] Jain, V.K., Kumar, R., Dixit, P.M. and Sidpara, A., (2009), "Investigations into abrasive flow finishing of complex work-pieces using FEM", *Wear,* Vol. 267, pp. 71-80.

[8] Gorana, V.K., Jain, V.K. and Lal, G.K., (2006), "Forces prediction during material deformation in abrasive flow machining", *Wear,* Vol. 260, pp. 128-139.

[9] Gorana, V.K., Jain, V.K. and Lal, G.K., (2004), "Experimental investigation into cutting forces and active grain density during abrasive flow machining", *International Journal of Machine Tools & Manufacture,* Vol. 44, pp. 201-211.

[10] Rhodes, L.J., (1987), "Abrasive flow machining with not-so-silly putty", *Met. Finish*., pp. 27-29.

[11] Rhodes, L.J., (1988), "Abrasive flow machining", *Manufacturing engineering*, pp. 75-78.

[12] Rhodes, L.J., (1991), "Abrasive flow machining: a case study", *Journal of Material Processing Technology,* Vol. 28, pp. 107-116.

[13] Perry, W.B., (1989), "Abrasive flow machining- principles and practices", *Non Traditional Conference Proceedings,* pp. 121-127.

[14] Ravishankar, M., Ramkumar, J. and Jain, V.K., (2009), "Experimental investigation and mechanism of material removal in nano finishing of MMCs using abrasive flow finishing (AFF) process", *Wear,* Vol. 266, pp. 688-698.

[15] Ravishankar, M., Jain, V.K. and Ramkumar, J., (2009), "Experimental investigations into rotating work-piece abrasive flow finishing", *Wear,* Vol. 267, pp. 43-51.

[16] Ravishankar, M., Jain ,V.K., Ramkumar, J. and Joshi, Y. M., (2011), "Rheological characterization of styrene-butadiene based medium and its finishing performance using rotational abrasive flow finishing process", *International Journal of Machine Tools & Manufacture,* Vol. 51, pp. 947-957.

[17] Ravishankar, M., Jain, V.K. and Ramkumar, J., (2010), "Rotational abrasive flow finishing (R-AFF) process and its effects on finished surface topography", *International Journal of Machine Tools & Manufacture,* Vol. 50, pp. 637-650.

[18] Rajesha, S., Venkatesh, G., Sharma, A.K and Kumar P., (2010), "Performance study of a natural based polymer media for abrasive flow machining process", *International Journal of Engineering and Material Science,* Vol. 17, pp. 407-413.

[19] Bahre, D., Brunnet, H. and Swat, M., (2012), "Investigation of one-way abrasive flow machining and in-process measurement of axial forces", in *Proceedings of 5th CIRP Conference on High Performance Cutting 2012,* pp. 419-424.

[20] Siddiqui, S.S. and Hameedullah, M., (2010), "Abrasive flow machining performance measures on work-piece surfaces having different vent/passage

considerations for media outflow", *International Journal of Computer Communication and Information System,* Vol. 2(1).

[21] Komanduri, R., Lucca, D.A. and Tani, Y., "Technological Advances in Fine Abrasive Processes", *Keynote Papers.*

[22] Kimberly, E. P., Richard, E.B. and Bopaya, B., (1998), "A neural network process model for abrasive flow machining operations", *Journal of Manufacturing System,* Vol. 17(1).

[23] Venkatesh, G., Singh, T., Sharma, A.K. and Dvivedi, A., "Finishing of micro-channels using abrasive flow machining". in *Proceedings of the International Conference on Research and Innovations in Mechanical Engineering.*

[24] Venkatesh, G., Sharma, A.K., Singh, N. and Kumar, P., (2014), "Finishing of Bevel Gears using Abrasive Flow Machining", in Proceedings of *12th Global Congress on Manufacturing and Management, GCMM 2014.*

[25] Cheema, M.S., Venkatesh, G., Dvivedi, A. and Sharma, A.K., (2012), "Developments in abrasive flow machining: a review on experimental investigations using abrasive flow machining variants and media", in *Proceedings of the Institution of Mechanical Engineers, Part B: Journal of Engineering Manufacture.*

[26] Chouhan, S. and Mittal, S., (2014), "Experimental investigation of machining parameters for AFM using round shaped of AISI D2",*International Journal of Current Engineering and Technology,* Vol. 2, pp. 92-103

[27] Chouhan, S. and Mittal, S., (2014), Abrasive Flow Machining: Major research areas & analysis", *International Journal of Research in Aeronautical and Mechanical Engineering,* Vol. 2, pp. 77-83.

[28] Junye, L., Lifeng, Y., Weina, L., Xuechen, Z. and Fenfyu, S., (2014), "Experimental research into technology of abrasive flow machining nonlinear tube runner", *Advances in Mechanical Engineering,* Vol. 2014.

[29] Abbas, F.I., Saad, K.S. and Wissam, K.H., (2014), "Studying Abrasive Flow Machining Conditions by Using Taguchi Method", *Engineering and Technical Journal,* Vol.32 (Part A).

[30] Abbas Fadhil Ibrahim, "Studying Material Removal in Abrasive Flow Machining by using SiC", *International Journal of Current Engineering and Technology,* Vol. 4, No. 5.

[31] Kenda, J., Duhovnik, J. and Tavear, J. and Kopac, J., (2014), "Abrasive flow machining applied to plastic gear matrix polishing", *International Journal of Manufacturing Technology,* Vol. 71, pp. 141-151.

[32] Kenda, J., Pusavec, F. and Kopac, J., (2014), "Modeling and Energy Efficiency of Abrasive Flow Machining on Tooling Industry Case Study", in *Proceedings of 2nd CIRP 2nd CIRP Conference on Surface Integrity (CSI),* Vol.13, pp. 13-18.

[33] Walia, R.S., Shan, H.S. and Kumar, P., (2009), "Enhancing AFM process productivity through improved fixturing", *International Journal of Manufacturing Technology,* Vol. 44, pp.700-709.

[34] Mali, H.S. and Kishan, J., (2014), "Developing alternative polymer abrasive gels for abrasive flow finishing process", in *Proceeding of 5thInternational & 26thAll India Manufacturing Technology, Design and Research Conference (AIMTDR 2014),* December 12th–14th, 2014, IIT Guwahati, Assam, India.

[35] Kavithaa, T.S., Balashanmugam, N. and Shashi, K. P.V., (2014), "Abrasive flow finishing process - a case study", in *Proceedings of 5th International & 26th All India Manufacturing Technology, Design and Research Conference (AIMTDR 2014),* December 12th–14th, 2014, IIT Guwahati, Assam, India.

[36] Brar, B.S., Walia, R.S., Singh, V. P. and Sharma, M., (2013), "A robust helical abrasive flow machining (HLX-AFM) process", *Journal of Institute of Engineers India,* Vol. 94(1), pp. 21-29.

[37] Kumar, R., Murtaza, Q. and Walia, R.S., (2014), "Three start helical abrasive flow machining for ductile materials", in *Proceedings of 3rd International Conference on Materials Processing and Characterisation (ICMPC 2014),* pp.1884-1891.

[38] Williams, R.E. and Rajurkar, K.P., (1992), "Stochastic modeling and analysis of abrasive flow machining", *Trans. ASME Journal of Engineering,* Vol. 114, pp. 74-81.

[39] Williams, R.E. and Rajurkar, K.P., (1989), *"*Metal removal and surface finish characteristics in abrasive flow machining", *ASME, PE,* Vol. 38, pp. 93-106.

[40] Williams, R.E., Rajurkar, K.P. and Rhodes, L.J., (1989), *"*Performance characteristics of abrasive flow machining", *SME technical paper,* pp. 898-906.

[41] Przyklenk, K., (1986), "Abrasive flow machining: a process for surface finishing and deburring of work-piece with a complicated shape by means of an abrasive laden medium", *ASME, PED,* Vol. 22, pp. 101-110.

[42] Loveless, T.R., Williams, R.E. and Rajurkar, K.P., (1994), "A study of the effects of abrasive flow machining on various machined surfaces", *Journal of Materials Processing Technology,* Vol. 47, pp. 133-151.

[43] Wang, A.C. and Weng, S.H., (2007), "Developing the polymer abrasive gels in AFM process", *Journal of Materials Processing Technology,* pp. 486-490.

[44] Davies, P.J. and Fletcher, A.J., (1995), "The assessment of the rheological characteristics of various polyborosiloxane/grit mixtures as utilized in the abrasive flow machining process", in *Proceedings of The Institution of Mechanical Engineers,* Vol. 209, pp. 409-418.

[45] Govl, K., Eyercioglu, O. and Cakir, C.V., (2013), "Hardness Effects on Abrasive Flow Machining", *Journal of Mechanical Engineering,* Vol.59, pp. 626-631.

[46] Agrawal, A., Jain, V.K. and Muralidhar, K., (2005), "Experimental determination of viscosity of abrasive flow machining media", *International Journal of Manufacturing Technology and Management,* Vol. 7(2-4), pp.142-156.

[47] Kendaa, J., Pusaveca, F., Kemoucheb, G. and Kopaca J., (2011), "Surface integrity in abrasive flow machining of hardened tool steel AISI D2", in *Proceedings of 1st CIRP Conference on Surface Integrity (CSI),* pp.172-177.

[48] Uhlmann, E., Mihotovic, V. and Coenen, A., (2009), "Modeling the abrasive flow machining process on advanced ceramic materials", *Journal of Materials Processing Technology,* Vol. 209, pp. 6062-6066.

[49] Uhlmnn, E., Doits, M. and Schmeidel, C., (2013), "Development of a material model for visco-elastic abrasive medium in Abrasive Flow Machining", in

Proceedings of 14th CIRP Conference on Modeling of Machining Operations (CIRP CMMO), Vol. 8, pp. 351-356.

[50] Tzeng, H.J., Yan, B.H., Hsu, R.T. and Chow, H.M., (2007), "Finishing effect of abrasive flow machining on micro slit fabricated by wire-EDM", *International Journal of Advance Manufacturing Technology,* Vol. 34, pp. 649-656.

[51] Tzeng, H.J., Yan, B.H., Hsu, R.T. and Lin, Y.C., (2007), "Self-modulating abrasive medium and its application to abrasive flow machining for finishing micro channel surfaces", *International Journal of Advance Manufacturing Technology,* Vol. 32, pp. 1163-1169.

[52] Fang, L., Zhao, J., Li B. and Sun, K., (2009), "Movement patterns of ellipsoidal particle in abrasive flow machining", *Journal of Materials Processing Technology,* Vol. 209, pp. 6048-6056.

[53] Walia, R.S., Shan, H.S. and Kumar, P., (2008), "Determining dynamically active abrasive particles in the media used in centrifugal force assisted abrasive flow machining process", *International Journal of Advance Manufacturing Technology,* Vol. 38, pp. 1157-1164.

[54] Walia, R.S., Shan, H.S. and Kumar, P., (2008), "Morphology and integrity of surfaces finished by centrifugal force assisted abrasive flow machining", *International Journal of Advance Manufacturing Technology,* Vol. 39, pp. 1171-1179.

[55] Hiremath, S., Vidyadhar, H. M. and Singaperumal, M., (2013), "A novel approach for finishing internal complex features using developed abrasive flow finishing machine", *International Journal of Recent advances in Mechanical Engineering,*Vol.2(4).

[56] Kim, J.D. and Kim, K.D., (2004), "Deburring of burrs in spring collets by abrasive flow machining", *International Journal of Advance Manufacturing Technology,* Vol. 24, pp. 469-473.

[57] Singh, S., Ravishankar, M., Jain, V.K and Ramkumar, J., (2014), "Modeling of finishing forces and surface roughness in abrasive flow finishing (AFF) process using rheological properties", in *Proceedings of 5th International & 26th All India*

Manufacturing Technology, Design and Research Conference (AIMTDR 2014), December 12th–14th, 2014, IIT Guwahati, Assam, India.

[58] Gupta, R. and Wandra, R., (2014), "Effect and optimization of Process Parameters on surface roughness in abrasive flow machining process", *IJITKM,* pp. 266-273.

[59] Wang, A.C., Cheng, K.C., Chen, K.Y. and Lin, Y.C., (2014), "Enhancing the surface precision for the helical passageways in abrasive flow machining", *Materials and Manufacturing Processes,* Vol. 29, pp. 153-159.

[60] Brar, B.S., Walia, R.S. and Singh, V.P., (2015), "Electrochemical-aided abrasive flow machining (ECA2FM) process: a hybrid machining process", *International Journal Advance Manufacturing Technology.*

[61] Wani A.M., Yadava V. and Khatri A.,(2007),"Simulation for the prediction of surface roughness in magnetic abrasive flow finishing (MAFF)", *Journal of Materials Processing Technology*, Vol. 190, pp. 282–290.

[62] Singh S. and Shan H.S., (2002), "Development of magneto abrasive flow machining process", *International Journal of Machining Tool Manufacture*, Vol. 42, pp. 953–959.

[63] Shinmura T., Takazava K., Hitano E., Aizawa T., (1985) "Study on magnetic abrasive process—process principle and finishing possibility", *Journal of Japanese Society of Precession Engineering*, Vol. 19 (1),pp. 54–55.

[64] Shinmura T., Takazava K., Hitano E., Aizawa T., (1984) , "Study on magnetic abrasive process—finishing characteristics", *Journal Japanese Society Precision Engineers*, Vol. 18 (4) 347–348.

[65] Shinmura T., Takazava K., Hitano E., Aizawa T., (1987),"Study on magnetic abrasive process—effect of various types of magnetic abrasives on finishing characteristics", *Journal Japanese Society Precision Engineers*, Vol. 21 (2), pp. 139–141.

[66] Hitomi Y. and Shinmura T.,(1997) “Study of the surface modification resulting from an internal magnetic abrasive finishing process”, *International Journal Machine Tool Manufacture,* pp. 997–1006.

[67] Jha S., Jain V.K., (2004), “Design and development of the magneto-rheological abrasive flow”, *International Journal of Machine Tools & Manufacture,* Vol. 44, pp. 1019–1029.

[68] Jha S. and Jain V.K.,(2006), “Modeling and simulation of surface roughness in magneto-rheological abrasive flow finishing (MRAFF) process”, *Wear,* Vol. 261, pp. 856–866.

[69] Shinmura T., Takazawa K. and Hatano E.,(1990),“Study of magnetic abrasive finishing”, *Annals of CIRP,* Vol. 39 (1),pp. 325–328.

[70] Das, M., Jain, V.K. and Ghoshdastidar, P.S., “Computer Simulation of Nano-finishing Process”. *Lecturer notes.*

[71] Paramvir, G. and Bhardwaj, D., “Modified Pts scheme based paper analysis of abrasive Flow machining through CFD Technique”, *International Journal of Electrical, Electronics and Mechanical Fundamentals,* Vol. 16.

[72] Wang, R. and Wang, M., (2010), A two-fluid model of abrasive water jet, *Journal of Materials Processing Technology,* Vol. 210, pp. 190-196.

[73] Deam, R.T., Lemma, E. and Ahmed, D.H., (2004), “Modeling of the abrasive water jet cutting process”, *Wear,* Vol. 257, pp. 877-891.

[74] Narayanan, C., Balz, R., Weiss, D.A. and Heiniger, K.C., (2013), “Modeling of abrasive particle energy in water jet machining”, *Journal of Materials Processing Technology,* Vol. 213, pp. 2201-2210.

[75] Annoni, M., Arleo, F. and Malmassari, C., (2014), “CFD aided design and experimental validation of an innovative air assisted pure water jet cutting system”, *Journal of Materials Processing Technology,* Vol. 214, pp. 1647-1657.

[76] Liu, H., Wang, J., Kelson, N. and Brown, R.J., (2004), "A study of abrasive waterjet characteristics by CFD simulation", *Journal of Materials Processing Technology,* pp. 483-493.

[77] Deepak, D., Anjaiah, D. and Sharma, N.Y., (2012), "Numerical analysis of flow through abrasive water suspension jet: The effect of garnet, aluminium oxide and silicon carbide abrasive on skin friction coefficient due to wall shear and jet exit kinetic energy", *International Science Index,* Vol.6 (10).

[78] Deepak, D., Anjaiah, D. and Sharma, N.Y., (2011), "Numerical analysis of flow through abrasive water suspension jet: The effect of inlet pressure on wall shear and jet exit kinetic energy", in *Proceedings of the World Congress on Engineering*.

[79] Deepak, D., Anjaiah, D. and Sharma, N.Y., (2011), "Effect of diameter ratio, volume fraction and abrasive grain size on the exit velocity by numerical simulation of flow through abrasive water suspension jet nozzle using DOE", *WJTA-IMCA Conference and Expo.*

[80] Deepak, D., Anjaiah, D. and Sharma, N.Y., (2012), "CFD Simulation of flow in an abrasive water suspension jet: The effect of inlet operating pressure and volume fraction on skin friction and exit kinetic energy", *Advances in mechanical engineering.*

[81] Lagumbay, R.S., Vasilyev, O.V. and Haselbacher, (2007), "Homogeneous equilibrium mixture model for simulation of multiphase/multicomponent flows", *International Journal for Numerical Methods in Fluids,* pp. 1-6.

[82] Manninen, M. and Taivassalo, V., (1996), "On mixture model of multiphase", Keynote papers, *Julkaisija-Utgivare, Publisher.*

[83] Zivkovic, V., Biggs, M.J. and Glass, D., "Granular pressure in a liquid fluidized bed", *Keynote Papers.*

[84] Fang, L., Zhao, J., Sun, K., Zheng, D. and Ma, D., (2009), "Temperature as sensitive monitor for efficiency of work in abrasive flow machining", *Wear,* Vol. 66, pp. 678-687.

[85] Tang, B., Ji, S. and Tan, D., (2010), "Structural surface of mould softness abrasive flow precision polishing machining method based on VOF", *International Conference on Electrical and Control Engineering.*

[86] Li, J., Liu, W., Yang, L., Li, C., Liu, B., Wu, H. and Sun, X. (2009), "Design and simulation for micro-hole abrasive flow machining", *The IEEE International-al Conference on Computer-aided Industrial Design & Conceptual Design*，Vol. 1, pp. 815-820

[87] Li, J., Liu, W., Yang, L., Yang, Z., Liu, W. and Zemin, Q., (2014), "Numerical thermodynamic analysis of two-phase solid-liquid abrasive flow polishing in U-Type Tube", *Advances in Mechanical Engineering.*

[88] Li, J., Liu, W., Yang, L., Liu, B., Zhao, L. and Li, Z., (2011), "The development of nozzle micro-hole abrasive flow machining equipment", *Applied Mechanics and Materials,* Vol. 44-47, pp. 251-255.

[89] Zheng, W., Junye, L. and Hao, G., (2012), "Three dimensional computer numerical simulation for micro-hole abrasive flow machining feature", International Review on Computers and Software, Vol. 7.

[90] Guo, H., Li, J. and Ma, T., "3-D numerical simulation on micro-hole of the common-rail pipe abrasive flow machining", *Applied Mechanics and Materials,* Vol. 437, pp. 202-206.

[91] Liu, W., Junye, L., Yang, L., Liu, B. and Zhao, L., "Design analysis and experimental study of common rail abrasive flow machining equipment", *American Scientific Publishers.* Vol. 5, pp. 576-580.

[92] Wan, S., Ang, Y.J., Sato, T. and Lim, G.C., (2014), "Process modeling and CFD simulation of two-way abrasive flow machining", International Journal Advance Manufacturing Technology, Vol. 71, pp. 1077-1086.

[93] ShiMing, J., FengQing, X. and DaPeng, T., (2010), "Analytical method for softness abrasive flow field based on discrete phase model", *Science China, Technological Sciences,* Vol. 53, pp. 2867-2877.

[94] Li, C., Shi-Ming, J. and Da-Peng, T., (2012), "Softness abrasive flow method oriented to tiny scale mold structural surface", *International Journal of Advance Manufacturing Technology,* Vol. 61, pp. 975-987.

[95] Wang, A.C., Tsai, L., Liang, K.Z., Liu, C.H. and Weng, S.H., (2009), "Uniform surface polished method of complex holes in abrasive flow machining", "*Transactions of Nonferrous Metals Society of China",* Vol. 19, pp. 250-257.

[96] Venkatesh, G., Sharma, A.K. and Singh, N., (2015), "Simulation of media behaviour in vibration assisted abrasive flow machining", *Simulation Modeling Practice and Theory,* Vol. 51, pp. 1-13.

[97] Venkatesh, G., Sharma, A.K. and Kumar, P., (2015), "On ultrasonic assisted abrasive flow finishing of bevel gears", *International Journal of Machine Tools & Manufacture,* Vol. 89, pp. 29-38.

[98] Yuan, Q., Ji, S., Wen, D. and Zhang, L., (2014), "Parameters optimization and numerical simulation for soft abrasive flow machining", *Sensors and Transducers,* Vol. 177(8), pp. 202-209.

[99] Arora, G., Sharma, A.K., Bhowmik, P. and Priyadarshini, S., (2013), "An FEM Approach to analysis of media used in the spiral flow assisted abrasive flow machining", *International Journal of Mechanical Engineering and Research,* Vol. 3(6), pp. 635-640.

[100] Chen, K.Y. and Cheng, K.C., "A study of helical passageways applied to polygon holes in abrasive flow machining", (2014), *International Journal of Advance Manufacturing Technology,* Vol. 74, pp. 781-790.

[101] Dong, Z., Gang, Y. and Lisheng, W., "Studies of model and cutting characteristics of abrasive flow machining based on slit", *Keynote Papers.*

[102] Wang, A.C., Liu, C. H., Liang, K.Z. and Pai, S. H., (2007), "Study of the rheological properties and the finishing behavior of abrasive gels in abrasive flow machining*", Journal of Mechanical Science and Technology*, Vol. 21, pp. 1593-1598.

[103] Das, M., Jain, V.K. and Ghoshdastidar, P.S., (2010), "Nano-finishing of stainless steel tubes using rotational magneto-rheological abrasive flow finishing process", *Machining Science and Technology,* Vol. 14, pp. 365–389.

[104] Das, M., Jain, V.K. and Ghoshdastidar, P.S., (2011), "Nano-finishing of flat work-pieces using rotational–magneto-rheological abrasive flow finishing (R-MRAFF) process", *International Journal of Advance Manufacturing Technology,* Vol. 62, pp. 405-420.

[105] Syamlal, M., Rogers, W. and O'Brien, T. J., (1993), MFIX Documentation: Volume 1, Theory Guide, National Technical Information Services, Springfield, VA.

[106] Gidaspow, D., Bezburuah, R. and Ding J., (1992) " Hydrodynamics of circulating fluidized beds, kinetic theory approach", In proceedings of *7th Engineering Foundation Conference on Fluidization, pp. 75-82.*

APPENDICES

The Brinell hardness number is given by

$$BHN = \frac{2F}{\pi D\left(D - \sqrt{D^2 - d^2}\right)}$$

where F = applied force in (kgf)

D = diameter of the indenter (mm)

d = diameter of indentation (mm)

putting $F = F_n$, $D = d_g$, $d = D_i$,

$$BHN = \frac{2F_n}{\pi D_g\left(D_g - \sqrt{D_g^2 - d^2}\right)}$$

$$= \frac{F_n}{\frac{\pi}{2} D_g\left(D_g - \sqrt{D_g^2 - D_i^2}\right)} \tag{20}$$

From the fig. 39,

$$t = \frac{D_g}{2} - \sqrt{\frac{D_g^2}{4} - \frac{D_i^2}{4}}$$
$$= \frac{D_g}{2} - \frac{1}{2}\sqrt{D_g^2 - D_i^2} \tag{21}$$

The cross-sectional area of the groove generated, A' (shaded portion of the grain) can be derived from the geometry.

The area of a circular section is given by,

$$A = \frac{R^2}{2}(\theta - \sin\theta)$$

The value of θ from the geometry (fig. 39) is given by

$$\theta = \sin^{-1}\frac{D_i}{D_g}$$

From the equation 21, the value of D_i is given by,

$$D_i = 2\sqrt{t\left(D_g - t\right)}$$

Putting the values of R = $\frac{Dg}{2}$, $\theta = \sin^{-1}\frac{D_i}{D_g}$ and Di $= 2\sqrt{t(D_g - t)}$,

$$A^{-1} = \frac{D_g^2}{2}\sin^{-1}\left(\frac{2\sqrt{t\left(D_g - t\right)}}{D_g}\right) - \sqrt{t\left(D_g - t\right)}\left(\frac{D_g}{2} - t\right) \qquad (22)$$

LIST OF PUBLICATIONS

International Journals:

1. R. Dash and K. P. Maity, Modeling of material removal in abrasive flow machining process using CFD simulation, *Journal of Basic and Applied Engineering Research*, Vol. 1, Number 2; October, 2014, pp. 73-78.
2. R. Dash and K. P. Maity, Simulation of abrasive flow machining process for 2D and 3D model, *Frontiers of Mechanical Engineering*, Vol. 10(4), pp. 424-432, Springer Publishers. (Indexed by SCOPUS)
3. R. Dash and K. P. Maity, Modelling of granular pressure in abrasive flow machining process for a rotary swaging die, *International Journal of Pure and Applied Research in Engineering and Technology (IJPRET)*, Vol. 3(9), pp. 23-29.
4. R. Dash and K. P. Maity, Numerical analysis of abrasive flow machining: Comparison of effects of different abrasives on granular pressure and skin friction coefficient, *Mathematical models and computer simulations*. (Communicated)

International Conferences:

1. R. Dash and K. P. Maity, Modeling of material removal in abrasive flow machining process using CFD simulation, International Conference on Innovative Trends in Mechanical, Material, Manufacturing, Automobile, Aeronautical Engineering and Applied Physics, JNU (New Delhi), 23rd and 24th August 2014.